5-2013

# Avβ8 Integrin Interacts With Rhogdi1 To Regulate Rac1 And Cdc42 Activation And Drive Glioblastoma Cell Invasion

Steve Reyes

αvβ8 Integrin Interacts with RhoGDI1 to Regulate Rac1 and Cdc42 Activation and Drive Glioblastoma Cell Invasion

Steve B. Reyes, B.S.

APPROVED:

_____
Joseph McCarty, Ph.D.

_____
Gary Gallick, Ph.D.

_____
Candelaria Gomez-Manzano, M.D.

_____
Anshu Mathur, Ph.D.

_____
Pierre McCrea, Ph.D.

APPROVED:

_____
Dean, The University of Texas

Graduate School of Biomedical Sciences at Houston

αvβ8 Integrin Interacts with RhoGDI1 to Regulate Rac1 and Cdc42 Activation and Drive Glioblastoma Cell Invasion

A

DISSERTATION

Presented to the Faculty of

The University of Texas

Health Science Center at Houston

And

The University of Texas

M. D. Anderson Cancer Center

Graduate School of Biomedical Sciences

in Partial Fulfillment

of the Requirements

for the Degree of

DOCTOR OF PHILOSOPHY

by

Steve B. Reyes, B.S.

Houston, Texas

May, 2013

αvβ8 Integrin Interacts with RhoGDI1 to Regulate Rac1 and Cdc42 Activation and Drive Glioblastoma Cell Invasion

Publication No._____

Steve Reyes, B.S.

Supervisory Professor: Joseph McCarty, Ph.D.

As an interface between the circulatory and central nervous systems, the neurovascular unit is vital to the development and survival of tumors. The malignant brain cancer glioblastoma multiforme (GBM) displays invasive growth behaviors that are major impediments to surgical resection and targeted therapies. Adhesion and signaling pathways that drive GBM cell invasion remain largely uncharacterized. Here we have utilized human GBM cell lines, primary patient samples, and pre-clinical mouse models to demonstrate that integrin αvβ8 is a major driver of GBM cell invasion. β8 integrin is overexpressed in many human GBM cells, with higher integrin expression correlating with increased invasion and diminished patient survival. Silencing β8 integrin in human GBM cells leads to impaired tumor cell invasion due to hyperactivation of the Rho GTPases Rac1 and

Cdc42. β8 integrin associates with Rho GDP Dissociation Inhibitor 1 (RhoGDI1), an intracellular signaling effector that sequesters Rho GTPases in their inactive GDP-bound states. Silencing RhoGDI1 expression or uncoupling αvβ8 integrin-RhoGDI1 protein interactions blocks GBM cell invasion due to Rho GTPase hyperactivation. These data reveal for the first time that αvβ8 integrin, via interactions with RhoGDI1, suppresses activation of Rho proteins to promote GBM cell invasiveness. Hence, targeting the αvβ8 integrin-RhoGDI1 signaling axis may be an effective strategy for blocking GBM cell invasion.

## Table of Contents:

## List of Illustrations:

## List of Tables:

## Introduction

### GBM Pathophysiology: Historical and Histopathology Perspective

Gliomas arise from the CNS and are derived from glial cell types (astrocytes, oligodendrocytes, and ependymal cells) and are named accordingly as astrocytomas, oligodendrogliomas, ependymomas, and mixed gliomas. Each tumor can differ in genetics and signaling, allowing researchers and physicians to better understand and exploit the pathways used by these cells(1,2). However, tumors defined by histological features alone have been shown to behave differently, suggesting that a molecular and genetic pathology classification would be advantageous(1). Additionally, in the past five years evidence has been accumulating that some brain tumor cells may behave similar to stem cells(3-5). The original nomenclature has become even more complicated as some of these cells have been found to transform into endothelial-like cells(6,7). Nonetheless the current naming convention has remained intact with an additional classification system further categorized by the World Health Organization (WHO).

Astrocytic gliomas have been broken divided into four stages with the first being largely separated by 2, 3, and 4. Stage I is characterized by their decreased ability to transform to a malignant state and are less invasive(7). An example of these is pilocytic astrocytomas. These less infiltrative tumors are often considered benign and can often be surgically resected, unlike higher stages(2). Stage II tumors, such as low-grade astrocytomas, are much more diffuse beyond the primary tumor mass and are not surgically curable. Stage III tumors, such as anaplastic astrocytomas, are increasingly more invasive and more proliferative(1).

Stage IV gliomas are yet more invasive, more proliferative, have increased vascularization, and are the most fatal. The most common gliomas diagnosed are glioblastoma multiforme (GBM), a WHO stage IV tumor(1).

Brain tumors do not have unique symptoms with the first sign being headaches, blurred vision, and nausea. As such patients and physicians do not often detect these tumors in their early stages. Typically the disease has progressed to the latest stage with the most severe symptoms before imaging is conducted, where the GBM is diagnosed(1). Because of this, most gliomas are diagnosed at a later stage and have worse outcomes. So while GBMs are rare, they are extremely fatal, when compared to other tumors. The typical survival time is 9-14 months from diagnosis(1-3). One of the distinguishing hallmarks of GBMs is their invasiveness. While a primary mass can be surgically resected, individual tumor cells that have invaded into the surrounding healthy tissue cannot be and form satellite tumors. This makes the invasive phenotype an important property to understand and why it was chosen for investigation herein.

**Gliomagenesis: Cell Biology and Genetics**

Neuroepithelial are stem cells that give rise to a majority of the cells in the CNS(6). These neuroepithelial cells progress along different pathways to differentiate into multiple cell types. As is understood in stem cell biology these cells typically assume two paths; (1) to asymmetrically divide to form a progenitor-like cell and a precursor cell or (2) to form two differentiated daughter cells slightly more restricted than the previous. At each stage of the subsequent divisions the

daughter cells gradually become a more defined cell type. Within the past 5 years considerable evidence has arisen suggesting GBMs may originate from an event that causes the differentiated cells to revert to a stem like state, exploiting aberrant signaling pathways along the way(6,7). It is therefore no surprise that many of the proteins and mechanisms of interest to cancer biologists are also used by the cells for development. Additionally, it is likely that relationships are also shared between GBMs and repair pathways. An example of this is nestin-positive reactive astrocytes and nestin-positive progenitors, which are known to migrate to a site of injury. This example is interesting as terminal astrocytes do not express nestin, yet it has been detected in GBMs.

The genetics of GBMs has also been of interest in recent years. One of the most well studied mechanisms in cancer biology involves p53, which is a transcriptional activator of p21, a cyclin-dependent kinase inhibitor which inhibits the cell cycle(4). Additionally, p53 is able to transcriptionally activate Bax while inhibiting Bcl-2, which are pro-apoptotic and anti-apoptotic respectively(8-11). Therefore, it is easy to understand how important p53 may be in GBM development and progression. Indeed evidence has accumulated that mutations in p53 are often found in low-grade gliomas whereas those that arise primarily often do not have p53 mutations(12). However, no prognostic advantage has been found with regard to p53 mutations in GBMs.

Interestingly those with functional p53 often overexpress EGFR or have mutated EGFR(12). These activated mutants are thought to lend a selective advantage, leading to increased proliferation while reducing apoptosis. Amplified

EGFR is associated with GBM and its activation has been found to influence the growth of both astrocytes and their precursors. EGFR overexpression correlates well with high grade GBMs and has long been thought to play a critical role in the formation of these tumors(12). With such influence over cell behavior it is no wonder this is a widely explored drug target with antibodies and small molecule inhibitors currently being developed(1,3,13). Other growth factors are also of interest including fibroblast growth factor (FGF), platelet-derived growth factor (PDGF), and insulin-like growth factor (IGF); lending much credit to the importance of extracellular signaling taking place across the ECM(14,15). However, as EGFR is the most commonly over-expressed receptor in gliomas, it is currently of the most interest.

It is also interesting that cells overexpressing mutated wild-type EGFR along with PTEN display the most favorable outcomes with EGFR inhibitors. However, loss of PTEN in GBM patients lend them a poor prognosis and it is mutated in GBMs with predictions of mutation in the 20% range(2). Wild-type PTEN has also been shown to rescue the mutated protein by halting proliferation. It is also thought that this protein may play a role in preventing invasion by interacting with FAK. However this claim has not been completely substantiated in GBMs and its all the more reason to further investigate these pathways(16,17).

**Integrins: Basic Function**

Integrin are defined by two unique chains, termed their α and β subunits. These obligate heterodimer receptors exist in 26 known combinations utilizing

eighteen α and eight β subunits. Most integrins are part of either the β1 or αv subfamilies, which is the breadth of this review(18). It is easily understood that the combination of these subunits determine the extracellular and intracellular binding and signaling events. The network of integrin-ligand interactions is vast: some integrins are ligand-specific while others bind many shared ligands. This overlap allows for one ligand to have multiple effects on a cell through different integrins while also maintaining its equilibrium. Conversely integrins are capable of inside-out signaling, making them a medium for large amounts of communication taking place within the microenvironment(19). During development this has been seen to regulate adhesion and migration. However in the context of tumorigenesis within the brain this is expanded to include proliferation, survival, and differentiation(20). Additionally, within the cell all integrins discussed here are link to the actin intracellular microfilament network.

**ECM Components: Basic functions**

The cellular environment is of great importance in GBM development and persistence. Gliomas develop alongside non-neoplastic endothelial cells and astrocytes as well as the native extracellular matrix (ECM). As a GBM develops it modifies its ECM into a niche that is further exploited by the tumor and is also a distinguishable fingerprint.

A prominent feature of integrins is their ability to connect to the ECM. The ECM itself is between astrocytes and blood vessels. Since astrocytic end-feet wrap around blood vessels, the integrin-ECM complex is extremely important. Integrins

are able to bind extracellular ECM scaffolding proteins such as laminins and collagens and also bind intracellular cytoskeletal elements such as talin. This direct link allows for the cell to detect its environment and heavily influences the how and where a cell migrates as well as communicates whether the given environment is suitable for growth. Downstream, these send signals through kinases such as FAK and Src. Beyond cell-ECM communication, integrins are also capable of influencing growth factors. These have been known to include Epidermal growth factor (EGF), Fibroblast growth factors (FGF), Vascular endothelial growth factor (VEGF), platelet-derived growth factor (PDGF), Interleukins (ILs), and Transforming growth factor beta and alpha family members (TGFβ/α). The wide influence of integrins also includes regulation of enzymes such at Matrix metalloproteinases (MMP) and tissue inhibitors of metalloproteinases (TIMP)(21-25). These highly responsive elements are capable of degrading components of the ECM, influencing cell motility. It is through these extra and intracellular components that we understand the intermediary role of integrins as translators of signals and through their known pathological behaviors we then classify integrins as major players of tumorigenesis.

**Various Roles of Integrins in Astrocytes:**

**β1s**

A substantial trait of GBMs is their invasiveness. While the β1 subfamily of integrins in astrocytes has not been reported to play a major role in GBM growth, they are involved in invasion. Integrins α2β1, α3β1, α5β1, and α6β1 have been seen to be over expressed in astrocytes (26, 27). It has been found that blocking monoclonals against is effective at slowing cell migration in vitro(28,29, 30). One of the highest expressing integrins, α3β1, has been seen to be involved in invasion both in-vitro and in-vivo (29,30). This is likely occurring through stimulation by its laminin ligand(31,32). While not all β1 integrin pairs have been investigated, it is likely that the non-invasive phenotype seen with dysfunctional β1 is attributed to α3β1 (29).

**αvs**

Even if a primary tumor mass can be fully resected, it is likely that individual cells have invaded into the surrounding tissue. These highly motile cells then spur secondary lesions. The involvement of integrins here is vast with αvβ1, αvβ3, αvβ5, αvβ6, and αvβ8 being involved in motility and growth(33-35). Knockout of αv, and thus absence of all the αv integrins, leads to severe cerebral hemorrhage and lethality(19). Other than the loss of the vast signaling pathways, this situation eliminates the formation of any αv integrin depend focal contacts. This is mostly due to the cytoplasmic portion of the β subunit being responsible for binding to the cytoskeletal proteins.

**αvβ1**

Angiopoietin-2 has been seen to act on αvβ1 to activate FAK and ERK1/2 as well as increase the expression of MMP2, which is of relevance to αvβ3 as described below (36). However this receptor is not expressed in all GBMs (37).

**αvβ3**

The integrin αvβ3 is known to have FN, VN, osteopontin, tenascin, and von Willebrand factor as ligands; however, the role of these within the tumor microenvironment has largely been unexplored. Along with the tumor vasculature, αvβ3 is also known to be expressed on GBM-glial cells (38). Following this observation, it has been seen that anti-αvβ3 inhibition can lead to reduced angiogenesis, tumor size, and invasion (39). αvβ3 dependent GBM invasion is known to utilize MMP2 (40,23,41). TGFβf2-stimulated invasion is reduced when either αvβ3 or MMP2 is inhibited in vitro (42). It is also likely that tissue inhibitor of metalloproteinases 2 (TIMP-2) is involved with MMP2, but more work needs to be carried out with GBM models (43,24,44). αvβ3 and αvβ5 are also involved with hypoxia(45-47). Under hypoxic conditions they are recruited to the cell membrane. In addition to being activated by hypoxic condition they also communicate the oxygenation state of the cell by activating GSK-3β, RhoB, and FAK to stabilize HIF-1α, implying a feedback mechanism (17). As αvβ3 has become associated with motility, it is of interest that it also inhibits tumor growth when over expressed (40,23,41,48). The Pieper group has also found that β3 over expression will result in smaller vessel size and a more hypoxic tumor. While these phenotypes could be

rescued by activating Akt and VEGF pathways common in GBMs, it presents an interesting situation in the context of hypoxia. Combining these data with the aforementioned hypoxic mechanism proposed by the Moyal group presents an interesting dilemma for GBM patients (17,48). Should a group of cell in the niche be αvβ3 high and become hypoxic, it may be possible for the signal to amplify itself and spread beyond the local site.

**αvβ5**

Besides being overexpressed in GBMs, αvβ5 has some interesting relations to αvβ3 (49,50,51). Externally, αvβ5 is able to activate latent-TGFB1 spurring TGFBRI/II the pathway while the αvβ3 is only able to change latent-TGFB1 conformation (52,53). Also, αvβ5 has been seen internalize VN, while αvβ3 was dependent on αvβ5 for it to internalize VN(54). PDGFR has also been seen to associate with αvβ3 but not αvβ5 in GBM samples (55). And while these differences occur, internally both integrins share the GSK-3- RhoB-FAK pathway that stabilizes HIF-1α under hypoxic conditions (17).

Interestingly, while both of these integrins can bind vitronectin, αvβ5 has been seen to be required for in-vitro motility independent of αvβ3 (56).

**αvβ6**

While αvβ6 is known to activate TGFB1 and TGFB3 in normal brain, its effects in GBM models have yet to be explored(57).

**αvβ8**

The normal brain depends on αvβ8 and its interactions with the ECM. The blood vessels of mice null for αv or β8 dilate, the blood barrier is compromised, and the mice suffer severe hemorrhaging(18, 58). As αv is known to form αvβ3, αvβ5, and αvβ8 integrin pairs, it is there for likely that the phenotype seen when αv is knocked out is caused by the loss of αvβ8. The current understanding of this integrin is that it binds to the RGD site of its ligand LAP-TGFβ1/3. Once bound it cleaves the LAP portion, leaving only the TGFβ1/3. It is this TGFβ1/3 that is considered active which can then signal by binding to the TGFβRI/II receptor. This receptor allows for the autophosphorylation of Smad2 and Smad3. These are then transported into the nucleus by Smad4 where TGFβ target genes are up regulated. It is also interesting to note that when TGFβ1/3 or TGFβR2 are ablated in endothelial cells hemorrhaging also results that is pathologically very similar to the ablation of αvβ8 this has led to a model where αvβ8, TGFβ1/3, and TGFβR2 are involved in the same signaling pathway (Figure). Interestingly, in both normal brain and GBM samples this pathway has been investigated for its role in motility (59,60). It has also recently been seen that αvβ8 plays a role in angiogenesis, which may be occurring through the negatively regulating mir-93; which leads to silencing β8 and an increase in tumor angiogenesis and size (61,62). This is of great clinical significance because numerous attempts are being made to elucidate the angiogenic pathways involved in GBMs(10,63-72). Additionally, many attempts are being made at targeting this hallmark of cancer(73-89).

**Various Roles for Integrins in Endothelial Cells:**

**α1β1 & α2β1**

A distinctive hallmark of GBMs is that they are highly vascularized. A critical factor in this process is the expression of β1 on endothelial cells (27,90). As a subunit involved in 12 integrin pairs its importance is self evident, with α1β1, α2β1, α3β1, α4β1, α5β1, α6β1, and α7β1 expression known to occur on endothelial cells and α2β1, α4β1, and α6β1 known to be over expressed in GBM endothelial cells(26). α1β1 and α2β1 have been show to promote angiogenesis in response to VEGF through the Erk1/Erk2 MAPK signal transduction pathway (69, 91-93). Antibodies directed against these integrins individually inhibited angiogenesis, in-vivo. Additionally, when used in combination the inhibition of these two integrins led to a significant reduction in tumor size and angiogenesis (91). Interestingly, α1-null mice which lack the α1β1 integrin do not harbor tumors well and illustrate a decrease in vascularization. Additionally MMP-7 and MMP-9 levels are elevated in α1-null mice, which are known to convert plasminogen into angiostatin, an inhibitor of angiogenesis (94-98). Although the involvement of α2β1 has not been clearly elucidated, it is likely involved in growth arrest (99,100). Upon α2β1 binding its laminin ligand, the ability of α5β1 to form focal adhesions is reduced. This limits the ability of α5β1 to communicate its downstream signals and inhibits cell proliferation (100).

**α5β1**

α5β1 is also a major endothelial player, being primarily influenced by its fibronectin (FN) ligand. α5-null teratocarcinoma are smaller and with less vascularization (101,102). Additionally, α5-null embryoid body formations also have delayed vascular differentiation (102). Interestingly, α5 and FN knockout mice are embryonic lethal and share angiogenic abnormalities(102,103,104,101). β1- null mice are also embryonic lethal with similar vascular pathologies, lending credence to the hypothesis that the β1-null phenotypes can be attributed to the α5β1 integrin(105). Clinically the anti-α5β1 monoclonal Volociximab is in early trials, being explored as an anti-angiogenic therapy(106-113). ATN-161, anti-angiogenic α5β1 targeting peptide, is in stage II head and neck clinical trials with plans for a glioblastoma trial (66,64,72,114).

**α3β1 & α6β1**

Due to early lethality, limited studies have been carried out exploring α3β1. However, the Hodivala-Dilke group has created conditionally knocked out α3 in endothelial cells. In non-brain ex-vivo and in-vivo models, loss of α3 led to larger tumors, more angiogenesis, and up-regulation of VEGF (65,115). α6β1 has been seen to be both upregulated and activated by VEGF in human brain cells along with several other interesting phenomena (116-125). Additionally, it is thought that they are the primary brain endothelial integrin involved in laminin adhesion (126).

**α4β1 & α7β1**

Integrin α7β1 knockout mice have interesting pathologies in regard to CNS vasculature. The mice are embryonic lethal possibly do to severe cerebrovascular hemorrhaging. Interestingly, mice that survived revealed hyperplastic and hypertrophic defects as well as down-regulated α5 in cerebral vasculature(127). While α4β1 is known to be expressed on endothelial cells, studies have been mostly carried out in human umbilical vein endothelial cells (HUVECs) and not of normal brain of GBM origin (20, 128).

**αvβ3 & αvβ5**

β3 and β5 double knockout mice are viable, have no obvious vascular pathologies (129), yet a different story is told in the context of tumorigenesis. αvβ3 and αvβ5 are over expressed in GBM endothelial cells and while its mechanism in GBMs has yet to be fully elucidated, there are promising developments with strong evidence of c-Abl involvement (40,130-132). Inhibition of αvβ3 and αvβ5 has been seen to induce endothelial apoptosis (67). An αvβ3 inhibitor has also been see to have similar success in vivo with a group developing a tracer for identifying GBM angiogenesis (19,63).

**Table 1.**

| Integrin | Structural ECM Ligands | Soluble Ligand | Expresssion (Cell Type) | Citation |
|---|---|---|---|---|
| αvβ1 | F V | TGFβ | A | (133), (134) |
| αvβ3 | F O V T W | MMP2 | EA | (135), (54) |
| αvβ5 | V | TGFβ | A E | (59), (134), (20), (54) |
| αvβ6 | F T | TGFβ | A | (133), |
| αvβ8 | L C F | TGFβ | A | (59), (134) |
| α1β1 | L C | | E A | (59), (136) |
| α2β1 | L C | MMP1 | E | (133), (27), |
| α3β1 | L F | | E A | (59), (27), (136),(38) |
| α4β1 | F O V | | E | (133), (20) |
| α5β1 | L F | | E A | (59), (27), (135), (136) |
| α6β1 | L | | E A | (59), (27), (136) |
| α7β1 | L | | | (133),(127) |
| α8β1 | F T | TGFβ | | (133), (134) |
| α9β1 | L O T | | E | (133), (137) |
| α10β1 | C | | | (133) |
| α11β1 | C | | | (133) |

**Table 1. Integrin-ECM Interactions**

**This expression table details a literature review of known ligands for given integrins as well as cell types they have been shown to be expressed on.**
**L = Laminin**
**C = Collagen**
**F = Fibronectin**
**O = Osteopontin**
**V = Vitronectin**
**T = Tenascin**
**W = von Willebrand factor**
**A = Astrocytes**
**E = Endothelial Cells.**

## A Role for αvβ8 Emerges in Gliomagenesis

As previously discussed, knocking out αvβ8 in the mouse brain results in significant hemorrhaging. Upon closer inspection it can be seen that there is endothelial cell hyperplasia as well as distorted and abnormal formation of the vasculature. In comparison, these phenotypes look very similar to the vasculature that is seen in GBMs. Tchaicha and colleagues were the first to draw a link between αvβ8 and the angiogenesis of astrocytomas. Transformed mouse astrocytes were cultured from both WT and β8 knockout mice and injected back into the mouse brain. Upon sacrificing the animal it was noted that $\beta8^{-/-}$ tumors displayed large amounts of hemorrhaging (Figure I1 A). These tumors were inspected more closely by performing immunohistochemistry for H&E as well as the blood vessel marker CD34 (Figure I1 B). It can be seen that the WT tumors have normal vasculature formation. However, when the integrin is knocked out the blood vessels become very distorted, which is a likely explanation for their hemorrhaging. Additionally, one can appreciate the hyperplasia with their being more endothelial cells per blood vessel and also more blood vessels in total. This has led out lab to a new model for αvβ8 in GBMs (Figure I1 C). Normal astrocytes and progenitors express the proper level of αvβ8. This allows for a homeostasis to take place which regulates blood vessel development via TGFβ signaling. At some point in a patient's life their cells transform through a preexisting genetic mutation or one that was induced through environment. As the pathology of the tumor progressed subpopulations of cells have varying levels of the integrin. Those with low levels of β8 lead to tumors that are more permeable and angiogenic as was described by Dr.

Tachicha or the McCarty lab(62). Preliminary results, along with published finding suggesting a role for αvβ8 in cell motility; therefore we predict high levels of β8 lead to increased invasiveness in GBMs. More specifically, this has led us to our hypothesis that αvβ8 integrin-dependent activation of TGFβ signaling pathways as well as cytoplasmic tail signaling drive astrocytoma cell migration and invasion (Figure I1 D). This data has been published(215).

**Figure I1.**

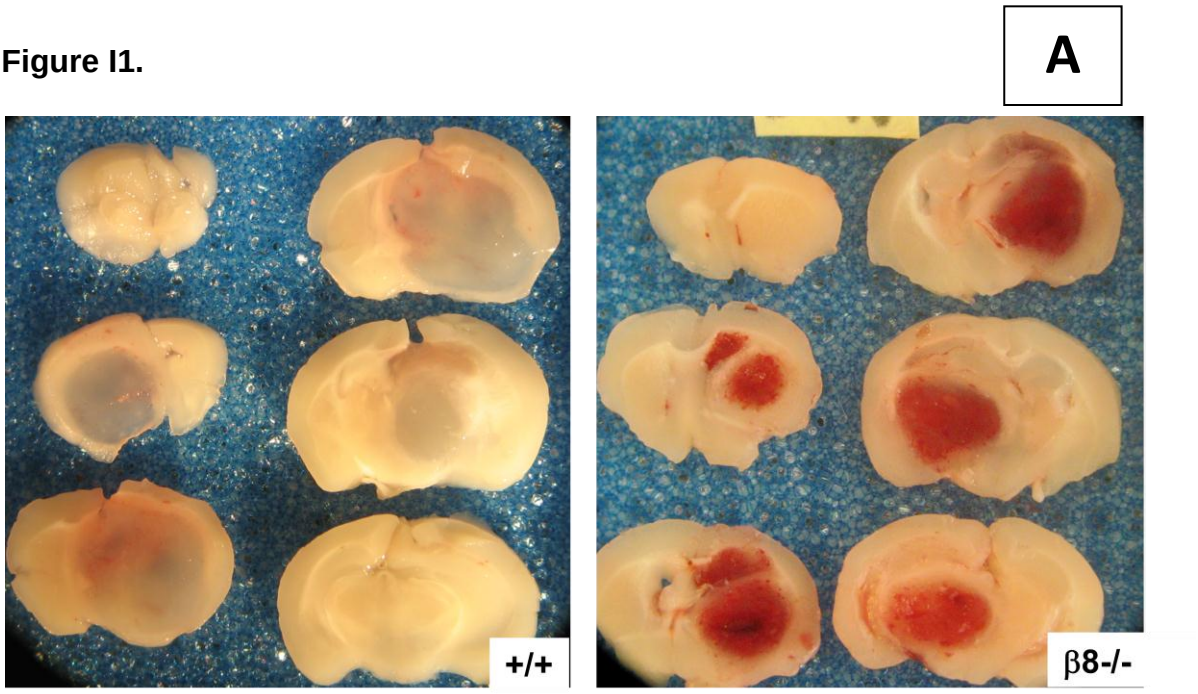

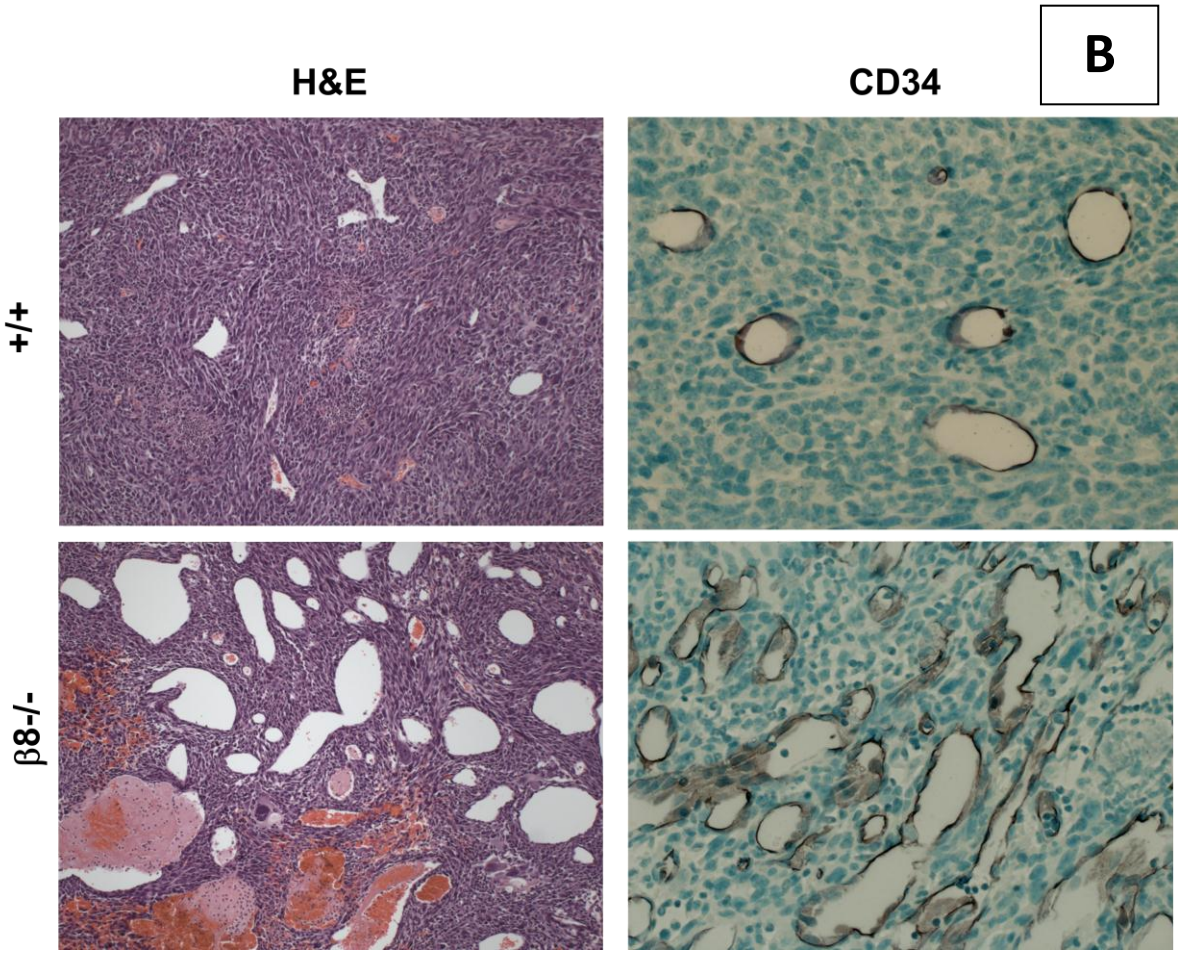
B
H&E
CD34
+/+
β8-/-

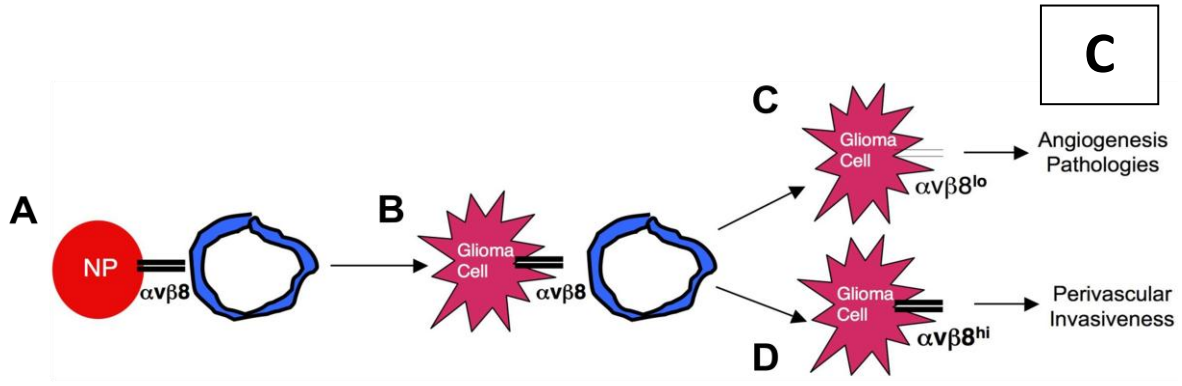
C
A
NP
αvβ8
B
Glioma Cell
αvβ8
C
Glioma Cell
αvβ8lo
Angiogenesis Pathologies
D
Glioma Cell
αvβ8hi
Perivascular Invasiveness

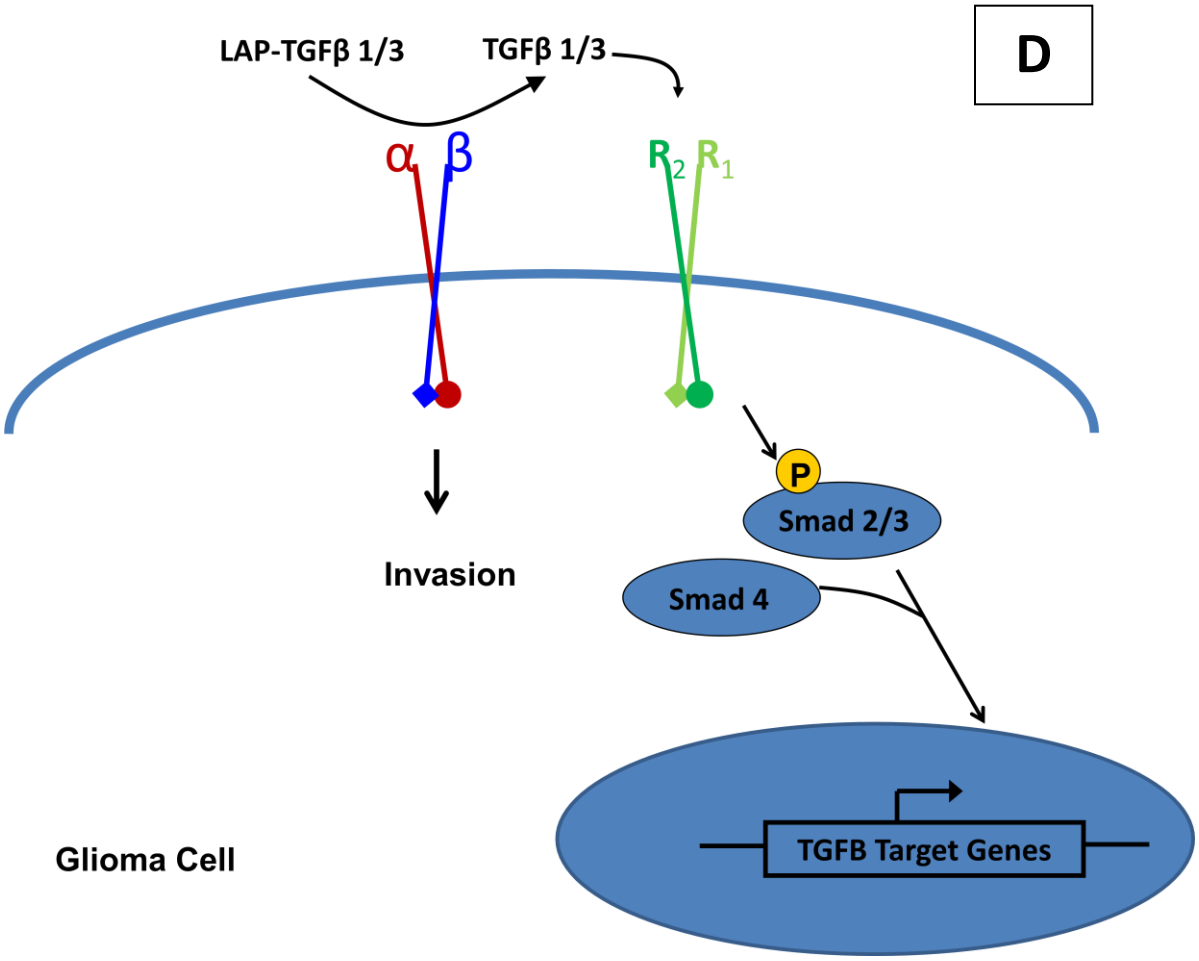


**Figure I1. A Model for β8 Regulated GBM Invasiveness**

**(A) WT transformed mouse astrocytes and $\beta 8^{-/-}$ transformed mouse astrocytes were injected into the brain of nude mice. Please note the large amount of hemorrhage that takes place when the integrin is knocked out. (B) Immunohistochemistry the tumors stained for H&E and blood vessel marker CD34. Please note the distorted vasculature present in the $\beta 8^{-/-}$ tumors. (C) A-Normal astrocytes and progenitors express αvβ8 and regulate blood vessel development via TGFβ signaling; B-Genetic mutations induce transformation; C-As the pathology progresses subpopulations have varying β8 integrin levels and low β8 leads to more angiogenesis and vascular permeability; D-High β8 leads to increased invasiveness. (D) Model for the role of αvβ8 in glioma invasiveness whereby separate signaling pathways take place. One originating from the cytoplasmic tail of β8 and the other from the extracellular portion of the αvβ8.**

## Chapter 2:

## Materials and Methods

### Immunocytochemistry and Immunofluorescence

When cells are ready to be analyzed they are washed twice with PBS. 4% PFA is then added for 10 minutes, washed twice with PBS, .5% NP40 Buffer added for 10 minutes, washed twice with PBS, and left in 10% serum of choice for blocking. All of this took place at room temperature. Fixed cells can then left at 4°C for long term storage. Primary antibody is added in the previously mentioned 10% serum of choice and left to incubate overnight at 4°C. This is then washed with .1% Tween20 for 5 minutes, and washed twice with PBS for 5 minutes. The secondary is added in the same serum and left at 4°C for 2 hours. This is removed, washed once with .1% Tween20, and twice with PBS for 5 minutes each. The edge of the coverslip is dabbed on a napkin to remove excess liquid and they are carefully set face down on a 10µl drop of soft-set DAPI stain. A modification of this procedure also allows for two primary and two secondary antibodies to be mixed and added at the same time. Additionally, this procedure is used for tissue sections in which the tissue is deparaffinized through sequential exposures to varying levels of Ethanol and Xylene, dried, and surrounded with a Pap-pen.

### Immunohistochemistry

Paraffin sections were first de-paraffinized by placing them in xylene for 4 minutes, xylene for 3 minutes, 100% ethanol for 2 minutes, 100% ethanol for 2

minutes, 95% ethanol for 1 minute, 95% ethanol for 1 minute, and 80% ethanol for 1 minute. The slides were then placed face up and the tissue outlined with a pap-pen (Invitrogen). PBS was added to the tissue for 5 minutes to rehydrate the tissue. This was removed and the tissue was blocked with 10% swine serum in PBS that was ran through a .45μM polyethersulfone filter (Whatman). This blocking step was done for 30 minutes at room temperature in a light sealed humidifying chamber. This was removed and the primary antibody was added. This was in the same filtered 10% swine serum and was added over night at 4°C. This was then washed twice in PBS+0.1% Tween-20 and then once with PBS. Washing steps were each 5 minutes and at room temperature. This was removed and the tissue was quenched with 0.3% hydrogen peroxide ($H_2O_2$) for 10 minutes. Fresh hydrogen peroxide is crucial as it reacts with ambient moisture over time. This is then carried through 3 washing steps of PBS, again at 5 minutes per wash and at room temperature. The secondary was added in 10% swine serum for 2 hours at room temperature (typically a swine anti-X biotin). This was washed off in 2 washes of PBS+0.1% Tween-20 and then once in PBS. This was then incubated with an ABC complex (Vectastain) for 30 minute at room temperature. This was then washed 3 times for 5 minutes at room temperature with PBS. The tissue was the developed with DAB (Vector Laboratories) for 10 minutes or until obvious color changes. This was then washed with water two times, 5 minutes each. The tissue was then immersed in Hematoxylin Gill's Formula (Vector Laboratories) for 3 minutes. This was then washed in water twice for 5 minutes each. It was then dipped in acid solution (2% glacial acetic acid in water) 10 times, dipped in water 10 times, dipped

in bluing solution (.45% $NH_4OH$ in ethanol) 10 times, and dipped in water 10 times. This was then ran through a sequence of alcohols that were 3 minutes in 75% ethanol, 3 minutes in 95% ethanol, 3 minutes in 100% ethanol, 3 minutes in 100% ethanol, 5 minutes in xylene, 5 minutes in xylene, and 5 minutes in xylene. These were then let dry briefly and Cytoseal-XYL (Richard-Allan Scientific) was added on top of the tissue. This was carefully covered with cover glass (Fisher Scientific) so as to prevent and minimize bubble formation.

**Frozen Sections**

As previously described, animals were cardiac perfused with 4% PFA (in PBS) and sectioned coronally in 2mm portions. These were left in 4% PFA over night. This was followed by placing them in 10% sucrose for 4 hours at 4°C and 20% sucrose overnight. These tissue sections were then placed in Cryomolds® (Tissue-Tek) with embedding medium (Tissue-Tek). This was flash frozen on dry ice and then stored at -80°C. These were then placed on positively charged slides by the MDACC Histology facility for H&E and other staining, as necessary.

**Paraffin Embedded Sections**

Following the previously mentioned cardiac perfusion and tissue sectioning, paraffin embedded sections were generated. Sections of coronally sliced tissue of 2mm thickness were placed in tissue cassettes. These were submitted to the MDACC Histology core where the samples were embedded in paraffin. 7μM

sections were subsequently placed on positively charged glass slides. The middle slide was H&E stained by the core for reference.

**Western Blot**

Cells are washed with PBS and lysed with either RIPA or NP-40 lysis buffer (dependent on specific experiment). The cells were removed with a cell scraper (Fisher Scientific) and put into 1.5ml Eppendorf tubes. These we set on ice for 10 minutes and then spun down for 15 minutes at 4°C at maximum RPM. The pellet was discarded and the supernatant kept. The resulting lysate was frozen and or BCA protein quantification was carried out. The lysate was made with lysis buffer up to the desired concentration. This was mixed with a loading buffer (either reducing or nonreducing) and boiled for 5 minutes at 100°C. The sample was then cooled on ice and spun down to remove droplets from the top of the tube. This was loaded onto a polyacrylamide gel for separation. Following this step the gel was transferred on a PVDF membrane. This membrane was washed in TBST 3 times, 5 minutes each. This was then blocked in 3% nonfat milk. The primary antibody was added in this milk and left to rock overnight at 4°C. This was removed and washed 3 times with TBST, 10 minutes each. The secondary antibody was added in 3% nonfat milk at room temperature for 1hr. This was washed 3 times with TBST, 10 minutes each. Following this the membrane was dried and chemiluminescent regents (GE Healthcare) were added for 1 minute. This was developed in a darkroom with chemiluminescent film (Fisher Scientific) for varying lengths of time.

**Immunoprecipitation**

Lysates were made with RIPA Buffer containing protease and phosphatase inhibitors. The cells were left on ice for 10 minutes and then spun down at maximum RPM at 4°C for 15 minutes. The supernatants were taken and then a BCA based protein quantitation method was used. These were pre-washed with the agarose conjugated secondary antibody of choice. This was tumbled at 4°C for 30 minutes. The supernatant was then removed and the primary antibody was added. This was tumbled overnight at 4°C. The secondary antibody was then added and tumbled for 2 hours at 4°C. This was spun down at 500RPM for 5min. The supernatant was removed, leaving just the agarose. This was then resuspended in 300µl of lysis buffer to wash and spun down at 500RPM. This was repeated two more time. Finally it was spun down so that only agarose remained. 15µl reducing buffer was added and the western blot process was carried out.

**In Situ Mixture Reaction Immunoprecipitation**

Pure proteins were added to a 1.5ml Eppendorf up to a final volume of 500µl. These are tumbled over night at 4°C.

| Peptides | Product Numbers | Peptide Amounts |
|---|---|---|
| Latent-TGFβ | 299-LT | 84ng |
| LAP | 246-LP | 55ng |
| αvβ8 | 4135-AV | 190ng |
| Cilengitide | BML-AM100 | 10µM |
| Control Peptide | BML-AM101 | 10µM |

The primary directed against β8 (Santa Cruz) is added and tumbled for 4 hours at 4°C. The agarose conjugated secondary is then added for 2 hours and tumbled at 4°C. This was then ran through the polyacrylamide gel separation and transfer procedure common to the immunoprecipitation protocol. This is then probed for LAP.

**Biotinylation of Cell Surface Proteins**

Wash cells 3x with 37°C PBS (semi confluent tumor cells grown on 10cm tissue cultures dishes). Add 6ml of Sulfo-NHS-Biotin (Thermo Scientific #21217) at 66ug/ml (in PBS) per dish for 20 minutes at 37°C. Wash 2x with PBS and 2x with TBS at room temperature. Lyse cells with 800µl NP-40 lysis buffer with protease and phosphatase inhibitors and cell scraper. Put on ice for 15 minutes and spin down for 15 minutes at maximum speed. Perform BCA and aliquot equal amounts

of protein into two tubes each. Pre-wash by adding 50µl washed anti-Rb-Agarose to each, bring volume to 600µl and tumble for 30 minutes at 4°C. Pull down agarose by spinning at 500RPM with microcentrifuge and transfer supernatants to new tubes. Add 2.5µg of β8-4627 and αV-cyto primaries per corresponding tubes and tumble overnight at 4°C. Add 25µl anti-Rb-agarose and tumble 30 minutes at 4°C. Spin down at 500RPM, remove supernatant, add 200µl lysis buffer, gently mix, spin, remove supernatant, and repeat this wash cycle two more times. Remove final supernatant, add 15µl of nonreducing sample buffer, boil for 5 minutes, run samples on 7.5% agarose gel. Transfer onto Immobilon-P membrane. Wash 3x with TBST, block in 3% BSA (in TBST) for 30 minutes at room temperature , wash 3x with TBST. Wash with streptavidin AB for 30 minutes at room temperature, wash 3x with TBST, then add chemiluminescence for development.

**GTPase Activation Assay**

GTP-bound Cdc42 and Rac1 were fractionated using GST-tagged p21 binding domain (PBD) of Pak1 as previously described. Rhotekin-conjugated to Agarose (Cytoskeleton, Inc.) was used for fractionating GTP-bound RhoA. Cells were harvested in $Mg^{2+}$ lysis buffer containing 25 mM HEPES, pH 7.5, 150 mM NaCl, 1% Nonidet P-40, and 10 mM MgCl2, supplemented with 1 mM DTT, 1 mM Na3VO4, 10 mM NaF, 10 mM β-glycerol phosphate, and EDTA free protease inhibitors (Roche). The lysates were incubated with PBD or Rhotekin beads for 20 min at 4°C. Following precipitation, the pellets were washed 3x with in Mg2+ lysis

buffer and then analyzed by Western blotting to determine levels of active Rac1,Cdc42 or Rho.

**Isolation of Primary Mouse Astrocytes**

P0-P2 neonates were taken from sacrificed WT, αvKO, and β8 KO litters. Incisions were made in ear canals down to the nose, and then upwards down the midline of the skull from anterior to posterior. The cranium was carefully opened with forceps and microscissors (Roboz Surgical Instrument Co. Inc.) and the brain removed and placed in a dish of sterile PBS on ice. The olfactory bulbs and hindbrain were removed as well as the thin meningeal layer surrounding the remaining cortex. The cortex was then split into its two hemispheres and opened so that the hippocampus could be removed. The remaining tissue is minced with sterile razors in a separate dish with new PBS. This tissue is again verified to not have meningeal tissue as it may lead to unnecessary heterogeneity of the cell culture. The PBS and tissue was placed into a sterile tissue culture grade 15ml conical and centrifuged at 1000RPM for five minutes. The PBS was removed and replaced with 5ml of a collagenase (Worthington) and DNase I (Sigma) in DMEM (Sigma) solution at 150units/ml and 40µg/ml, respectively. This was resuspended and pipetted up and down several times for mixture. This was placed on a rocker for 30 minutes at 37°C. The tubes were centrifuged and the media aspirated. 5ml of low glucose DMEM (Sigma) with 10% calf serum (Thermo Scientific) and 1% Pen-Strep (Sigma) was used to resuspend the pellet and titrate it 20 times. This homogenized tissue was then ran through a 70µm nylon sieve. An additional 15ml

of media was ran over the cell strainer to push remaining bits through into a 50ml sterile conical. This cell homogenate was then placed into canted neck 75cm$^2$ tissue culture flasks that were coated with 10µg/ml murine laminin (Sigma). These cells are grown at standard tissue culture condition in an incubator at 37°C 5%CO2. After a week or full confluence the cells are shaken over night at 37°C and 250RPM. This was to prevent contaminating microglia and fibroblasts, which sometimes loosely grow on the surface of monolayers of astrocytes. Other than cell type contamination, microglia presence is unfavorable because they release toxic cytokines. These are then placed back in standard culture incubating conditions for recovery.

**Culturing Human GBM and Assorted Cell Lines**

GBM cell lines U87, LN18, SNB19, LN229, LN428, LNZ208, and U373 were acquired from ATCC. With U251 being kindly provided by Professor Oliver Bögler in the Department of Neurosurgery at M. D. Anderson. These cells were grown in 10% fetal bovine serum (Thermo Scientific) and 5% Pen-Strep (Sigma) in DMEM/F12 50/50 (Cellgro) as recommended by ATCC. These medias were also supplemented with construct specific antibiotics, as necessary. Norma human astrocytes (NHA) were acquired from Lonza and grown in Lonza provided media and supplements. Transformed human astrocytes (THA) were donated by Dr. Russell Pieper and were derived from NHAs as previously described. 293T cells were acquired from ATCC and grown in DMEM-High Glucose media (Sigma)

supplemented with 10% fetal bovine serum (Thermal Scientific) and 1% Pen-Strep (Sigma). This same media was also used for Mink lung epithelial cells (MLEC).

Note: The previous protocol includes specific numbers, antibodies, and reagents that can be exchanged depending on specific experiment requirements.
Prepare Anti-Rabbit IgG-Agarose by taking 1300µl, spinning down at low RPM, and removing the supernatant. Add 600µl NP-40 lysis buffer with protease inhibitor (complete mini EDTA free) and phosphatase inhibitor(PhosSTOP), mix, spin down, remove supernatant, and repeat two more times. Then add 600µl lysis buffer. This mixture should always be resuspended before use, resulting in an approximate 1:1 ratio of agarose:buffer.

**Transformation and Plasmid Preparation**

Thaw tubes of NEB-5α cells, Puc-19 DNA, and constructs on ice. Transfer the 50µl of cells into a pre-chilled round bottom tube and add 1µl of DNA. Flick to mix and incubate on ice for 30 minutes. Heat shock in a water bath at 42°C for 30 seconds and place back on ice for 5 minutes. Add 950µl SOC medium to each tube and shake for 1 hour at 37°C. Transfer these cells onto a plate with appropriate antibiotics, smear, and let grow at 37°C over night. Remove one colony and place into 5ml of 1X LB with appropriate antibiotics. Shake at 37°C for 8 hours. Transfer this into 50ml of 1X LB with antibiotics and shake at 37°C overnight. Spin down for a pellet of bacteria that can be lysed and used for a Qiagen Midi Prep.

**Virus Synthesis**

Retroviral and Lentiviral vector DNA was transfected into ecotropic Phoenix cells rendering the viral product capable of delivering genes into dividing murine cells. The following day the media was replaced with fresh, vectorless and reagentless media. This media was incubated on the cells for 2 days.

Cells of interested were washed with PBS once. The virus containing media was then incubated with polybrene at a final concentration of 6µg/ml for 10 minutes at 37°C. This was then added to the cells of interest and let incubate at 37°C until the cells became semi-confluent. The cells were then selected for and/or analyzed for appropriate proteins expression levels.

**Transfections**

In a 60mm tissue culture dish 1µg DNA, 8µl Enhancer reagent (Qiagen), and 8µl EC Buffer (Qiagen) is added to a total volume of 150µl. This is mixed by pipetting 10 times and incubated at room temperature for 5 minutes. 25µl Effectene reagent (Qiagen)is added, mixed by pipetting, and incubated at room temperature for 8 minutes. During this incubation time the cells are washed once with PBS and 2ml media added. After incubation, the mixture is filled to a total of 1.5ml with media, mixed, and added to the cells. Construct specific selection agents are then used for selection.

**shRNA Development**

cDNA sequences to three different regions of human origin αv and β8 subunits were chosen and verified to have minimal homology. These were submitted externally (Integrated DNA Technologies) for synthesis of DNA oligonucleotides. Each oligonucleotides was annealed into the pLB system with XhoI and HpaI restriction sites. DH5α competent E. coli were transformed with the lentiviral vectors and grown on amp resistant LB plates. Colonies were isolated and a Midi prep (Qiagen) was performed and the DNA was purified. The sequence was verified (Lone Star Labs). This was then transfected into 293-FT cells as previously described to generate lentivirus. This was subsequently added to LN229, SNB19, and THA cells. Knock down was examined by western blot, the best shRNAs were determined, and the cells were FACS sorted for further knockdown power. The final selection was αvshRNA-#4 and β8shRNA-#6.

**siRNA Mediated Knockdown**

Cells are plated at less than 50% confluency on 60mm tissue culture dishes. 30µl of 20 µM siRNA is added to 30µl of antibiotic and serum free media. Mix by pipetting. In parallel, 3µl Dharmafect Reagent #2 is added to 147µl of antibiotic and serum free media and mixed by pipetting. These two reactions are incubated for 5 minutes at room temperature and then combined and incubated for 20 minutes at room temperature. Cells are washed with PBS, and 4ml of serum containing media is added. The contents of the reaction tube are added and the cell incubated at

37°C for 24 hours. The media is then replaced with fresh media and a lysate is made 2 days later. This amounts to 3 days after the initial addition of siRNA.

**Fluorescence-Activated Cell Sorting**

FACS was carried out at the M. D. Anderson FACS facility on BD FACSAria II flow-cytometry cell sorters and assisted by Laboratory Manager with over 20 years of FACS experience. Cells trypsinized, placed in PBS and sorted into chilled serum containing media. Cells were gated to cell size, and fluorescence intensity as specified per experiment.

**Dish Coating Substrates**

Substrates were used in tissue culture at the following concentrations.

Fibronectin Sigma F2006

A 24-well dish has 1.9cm$^2$ of surface area. It is recommended to be used at 2-5µg/cm$^2$, so I used it at 2µg/cm$^2$. This came out to 38µl of stock fibronectin plus 462µl PBS per well. Stock was made to 100µg/ml.

Laminin L2020

This was used consistently at a 1:300 dilution in PBS. This comes out to 101ng/cm$^2$.

Vitronectin V8379

This was recommended to be used at .1µg/cm$^2$ which equates to 38µl stock into 462µl PBS per well. The stock concentration was 5µg/ml

PDL P6407 70,000-150,000 mol wt (though the [30,000-70,000 mol wt P7280 is also possible for use) With a larger weight the P6407 has a higher binding site density.

This was made into a stock at 25µg/ml. When using 500µl in a 24 well plate this works out to 0.526µg/cm$^2$.

**Adhesion Assay**

A 24-well plate was coated as dictated in the chart below for 2 hours at 37°C. The wells were washed three times with PBS and blocked with 300µl of 3% BSA for 30 minutes. The wells were then washed three times with PBS and the cells were left to adhere for 48 hours.

**Table 2.**

| | Added per Well | PBS per Well | [Stock] | µg/cm$^2$ |
|---|---|---|---|---|
| Laminin | 1.667µl | 498.33µl | 1mg/ml | .0033 |
| Vitronectin | 38µl | 462µl | 5µg/ml | .1 |
| Fibronectin | 38µl | 462µl | 100µg/ml | 2 |
| LAP | 300µl | 200µl | 5µg/ml | .7895 |
| PDL | 500µl | 0µl | 25µg/ml | .526 |

| | | | | |
|---|---|---|---|---|
| PBS | - | 500µl | - | - |

**Table 2. Substrate Dilutions**

**Dilutions for various experiments that required the above substrates**

**Proliferation Assay**

For this assay, 25,000 cells were trypsinized, counted, and evenly distributed into wells of a 24-well plate. Each time point consisted of 6 wells per time point. Each well was trypsinized and counted by hand under a microscope with a hemocytometer. Time points were taken at 24 hour intervals.

**Scratch Assay**

Cover glass with a 12mm diameter (Fisher) was placed in wells of 24-well plates. Cover slips were coated with Laminin (Sigma) at 1:300 in PBS for 2hrs at 37°C. They were then washed with PBS and cells added in normal growing medium. The cells were allowed to grow until confluent and were scratched linearly with a p10 pipette tip. These were washed 1x with PBS to remove free-floating and weakly attached cells at the scratch margin and replaced with growth media. The cells were fixed by washing once with PBS, adding 4%PFA for 10 minutes, washing once with PBS, adding .05%NP40 Buffer, washed once with PBS, and kept in 10% goat, donkey, horse, or swine serum.

**Invasion Assay**

BD BioCoat™ Matrigel™ Invasion Chambers were used with 6.4mm chamber size, .3cm$^2$ membrane surface area and of 8μM pore size. Inserts were rehydrated with 1% serum containing media (cell-line specific) and place at 37°C for two hours prior to the start of the assay. Cells were trypsinized and resuspended in 1% serum containing media (cell-line specific). Cells were counted by hemocytometer and added at 50,000 cells per well into the top chamber with a total volume of the top chamber being .500ml. .750ml of 10% serum containing media (cell-line specific) was added to the bottom chamber as the chemoattractant. This was placed back at 37°C for 24 hours and invasion allowed to occur. The following day the chambers were removed and the inside of the upper chamber was swabbed with cotton swabs to remove adherent but non invasive cells. The upper chamber was then washed once with PBS. The insert were then fixed in 2.5% grade II glutaraldehyde (Sigma) for 15 minutes. This was removed and then incubated with 0.5% Triton X-100 (Fisher) to permeabilize the cells for 3 minutes. They are then submerged in filtered Gill's formula hematoxylin (Vector Laboratories) for 30 minutes. This is then washed with dd$H_2O$. Membranes were out with a scalpel and placed cell-containing-side down on a drop of water on a glass slide. The entire membrane was imaged at magnification (cell size dependent) to take overlapping pictures. Images were then printed, and a macro sized membrane was constructed. All the cells were counted. "Invasion Index" was calculated as giving a percentage of invasion relative to the control cell line. The number of cells for the control cell line was used as the denominator for both that cell type and for the experiment cell

types. This appears as Control Invasion Index = (Control #)/(Control #) ; Experimental Invasion Index = (Experimental #)/(Control#). In this way the Control is always 1 (or 100%) while the experimental cell type can easily be viewed as a percentage relative to the control.

**Live Cell Imaging, Quantitation, and Track**

Imaging was carried out with an Olympus IX81 inverted microscope. This was manufacturer modified with a Retiga camera capable of capturing bight and fluorescent wavelengths (QImaging). Addition modifications included a motorized stage (ASIimaging), manual analog-stick apparatus (Applied Scientific Instrumentation) and a built-to-order live cell environmental chamber (PrecisionControl) with a temperature and $CO_2$ controller (PrecisionControl). This was attached to an external CO2 tank (Matheson Tri-Gas) and regulator (Fisher Scientific). The software used was SlideBook 4.2 (Intelligent Imaging Innovations). Prior to start of the assay the microscope is warmed to 37°C with 5% $CO_2$ and the humidifier is activated over night. Cells were plated to confluence on coated 24-well glass tissue plates (Greiner Bio-One) and scratched with a p10 pipette tip vertically. This was washed with PBS to remove floating cells and fresh media was added. Images were taken at 100x every 30 minutes over a 48 hour period. Movies were then compiled from these snap shots in SlideBook. Fluorescent images were taken with exposure of one wavelength at a time and overlaid with the software during the

compiling process. This was to generate the clearest images as well as to prevent fluorophore cross excitations.

**Luciferase Assay**

Previously described mink lung epithelial cells (MLEC) were transfected with a stable PAI1-Luciferase construct. These cells were plated on poly-lysine (Sigma) coated dishes. The tumor cells (cells of interest) were grown until 80% confluent. These are washed with PBS to remove serum and add serum-free media over night. The MLECs were also washed with PBS and replaced with serum-free media. The following day the media from the tumor cells is added to the MLECs for 4 hours. Control medias were also used with exogenous TGFβ. These cells were washed with PBS and lysed with proprietary buffers (BD Biosciences). Luciferase reporter reagent and instructions were used for subsequent steps.

**Stereotactic Injection of Modified and Non-Modified GBM Cell Lines**

"Nude" male NCR $^{nu/nu}$ mice (Jackson Laboratories) were used for all in-vivo tumor model work. These mice were anesthetized with Avertin at the recommended 0.25mg/g. After intraperitoneal injection the mice were continuously checked for paw sensitivity and other symptoms of general anesthetic induced unconsciousness. The mouse was then placed in a stereotactical surgical frame with a fixed needle to stabilize the mouse and to allow for geographically consistent injections (Image 1A and 1B). The surgical area was sterilized and with a sterile

surgical scalpel (BD Biosciences) an anterior to posterior incision was made to expose the cranium (Image 1B). Once open, coordinates 1.5mm rostral and 1.5mm anterior of the bregma were set and recorded on the skull. This spot was drilled with a small bit dental drill. Once open the needle was placed 3mm below the pail surface and a 3µl solution of cells was injected containing 100,000 cells over a 3 minutes period using an automated micropump (Stoelting Instruments). The hole was filled with bone wax and the skull was closed with surgical stables. In these experiments the cells were sorted for GFP, counted, and directly injected for the best knockdown. Animals were kept in MDACC animal facility and watched daily for neurological phenotypes, physical weight loss, and other abnormalities.

Tumor-bearing and control mice were sacrificed within 24 hours of each other. These mice were anesthetized with .5-1mg/g of Avertin. Their chests were entered through the diaphragm and opened. A needle was inserted in the lower left ventricle of the heart. This needle was attached through surgical tubing to an open syringe containing 4% PFA. As the heart began to swell the right auricle was snipped. This allowed an exit point for blood and PFA as the mouse was cardiac perfused. The brains were then carefully removed and set into a brain shaped cassette where they were coronally sliced in 2mm sections, accounting to tissue shrinkage that occurs with PFA exposure. The tissue was then submitted to MDACC Histology Core for serial 7µM sections that were placed on glass slides for later staining and examination.

## VEGF ELISA

For this assay 500, 000 cells placed in 6-well plates. The serum containing media was washed with PBS to remove residual VEGF and replaced with serum-free media over night. This media was harvested and filtered through a .45μM filter to remove cell debris. This, along with control medias (serum containing, serum free, and serum free with VEGF) were used with the VEGF kit (R&D Systems).

## Statistical Analysis

Invasion assays were normalized to the control by dividing the experiment and control samples by the average of the controls. This gave the control a value of 1 and the experimental a value relative, in percentage, to the control for best perspective. Statistical significance was determined by the student's t-test.

## Antibody Usage Guidelines

**Table 3.**

| Name | Company Product Number | Dilution | Mol Wt | Applications | |
|---|---|---|---|---|---|
| Nestin | Neuromics CH23001 | 1:100 | - | IF | Chicken |
| Smad3 | Epitomics 1880-1 | | 60 | WB | |
| Actin | | 1:5000 | 37 | WB | |
| PKCzeta | Cell Signaling 9372 | | 78 | WB | |
| Desmin | 40245 | | 53 | WB | |
| GFAP pAb | | 1:200 | - | IF | Rabbit |

| | | | | | |
|---|---|---|---|---|---|
| GFAP mAb | | 1:250 | - | IF | Mouse |
| S100 | Abcam | 1:100 | - | IF | Mouse |
| NeuroFilamen | | 1:250 | - | IF | Mouse |
| pERK | Cell Signaling 9106s | 1:1000 | 42, 44 | WB | |
| pAKT | Cell Signaling 9271s | 1:1000 | 60 | WB | Rabbit |
| Total AKT | Cell Signaling 9272 | 1:1000 | 60 | WB | |
| αv-cyto | Custom | 1:3000 | 150 NonRed | WB/IP | Rabbit |
| B8-4627 | Custom | 1:3000 | 100 | WB/IP | Rabbit |
| IgG | Santa Cruz-2027 | | - | IF/IP | Rabbit |
| GDI-1 | | | 28 | WB/IP | |
| GDI-2 | | | 28 | WB | |
| Rac1 | Millipore | 1:500 | 21 | WB | |
| GFP | AB290 | 1:3000 | 25 | WB/IP | |
| GFP | | 1:3000 | 25 | WB/IP | |
| Myc | Santa Cruz 789 | | as tagged | WB | |
| αv | BD Biosciences | | 125 | WB/IP | Mouse |
| pSrc | Cell Signaling 2101s | 1:1000 | 60 | WB | Rabbit |
| pSmad2 | Cell Signaling 3101s | 1:1000 | 60 | WB | Rabbit |

| | | | | | |
|---|---|---|---|---|---|
| pSmad2 | Cell Signaling 3104s | 1:1000 | | WB | Rabbit |
| pSmad1 | Cell Signaling 9511s | 1:1000 | 60 | WB | Rabbit |
| Hif1α | | 1:1000 | 125 | WB | |
| FAK | Cell Signaling 3284s | 1:1000 | | | Rabbit |
| P2Y2 | | 1:600 | | | Rabbit |
| p-β Catenin | Cell Signaling 9561s | 1:1000 | | | Rabbit |
| pFAK | FM1211 | 1:1000 | | WB | Mouse |
| B1 | Millipore MAB1997 | 1:1000 | | WB/IP | Rat |
| B3 | AB1932 | 1:1000 | | WB/IP | Rabbit |
| B5 | Ab1926 | 1:1000 | | WB/IP | Rabbit |
| B6 | Santa Cruz 15329 | 1:1000 | | WB/IP | Rabbit |
| Smad 2/3 | 3102 | 1:200 | | | Rabbit |
| PTEN | MAB4037 | 1:50 | | | Mouse |
| N-Cadherin | SC-1502 | 1:200 | | | Goat |

**Table 3. Antibody Information**

**A catalog of various antibodies used throughout this work.**

## Chapter 3:

## αvβ8 Extracelluar Signaling: Determining Functional Roles for αvβ8 Integrin in Glioma TGFβ-Induced Invasiveness.

### Introduction

Glioblastoma multiforme (GBM) is the most common type of primary malignant brain tumor. While their overall rate of occurrence is low, at around 25,000 new cases per year in the United States, they cause a very high mortality rate(138). One of the distinguishing hallmarks of GBMs is their invasiveness. While a primary mass can be surgically resected, individual tumor cells that have invaded into the surrounding healthy tissue cannot be which can lead to satellite tumors. This makes the invasive phenotype an important property to understand.

Previously, our laboratory has shown that αvβ8 plays a key role in development of the vascular network of the mouse brain. More recently this work has been extended to show a role in GBM angiogenesis. The pathway investigated in the process of deciphering angiogenic phenotypes was an extracellular signaling pathway that involved the activation of LAP-TGFβs by αvβ8. Here we begin to explore how this extracellular activation of TGFβ plays a role in GBM invasiveness, and investigate it in the context of autocrine and paracrine GBM cell - GBM cell signaling. Previously differences in cell polarity, morphology, and invasiveness were seen with manipulation of β8 levels but these phenotypes were left largely unexplored.

Here we hypothesize that abnormal αvβ8 expression contributes to the characteristic invasive phenotype of GBMs through TGFβ signaling. Herein, molecular biology and cell culture techniques were used to manipulate β8 expression and distinguish potential new roles for αvβ8 in in-vitro invasive phenotypes.

**Primary Astrocyte Isolation**

Though previously conducted, this exercise was repeated for verifying previous results and accountability for those thereafter. P0-P2 pups were taken from wild type (+/+), αv knockout (αv-/-), and β8 knockout (β8-/-) litters. Pups were segregated based on obvious intracerebral hemorrhaging and placed into likely categories of knockout and wild-type (WT). Genomic tail DNA was then used for PCR to verify individual mice as their astrocytes were being cultured in-vitro. The cells were placed on dishes coated with the basement membrane Laminin, which is known to support primary astrocyte growth (139). Additionally, the McCarty lab generated β8 antibody was used to verify knockout of this integrin in $\beta8^{-/-}$ astrocytes for future use (Figure 1).

**Figure 1.**

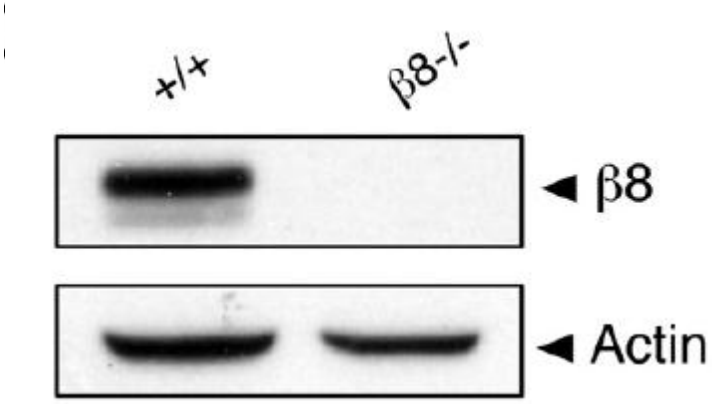


**Figure 1. 1° Astrocyte Western**
**β8 knockout and Wild-Type mouse astrocytes were blotted with an generated antibody against the cytoplasmic portion of β8 and with Actin.**

Wild-type, αv knockout, and β8 knockout primary astrocytes were then transduced to forcibly express E6 and E7 proteins of the human papilloma virus (HPV). The E6 oncogene inhibits the p53 tumor suppressor by stimulating its ubiquination and proteosome degradation while the E7 inhibits Rb by preventing its interaction with transcription factor E2F. This leads to a perpetually activated cell cycle. This process generated immortalized cell lines that are biologically relevant since p53 and Rb loss of function has been seen in human glioblastoma multiforme. Using the same delivery system, human oncogenic Ras (HRasV12) was also transduced into the cells.

The transformed human astrocytes (THAs) underwent a similar process except utilizing amphotropic Phoenix cells that are capable of delivering genes into human cells. Additionally human telomerase reverse transcriptase (hTERT) was used to prevent telomere shortening to lead to immortalization.

Additionally, it is critical to identify integrin expression at the cell surface as that is required for extracellular TGFβ activation and TGFβ mediated pathways. This was accomplished with the use of amine-reactive biotin to label all of the extracellular amine sites of the proteins. Since no expression of αv or β8 was seen in the knockout cells, biotinylation was carried out on WT cells. All of the cell surface proteins were biotinylated and those associated with αv were pulled down and blotted with reagents reactive to biotin(Figure 2). This revealed the presence of both αv and β8 proteins in the primary, immortalized, and transformed cells (Figure 2). Additionally, it revealed that as the transformation process takes place

there is less extracellular αv and β8 expression. This was also seen in the expression levels of these proteins by western blot (Figure 2).

**Figure 2.**

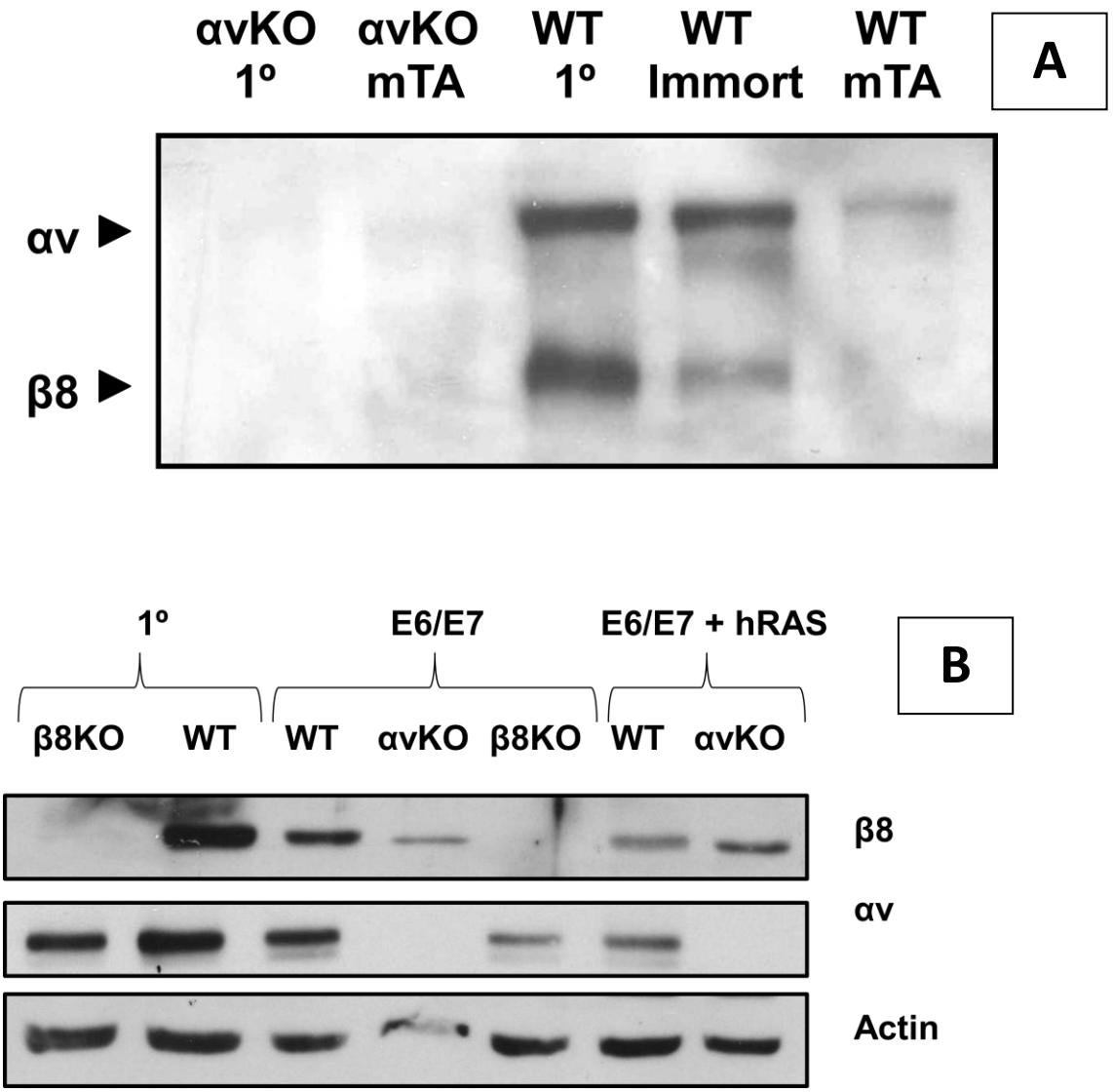


**Figure 2. Mouse Astrocytes Lose Integrin with Transformation**

**(A) Primary (1°), immortalized (I), and transformed (mTA) mouse astrocytes were biotinylated. An anti-αv antibody was used to pull down all associated proteins and blotted with a biotin reactive agent. This revealed two bands being associated with αv and β8. Note the lack of αv and β8 expressed on the surface of primary and transformed αvKO cells. (B) Primary (1°), immortalized (E6/E7), and transformed (E6/E7 + hRAS) mouse astrocytes were analyzed by western blot. Wild-type cells show that as they are immortalized and then transformed expression levels of β8 and αv decrease. β8 knockout and αv knockout cells lines were also used as controls to verify antibody specificity.**

Additionally, the transformed cells were checked for surface expression of various integrins where it was seen that α5, α6, and β1 surface expression was present in all cells and that this expression did not change with immortalization (Figure 3). Additionally, this experiment verified that β8 does not pair with these alpha subunits as they would also have been biotinylated. This also revealed that β1 does not pair with α6 or α5 in transformed mouse astrocytes as was previously thought.

**Figure 3.**

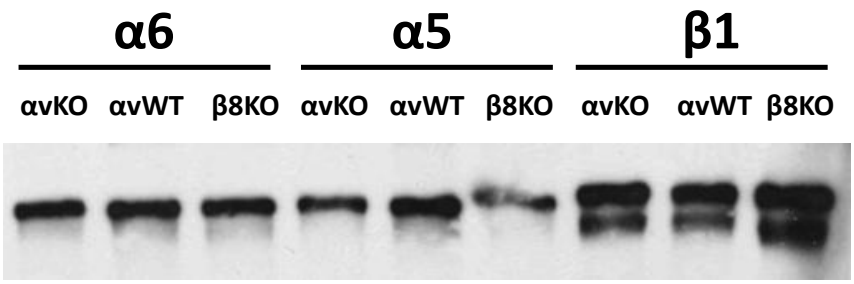


**Figure 3. α6, α5, and β1 Biotinylation**

**Transformed mouse astrocytes were biotinylated and pulled down with α6, α5, and β1 antibodies, revealing proteins paired with them. β8 did not pair with these proteins. Note, during pull down of β1 the lower band is β1 and the upper band is an α subunit.**

**Human GBM Cell-Line Characterization**

Human GBM cell-lines were then characterized for expression of αv and β8 integrins. Figure 4 demonstrates the expression levels of the integrin in various cells lines. Here it is seen that while αv remains relatively unchanged in human GBMs the level of β8 varies. It is also interesting that transformation of human astrocytes decreases the expression of both integrins, just as was seen in transformed mouse astrocytes. Due to their low expression of β8, U87 was selected for further studies. As we believe high levels of β8 integrin positively influence the invasiveness in GBMs, SNB19 and LN229 cells were chosen for their robust levels of the integrin as well as their ubiquity in the literature.

**Figure 4.**

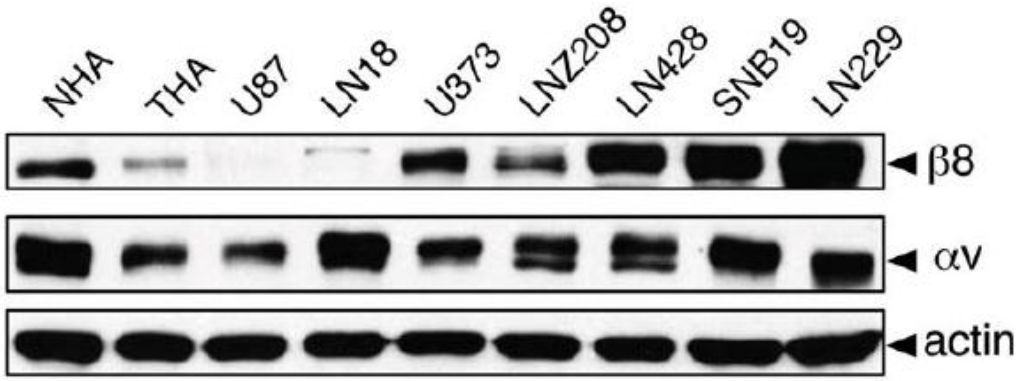


**Figure 4. GBM Cell Lines Express Varying Levels of Integrin β8**

**Detergent-soluble lysates were made from seven different GBMs of human origin as well as transformed human astrocytes (THA) and the normal human astrocytes (NHA) they were derived from. Note that GBM cell lines express varying levels of integrin β8 and near constant levels of integrin αv.**

Following this it was critical to determine if that these integrins were also expressed on the cell surface. Membrane-impermeable amine-reactive biotin was added and proteins αv and β8 were pulled down. It was seen that not only were the integrins expressed on the cell surface, but that this expression also correlated with the levels seen in whole cell lysates (Figure 4-2). i.e. High expression of total and surface β8 in LN229 and low expression of total and surface β8 in U87 cells were correlated.

**Figure 4-2.**

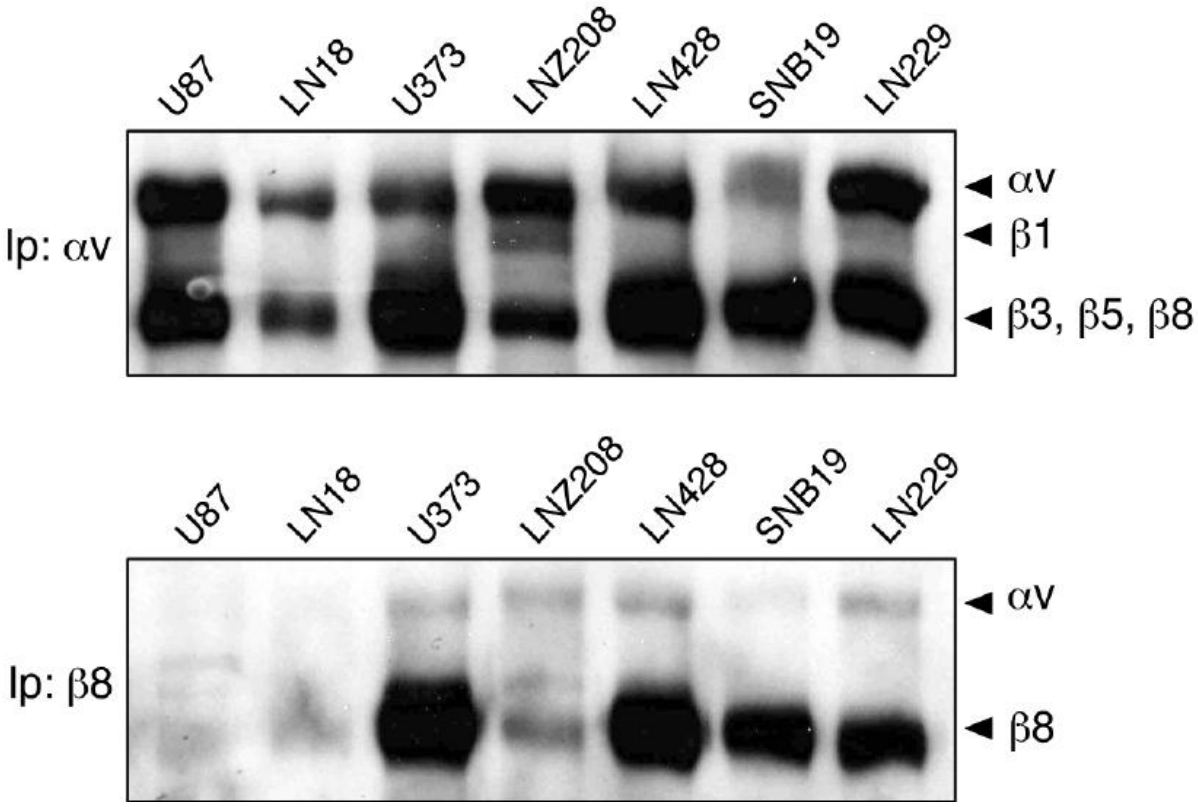


**Figure 4-2. Integrin Subunits αv and β8 Pair in GBM Cell Lines**

**Membrane-impermeable amine-reactive biotin was used to label extracellular proteins. Antibodies targeting the cytoplasmic domains of αv and β8 integrins were used to immunoprecipitate the respective complexes. These were then reduced to disrupt subunit interactions and subsequently probed.**

**Overexpression of β8 in GBM U87 cells Correlates with VEGF Expression**

A previous study by our lab has suggested that levels of the integrin β8 may be involved in angiogenesis. Therefore we decided to further investigate this here; anticipating changes in VEGF levels with β8 integrin manipulation. U87 cells were transfected with a pcDNA4.0 plasmid harboring the full-length human β8 cDNA which overexpressed β8 in U87 cells (Figure 5). While it was seen that β8 was over expressed, αv was not. Morphologically these cells also appeared longer in comparison to untransfected and mock transfected U87 cells. Additionally, β8 expression correlated with high amounts of VEGF secretion, as measure by hVEGF ELISA. However, this correlation did not extend to the varying levels of β8 in LN229 cells with high and knocked down β8 (Figure 5). This may be due to a specific genetic difference between the two cell lines. Interestingly, THAs with the integrin β8 knocked down using shRNA showed a decrease in VEGF when compared to the control non-targeting shRNA cells (NT-pLB), as determined by ELISA. This fits with the previously mentioned results in U87 cells.

**Figure 5.**

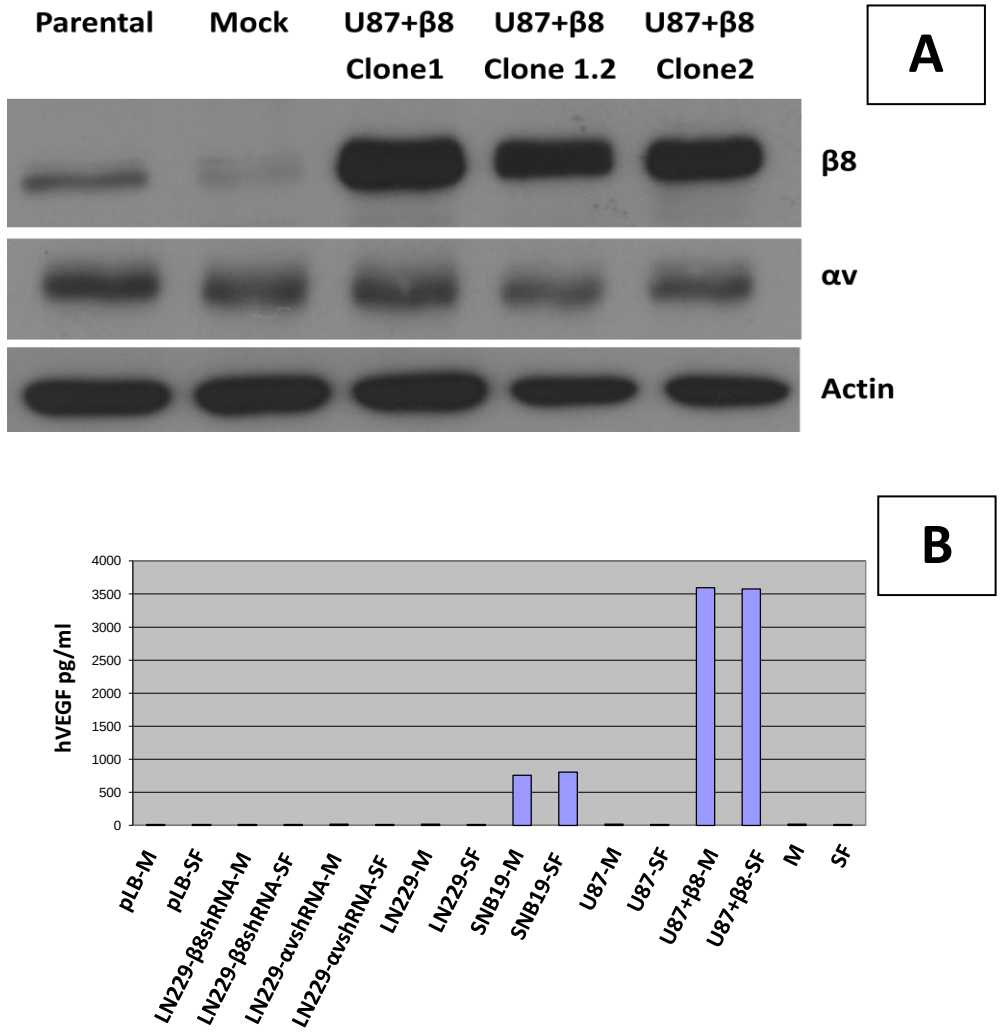
Parental
Mock
U87+β8 Clone1
U87+β8 Clone 1.2
U87+β8 Clone2
A
β8
αv
Actin
B
hVEGF pg/ml
4000
3500
3000
2500
2000
1500
1000
500
0
pLB-M
pLB-SF
LN229-β8shRNA-M
LN229-β8shRNA-SF
LN229-αvshRNA-M
LN229-αvshRNA-SF
LN229-M
LN229-SF
SNB19-M
SNB19-SF
U87-M
U87-SF
U87+β8-M
U87+β8-SF
M
SF

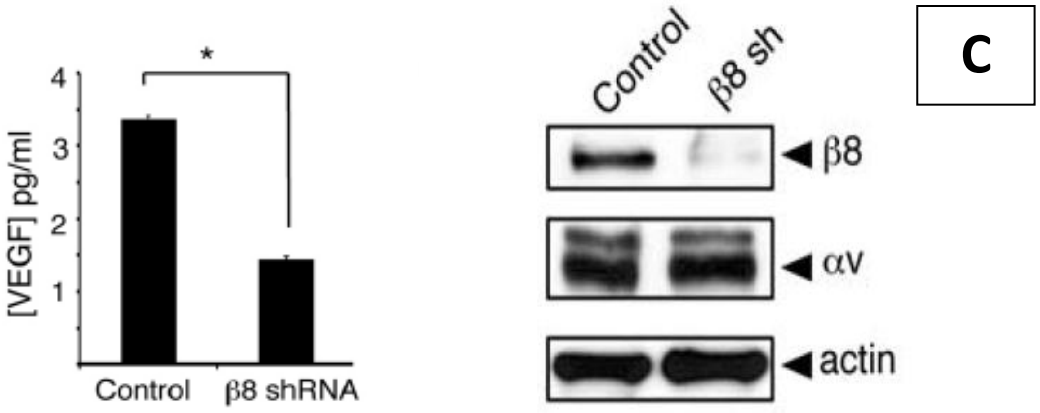


**Figure 5. U87 Cells Secrete VEGF with β8 Overexpression**

**(A) Parental, mock transfected, and three clones of U87 cells overexpressing the integrin β8 were blotted for the protein. While the integrin increased, the levels of αv did not change. (B) Various cell lines, including U87 and U87+β8 were checked for VEGF levels with an ELISA. Please note the relatively low levels of VEGF in U87 cells with low β8 expression and high VEGF levels in U87 overexpressing β8. (C) THA cells were transfected with control and β8shRNA. Please note the decreased expression of the integrin did not change the levels of αv protein. Decreased β8 integrin levels resulted in decreased VEGF secretion.**

**Manipulation of β8 Integrin Levels in LN229 and SNB19 Human GBM Cells**

LN229 human GBM cells were transfected with lentivirus to express an empty non targeting (NT) pLB construct and a pLB-β8shRNA construct that were previously described. This system allowed for the co-expression of GFP and an shRNA. Due to this, the cells with higher GFP expression often result in better knock down. This also allowed for the use of FACS to select the desired level of knock down. After addition of the shRNAs there was no obvious phenotypic difference between the cells. It is interesting though that after passaging the pLB-αvshRNA cells could not adhere to plastic tissue culture dishes or culture dishes coated with Laminin. This resulted in total cell death. By definition, loss of αv means the loss of αv containing integrins, so it is likely that one or a combination of these integrins are required for cell adhesion and or survival(19,134,140). This situation was also the case for SNB19 cells with pLB-αvshRNA (data not shown). For this reason pLB-αvshRNA LN229 and SNB19 cells were not pursued for further *in vitro* work. However, it remains to be seen whether αv integrin is required for *in vivo* cell survival.

LN229 NT and LN229 pLB-β8shRNA #6 cells were sorted for the top 10% of GFP positive cells. This resulted in the additional knockdown that is seen in Figure 6B. Additionally the knockdown was seen to decline from cells passaged twice, to five time, to seven times (data not shown). Because of this, cells used thereafter were of low passage. Due to the cell death that occurred along with αv knockdown, it was imperative to check the growth patterns of the LN229 β8shRNA cells. A

proliferation assay was conducted and it was seen that growth differences were not seen as cells grew to confluence in-vitro, which was up to 72 hours (Figure 6C).

Utilizing these same shRNAs, β8 integrin was also knocked down in SNB19 and THA cells. After sorting for the top 10% of GFP positive cells the knockdown was measured (Figure 7). Additionally, it was seen that there are no differences in proliferation between the two shRNAs when placed into SNB-19 cells (Figure 7).

**Figure 6.**

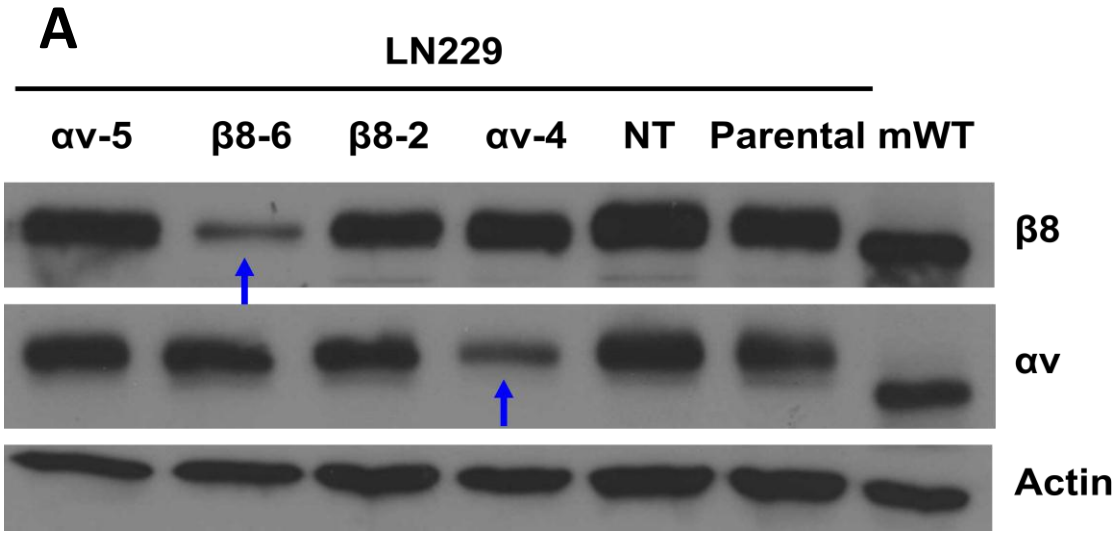
A
LN229
αv-5
β8-6
β8-2
αv-4
NT
Parental
mWT
β8
αv
Actin

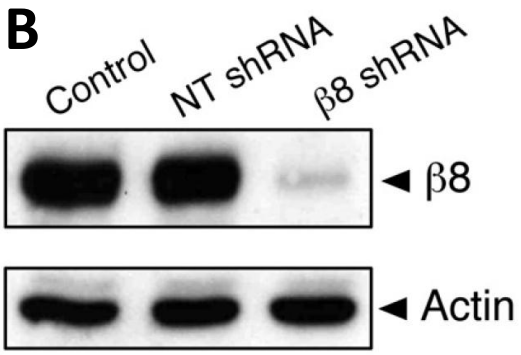
B
Control
NT shRNA
β8 shRNA
β8
Actin

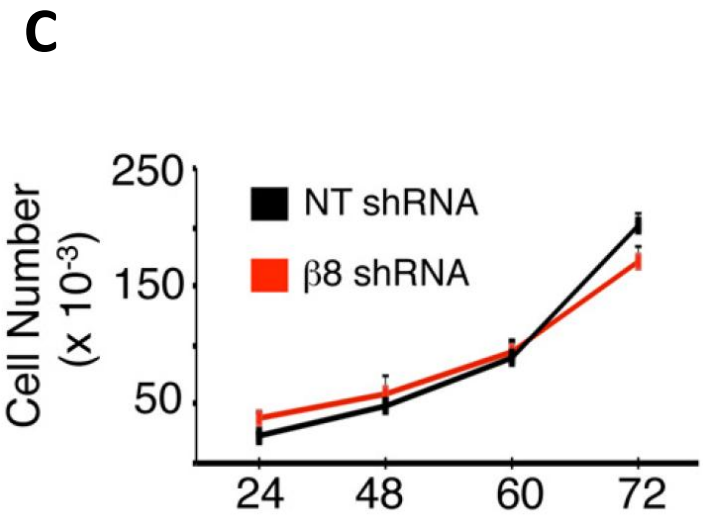
C
Cell Number (x 10-3)
250
150
50
NT shRNA
β8 shRNA
24
48
60
72

**Figure 6. shRNA Mediated Knockdown of β8 in LN229 Cells Does Not Influence In-Vitro Growth**

**(A) Human GBM LN229 cells were transduced with two constructs directed against αv and two directed against β8. Note the low levels of integrin expression for #6 and #4 relative to parental cells. mWT are WT whole mouse cortex lysates. (B) β8shRNAs #6 was then taken and sorted for the top 10% of GFP positive cells. This resulted in the additional knockdown seen. (C) This proliferation assay revealed there is no difference in in-vitro growth when the integrin is knocked down with shRNA.**

**Figure 7.**

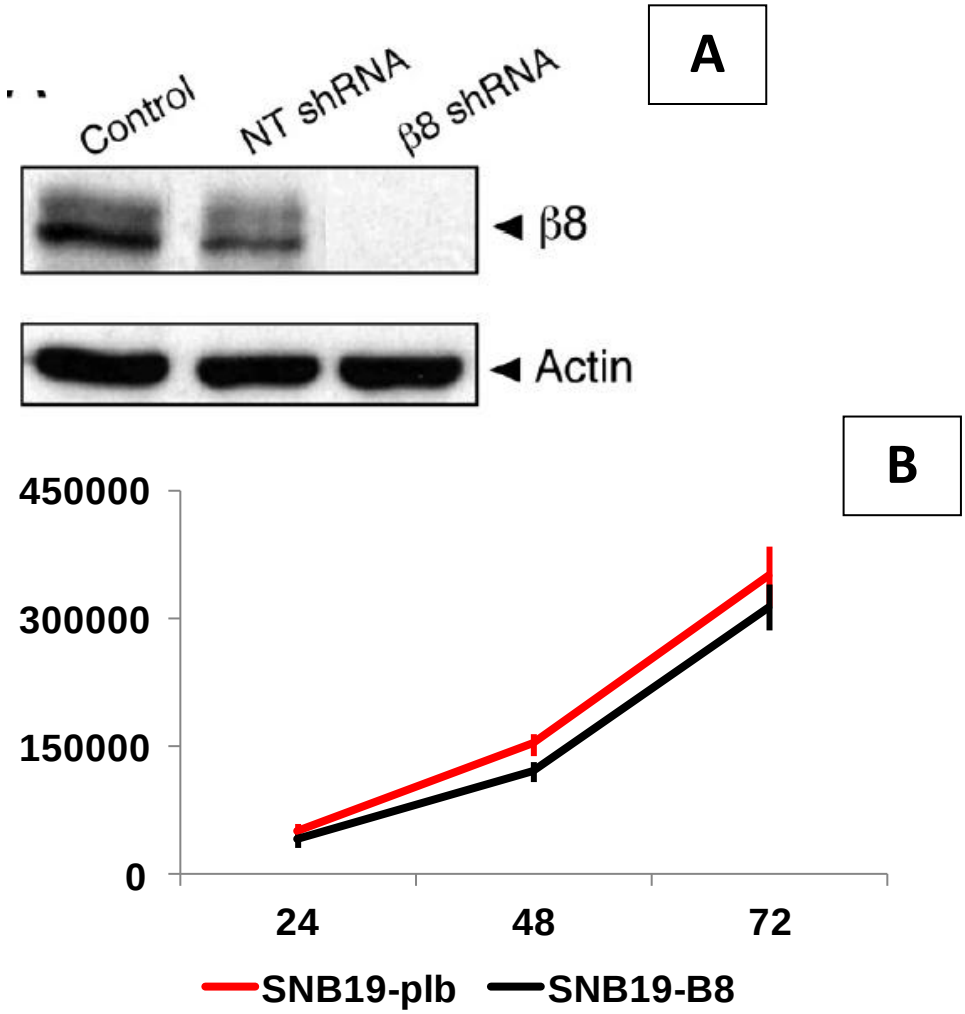


**Figure 7. shRNA Mediated Knockdown of β8 in SNB19 Cells Does Not Influence In-Vitro Growth**

**(A) Parental control, non-targeting, and β8shRNA SNB19 cells were blotted for integrin expression. Note the β8 knock down in the β8shRNA cells . (B) This proliferation assay revealed there is no difference in in-vitro growth when the integrin is knocked down with shRNA.**

**Integrin Subunit αv Plays a Major Role in Migration**

WT and αvKO transformed mouse astrocytes were analyzed for migration related differences by plating them on laminin coated glass coverslips and scratching them once they were confluent. This revealed a striking difference where the cells did not move in to fill the wound as they did with WT cells. This is of interest because those with αv knocked out had no αv associated integrins. Further experiments with live cell imaging revealed that the transformed αvKO cells were indeed moving, but just not into the wound (video not shown). The cells would migrate towards the scratch wound, but not fill it as though a barrier was present. They would then move vertically along the margin of the wound. The cells continued to move in this pattern over the 48 hours period analyzed (data not shown). The cells were let go beyond confluence up until cell death; they still did not cross the barrier. Though real time video capture cannot be displayed Figure 9 best represents the pattern of cell movement just after a scratch is made. Note the original scratch is not a smooth line (Figure 9). However, after 24 hours the cells move towards the scratch barrier and halt forward progress and only move parallel to the margin.

Following this observation, a rescue experiment was attempted to see whether WT transformed mouse astrocytes could rescue the migration defect seen when αv integrins are knocked out. For this the transformed mouse astrocytes were stably transfected with an RFP vector while the αv knockout cells were transfected with a stable red fluorescent protein (GFP) construct. Both sets of cells were sorted for maximum fluorescence. Cells were first imaged separately where

the phenotypes seen in non transfected cells persisted. The two cell types were then mixed in a 50:50 ratio and scratched as done before. It was seen that as time elapsed the αvKO cells were preventing the WT cells from filling the wound in the manner they do when only WT cells are present (Figure 10). Following this 293T cells were transfected with RFP and also ran through this mixing experiment. It was again seen that the αvKO cells inhibited the migration of another cell type. Interestingly, 293T cells do not express β8 (data not shown), while WT cells do.

WT cells contain β8 integrin which is able to activate TGFβ while αvKO cells do not. The rationale behind this mixing experiment was that the WT cells would be able to activate the TGFβ which could then signal on the αvKO cells, rescuing the phenotype. However, since this did not happen it suggests an additional pathway is present that is independent of TGFβ activation. These experiments were also repeated in reverse with WT transformed mouse astrocytes expressing the RFP and the αvKO transformed astrocytes and 293T cells expressing GFP.

**Figure 8.**

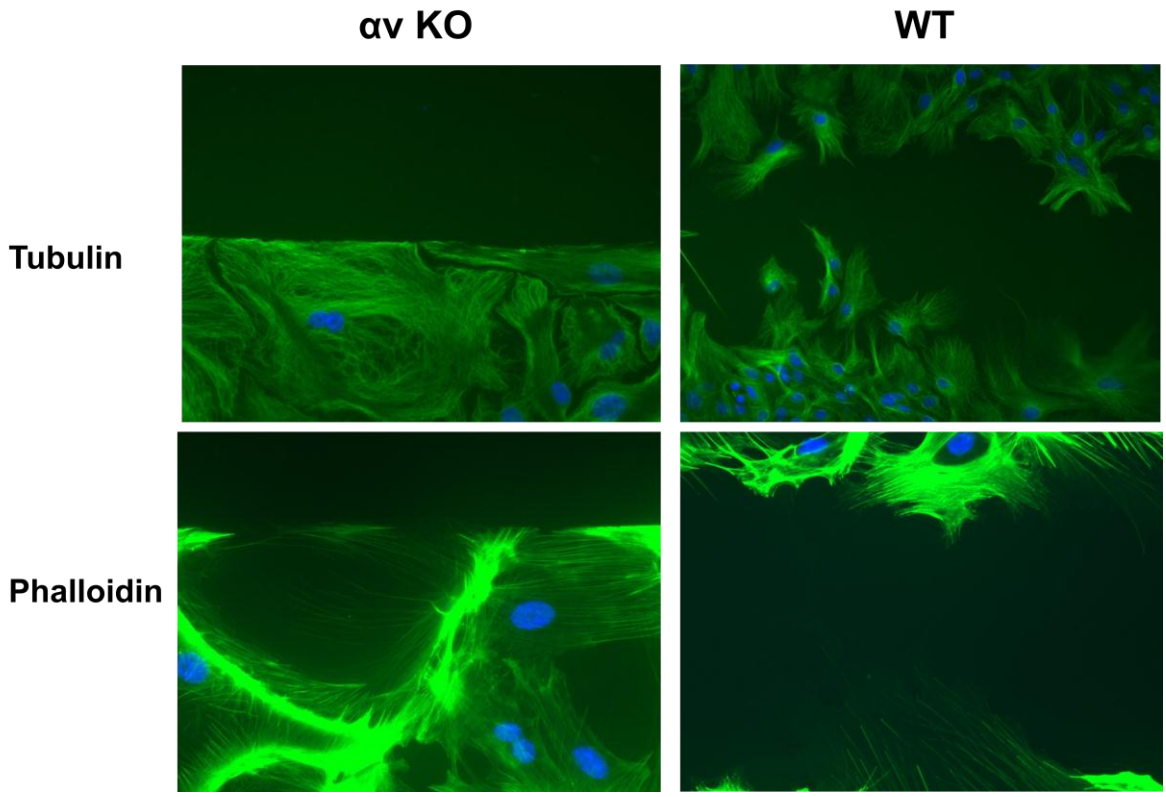


**Figure 8. Loss of αv in Transformed Mouse Astrocytes Alters In-Vitro Cell Migration**

**Wild-type and αv knockout transformed mouse astrocytes were grown to confluence on laminin coated glass cover slips. They were scratched and fixed after 12 hours. Immunofluorescence was conducted with a green 488nm secondary and tubulin and phalloidin primary antibodies. Tubulin stains for microtubules while phalloidin marks the actin. Note the complete lack on migration into the wound in αvKO mouse transformed astrocytes.**

**Figure 9.**

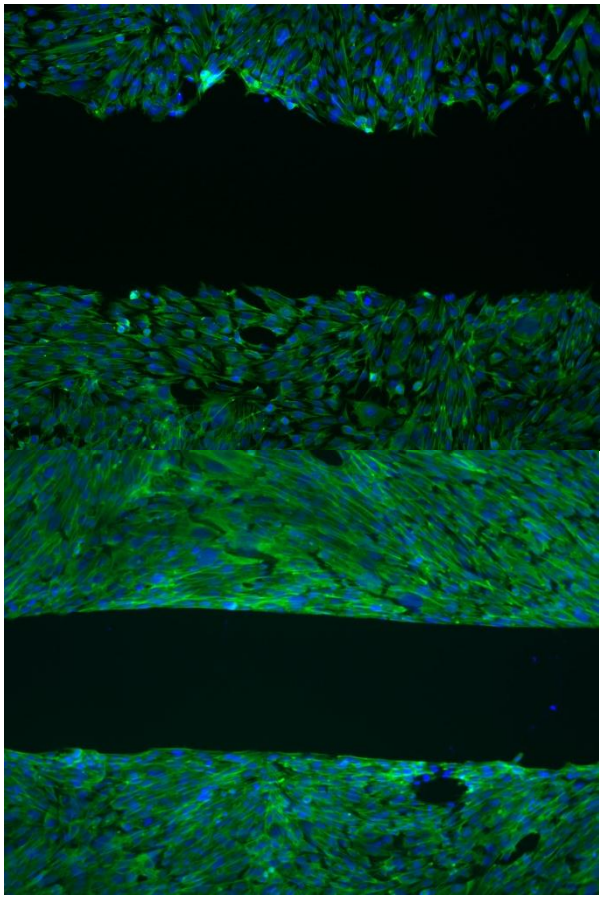

**Figure 9. Loss of αv in Transformed Mouse Astrocytes Does Not Inhibit Cell Movement**

**Two scratch wounds were fixed at two time intervals after the scratch of αvKO cells. The 0hr (left) scratch has a jagged and uneven edge as cells were torn away from the wound with the scratching motion. After 24 hours (right) it is seen that the cells will migrate to the wound edge, but not farther.**

**Figure 10.**

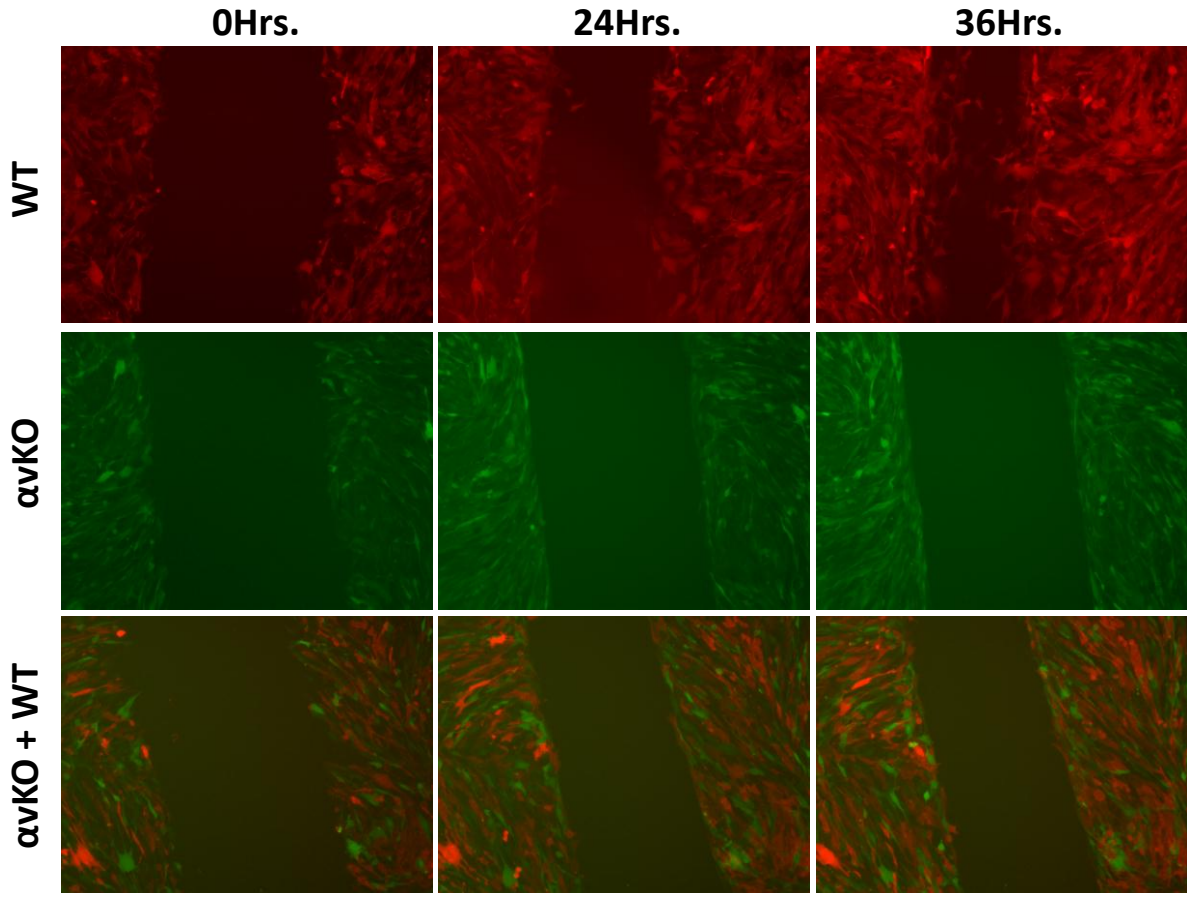

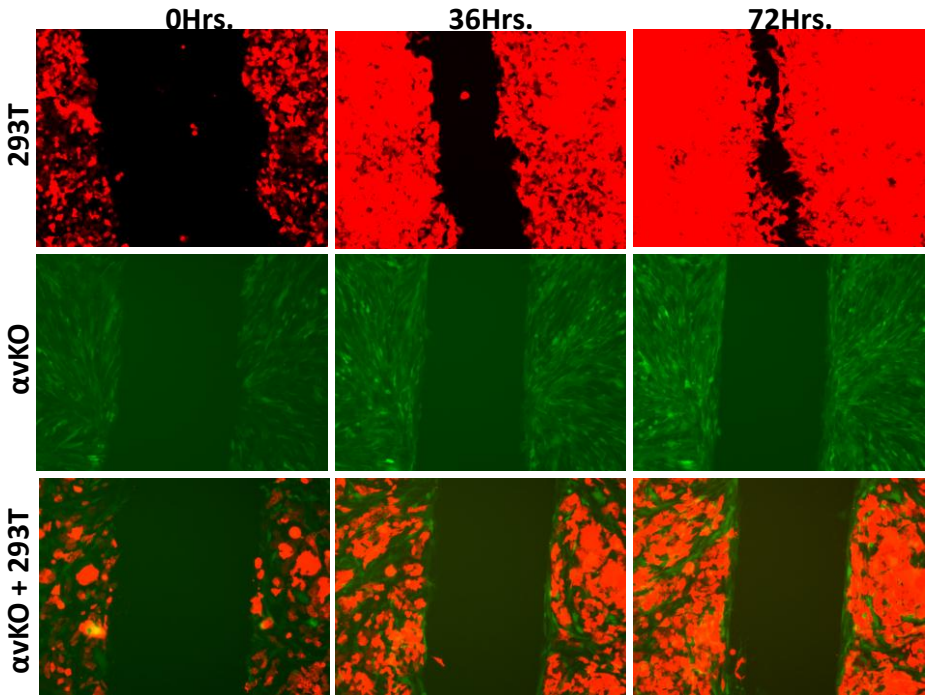


**Figure 10. WT mTAs Cannot Rescue the $\alpha v^{-/-}$ mTA Phenotype**

**(A) Using a live imaging microscope cells were imaged over 36 hours. The images depicted are from the same well and are screen captures of a movie generated. In the top three panels transformed wild-type mouse astrocytes stably expressing RFP were plated, scratched and imaged. The second set is transformed αvKO mouse astrocytes. The bottom row of panels is a 50:50 mixture of the two cell types. Note the migration of WT cells and lack of migration for the αvKO cells and also how the αvKO cells inhibit the migration of WT cells when the two are mixed. (B) 293T cells were also transfected to stably express RFP. Note how in the mixture experiment the GFP positive αvKO cells inhibit the migration of the RFP positive 293T cells.**

**Integrin Subunit β8 Plays a Major Role in Migration**

Transformed human astrocytes (THA) with the previously described non-targeting shRNA and β8-targeting shRNA were used for a migration assay. These cells were plated onto laminin coated glass wells of a 24-well plate, scratched, and imaged over 36 hours. Wells with and without exogenous TGFβ were analyzed. By following the time lapse file frame by frame it was seen that knocking down β8 reduces the time it takes for the scratch region to fill (Figure 11). Additionally, it was seen that the addition of exogenous TGFβ can partially rescue this defect. This was further quantified and there was a statistically significant decrease in the amount of time it took the NT and β8shRNA cells to fill the wound (p-value = .006). There was also a significant difference (p-value = .03) for β8shRNA THAs with and without the exogenous TGFβ (Figure 11). As TGFβ rescued this phenotype it suggests that the pathway involved with this molecule is the origin on the phenotype.

In analyzing this phenotype polarity proteins were also examined. Confluent THAs expressing the NT-shRNA or the β8shRNA were scratched and fixed after the initial stages of cell polarity. These were stained with paxillin, a marker of focal contacts and the actin marker, phalloidin. It may been that the control THAs polarize into the wound region as expected while those with less β8 illustrate abnormal cell-ECM contacts (Figure 12). The focal contacts are at the leading edge of the cell in the control panel but are dispersed when β8 is knocked down. Additionally, the actin cytoskeleton is stretched in the direction of cellular

movement, into the wound, for the control. While with β8shRNA the actin pattern is hashed with no consistent direction (Figure 12).

**Figure 11.**

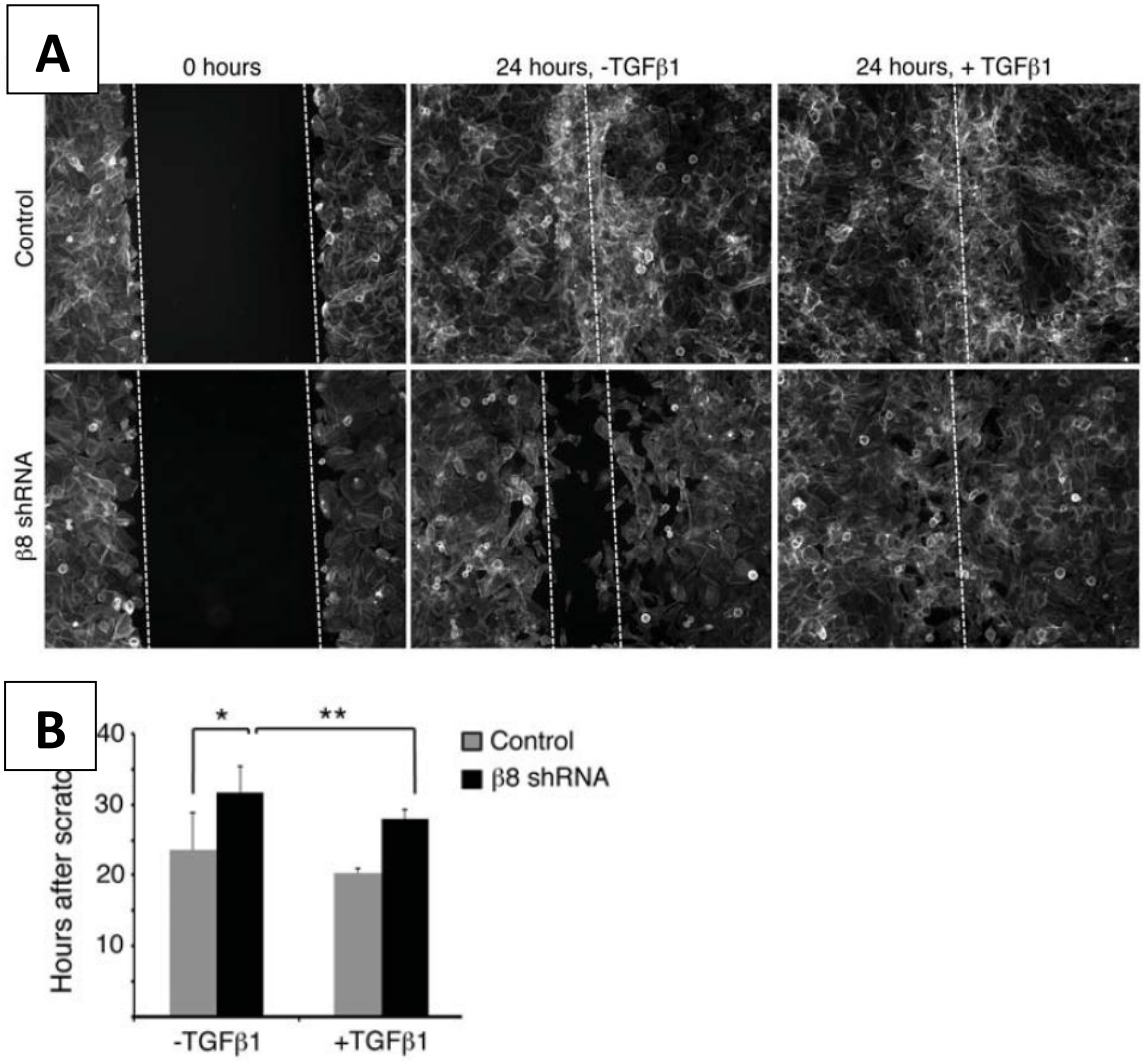


**Figure 11. β8 Dependent Migration Defects Are Partially Rescued by Exogenous Active-TGFβ**

**(A) Transformed human astrocytes (THAs) control (Non-targeting shRNA) and β8shRNA cells were time-lapse imaged. It can be seen that THA-β8shRNA cells migrate to fill the wound slower than those with the THA-NTshRNA. Note the partial rescue of this phenotype with exogenous 1ng/ml TGFβ is added. (B) Quantitation of scratch assay. *P-value = .006 **P-value = .03**

**Figure 12.**

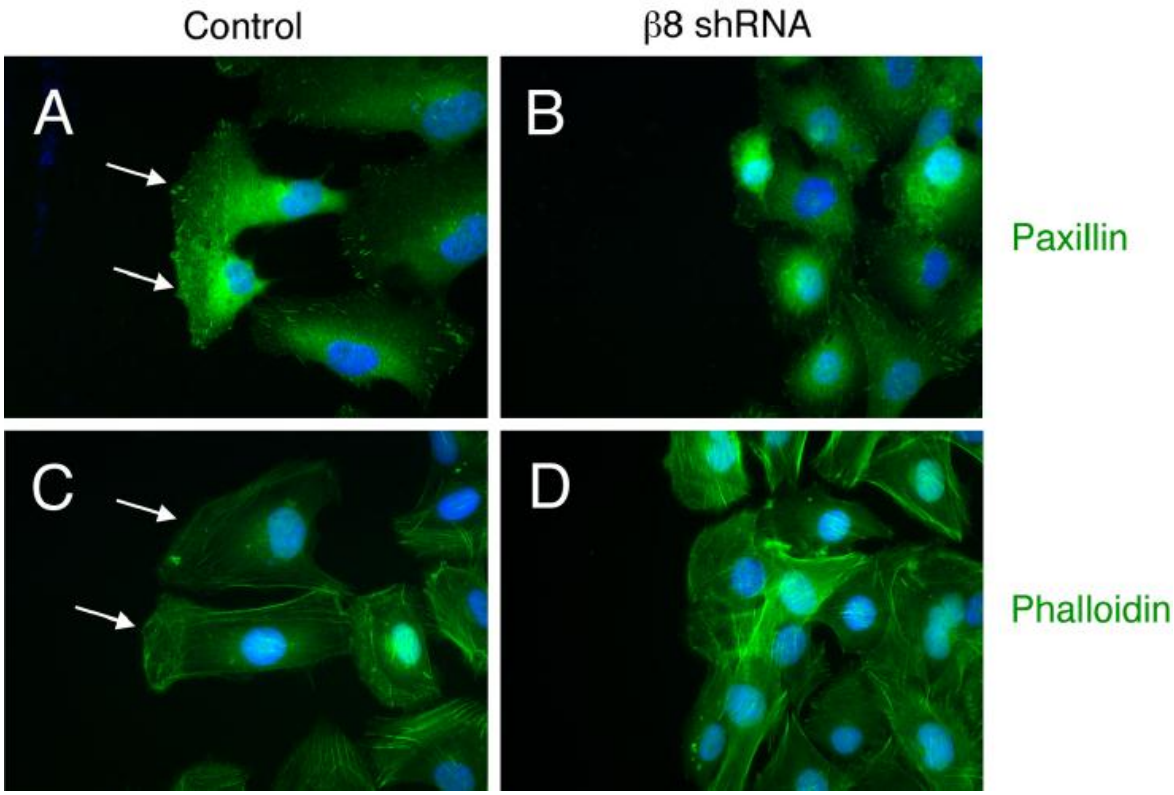


**Figure 12. β8 Knockdown Induces Polarity Dependent Phenotypes**

**A scratch assay was performed on a confluent monolayer of THAs with control NT-shRNA (A) and β8shRNA (B). The initial states of polarity can be seen with anti-paxillin and anti-phalloidin. Note how control cells polarize into the wound region while when β8 integrin is knocked down obvious defects are present. These images are shown at 400x magnification.**

**Integrin Subunit β8 Plays a Major Role in Invasion**

Following the previously demonstrated phenotype of primary and transformed mouse astrocytes lacking their full migratory potential, invasion assays were performed to gain further perspective. Primary mouse astrocytes were cultured from WT, $\beta8^{-/-}$, and $\alpha v^{-/-}$ mice. These cells were run through an *in-vitro* invasion assay. The same number of cells was added into 1% serum containing media. Aliquots were made that contained cells at a concentration of 50,000 cells per 500 microliters media for each cell type and loaded into the chamber. The chemo-attractant was set at 10% serum containing media in the lower chamber. It was seen that half as many $\beta8^{-/-}$ primary astrocytes invaded compared to WT astrocytes. $\alpha v^{-/-}$ cells invaded minimally with just a few cells making it to the bottom of the membrane (Figure 13A). Following this transformed mouse astrocytes were analyzed by the same method to determine their invasive potential. It was seen that these cells followed a similar pattern where loss of β8 reduced in-vitro invasiveness by about 50% and loss of αv resulted in severe and near complete loss of invasion (Figure 13B). Following these results an experiment was performed to determine if this phenotype could be rescued. β8 was overexpressed in $\beta8^{-/-}$ cells as determined by western blot (Figure 5). These were run through an invasion assay where it was determined that forcibly expressing β8 can increase the invasive potential by about 60% over the $\beta8^{-/-}$ cells (Figure 13C).

**Figure 13.**

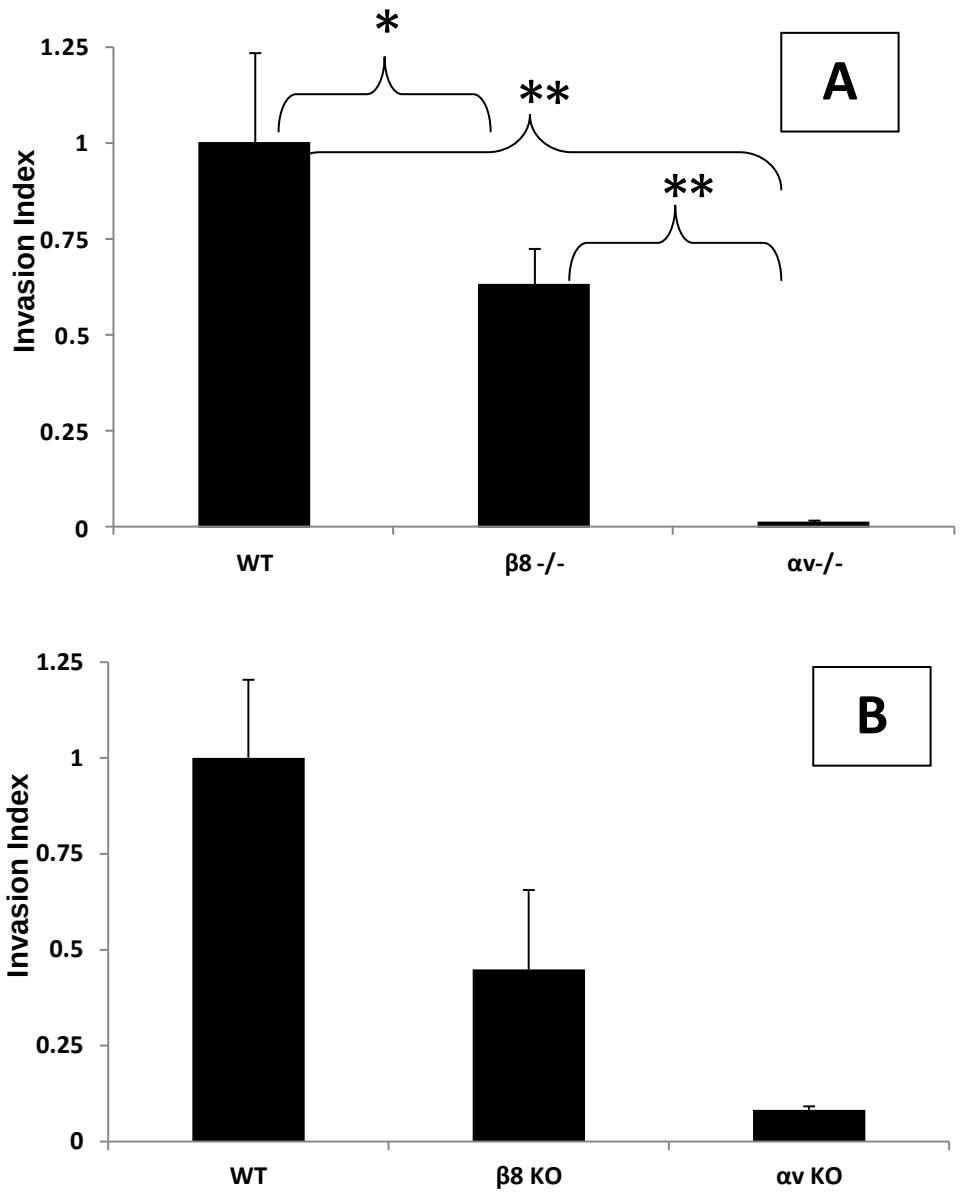
A
*
**
**
Invasion Index
1.25
1
0.75
0.5
0.25
0
WT
β8 -/-
αv-/-
B
Invasion Index
1.25
1
0.75
0.5
0.25
0
WT
β8 KO
αv KO

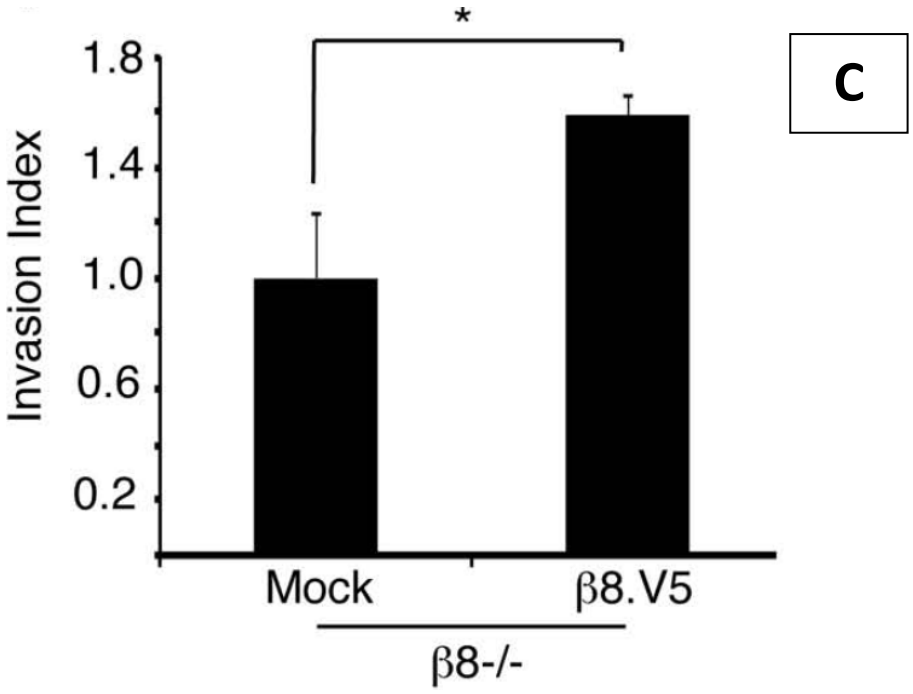


**Figure 13. Loss of β8 Reduces Invasion and can be Rescued in a β8 Dependent Manner in Transformed Mouse Astrocytes**

**(A) Invasion assays were performed on primary mouse astrocytes, (B) transformed mouse astrocytes, and (C) $\beta 8^{-/-}$ transformed mouse astrocytes forcibly expressing β8. Note how the loss of β8 reduces in-vitro invasiveness while re-expressing this integrin in knockout cells causes a statistically and biologically significant increase in invasiveness. **p-value <.005 ; All other p-values < .05**

Human glioblastoma cell lines were analyzed to determine how β8 may play a role. A pool of siRNA directed against β8 and a pool of scrambled siRNAs were used on the SNB-19 glioblastoma cell line. This expression was check by western blot (Figure 14A). These cells were then ran through an in-vitro invasion assay where it was seen that knocking down β8 in the SNB19 human GBM cell line results in about 50% loss in invasiveness when compared to cells treated with scrambled siRNA (Figure 14B). Additionally, this was attempted in LN229 human GBM cells. The knockdown of β8 was verified by western blot (Figure 14C). These cells were run through an invasion assay using the same protocol as with the SNB19. Knocking down expression of β8 in human GBM LN229 cells resulted in approximately 50% reduced invasiveness suggesting role for this protein in GBM cells' invasive phenotype (Figure 14D).

**Figure 14.**

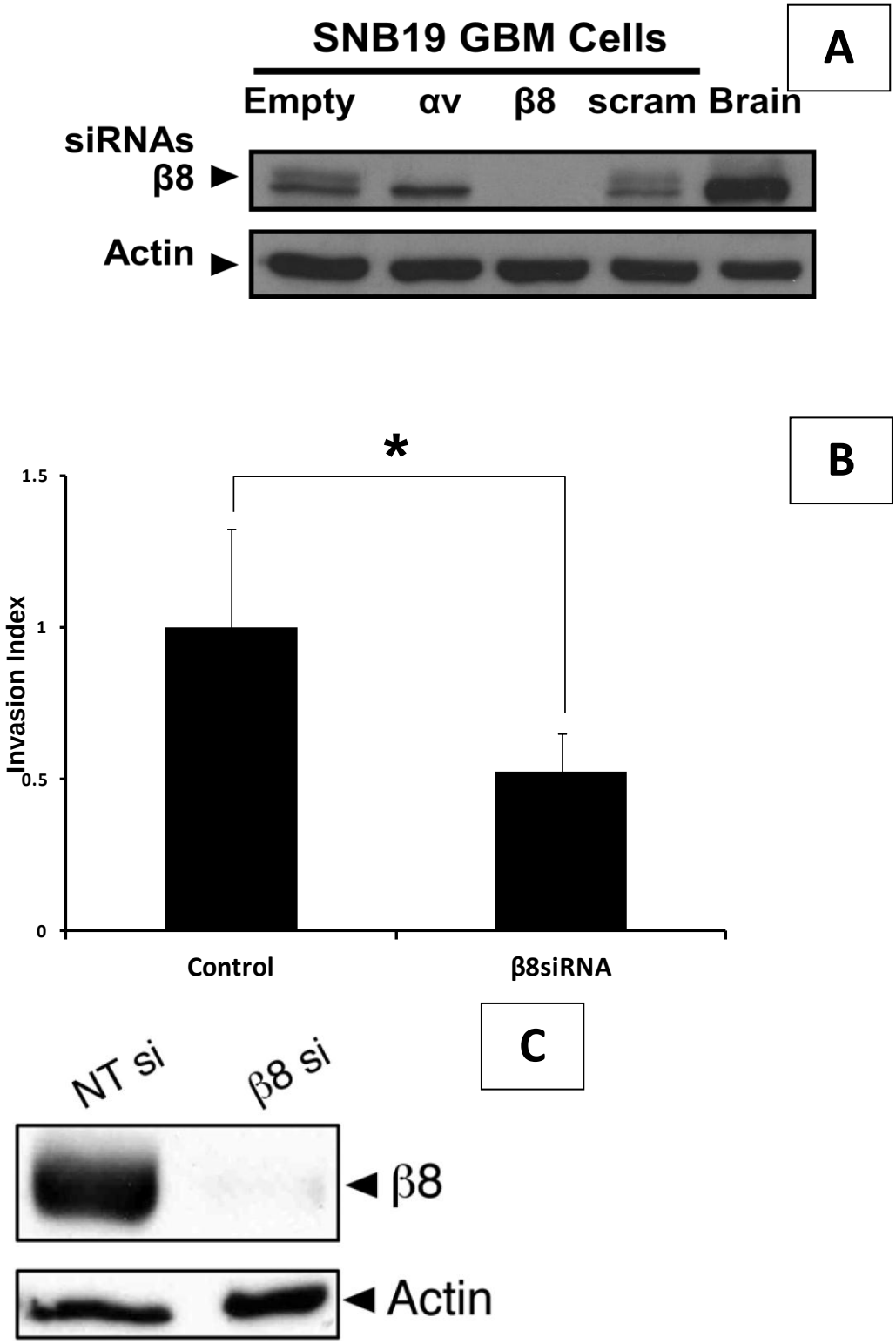
A
SNB19 GBM Cells
Empty
αv
β8
scram
Brain
siRNAs
β8
Actin
B
*
Invasion Index
1.5
1
0.5
0
Control
β8siRNA
C
NT si
β8 si
β8
Actin

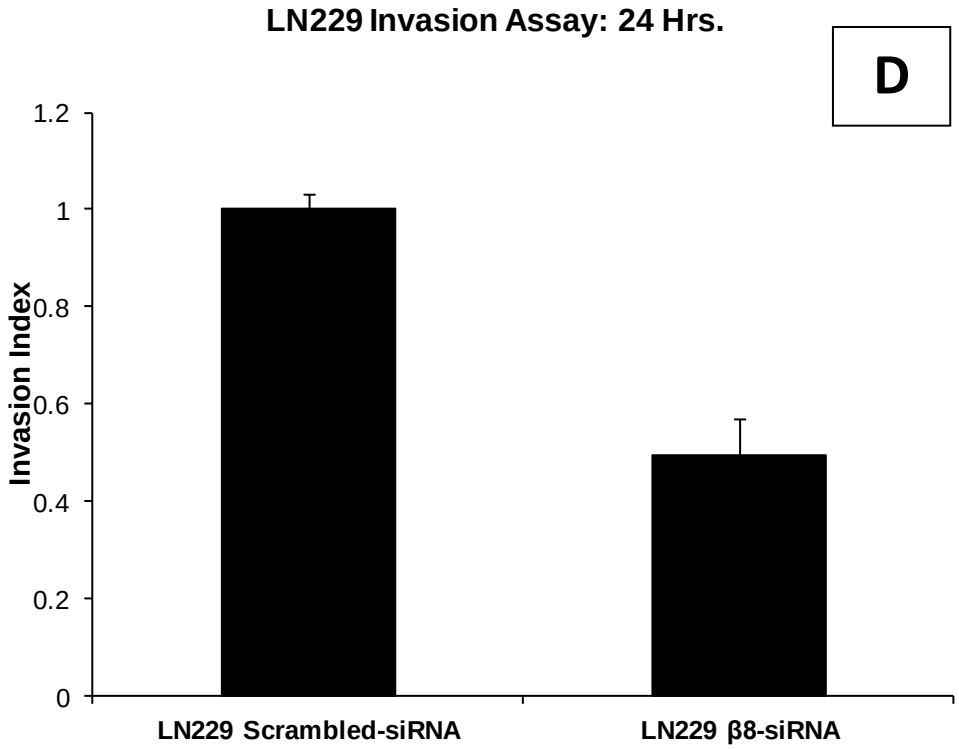


**Figure 14. Silencing of β8 Reduces Invasion in SNB19 and LN229 GBM Cells**

**Untransfected, αv-siRNA, β8-siRNA, and scrambled-siRNA were added to GBM cell line SNB-19. Normal mouse astrocytes (Brain) were used for antibody reference. (A)Note the reduced expression of β8 when β8siRNA is added. (B) When β8 is knocked down in SNB-19 human GBM cells, in-vitro invasiveness decreases by about 50%. (C) Knockdown of β8 was verified by western blot in LN229 cells. (D) In-vitro migration assay of LN229 human GBM cells with β8siRNA and scrambled siRNA. Note how silencing of β8 reduces invasiveness by about 50%. p-value < .05**

Further verification was taken by checking the invasiveness with shRNAs. The previously used SNB19 cells with known shRNA knockdown levels were used (Figure 7). It was seen that this caused a roughly 50% reduction in in-vitro invasiveness (Figure 15A). Additionally a second GBM cells line, LN229 was checked. The shRNA knockdown levels were previously identified (Figure 6B). In these cells we also see a roughly 50% reduction of invasiveness when β8 is knocked down (Figure 15B). In addition to these new shRNAs were used. For clarification all previous experiments used a single shRNA sequence. Here two new sequences were tested on LN229 cells (Figure 16A). This knockdown worked well and it was next determined that these new β8 targeting shRNAs also lead to reduced invasiveness. In LN229 cells this was seen to be a roughly 40% reduction in invasiveness. As these shRNAs have weaker knockdown, all subsequent experiments used the original shRNA which has the best knockdown (Figure 6). Following this, previously described transformed human astrocytes (THA) were analyzed for their invasive potential. The knockdown was verified by western blot and they were shown to reduce invasiveness by about 80% (Figure17).

**Figure 15.**

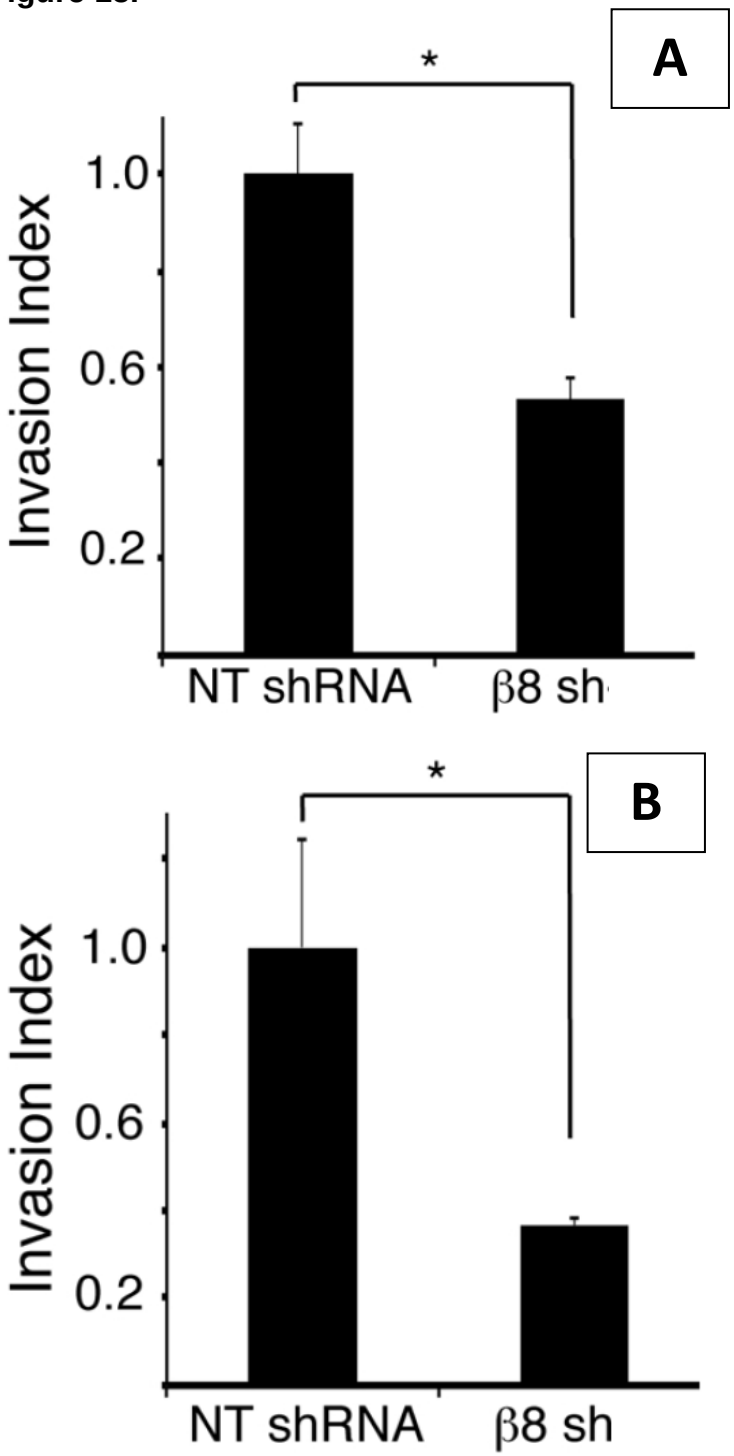
A
*
Invasion Index
1.0
0.6
0.2
NT shRNA
β8 sh
B
*
Invasion Index
1.0
0.6
0.2
NT shRNA
β8 sh

**Figure 15. Knockdown of β8 Reduces Invasion in SNB19 and LN229 GBM Cells**

**Previously described human GBM cells (A) SNB-19 and (B) LN229 were used for invasion assay. Note how knocking down integrin β8 reduces invasiveness by ~55% and ~65%, respectively. Knockdown efficiency previously demonstrated (Figure 7 and 6B).**

**Figure 16.**

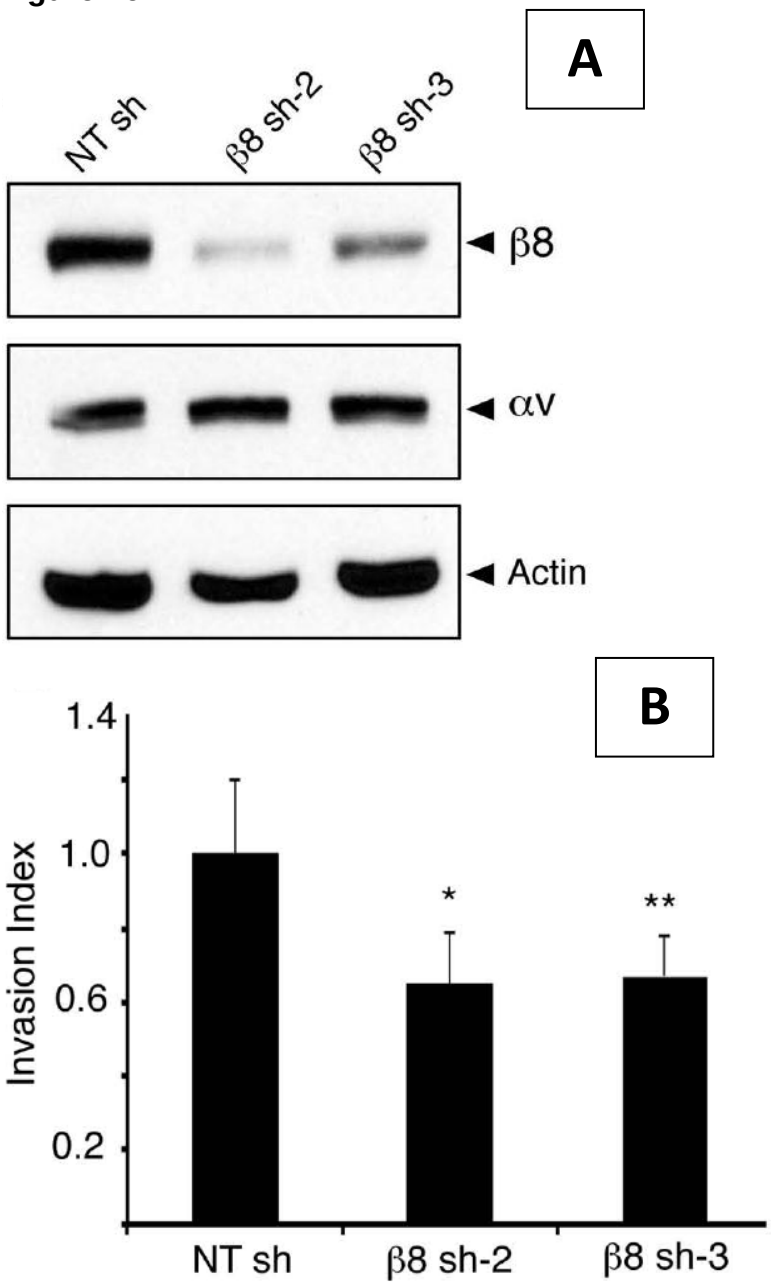


**Figure 16. Knockdown of β8 with Additional shRNA Sequences Reduces Invasion in LN229 GBM Cells**

**(A) Two new shRNAs were placed into LN229 GBM cells. (B) These same cells showed a decrease in invasiveness when ran through an invasion assay.**

**Figure 17.**

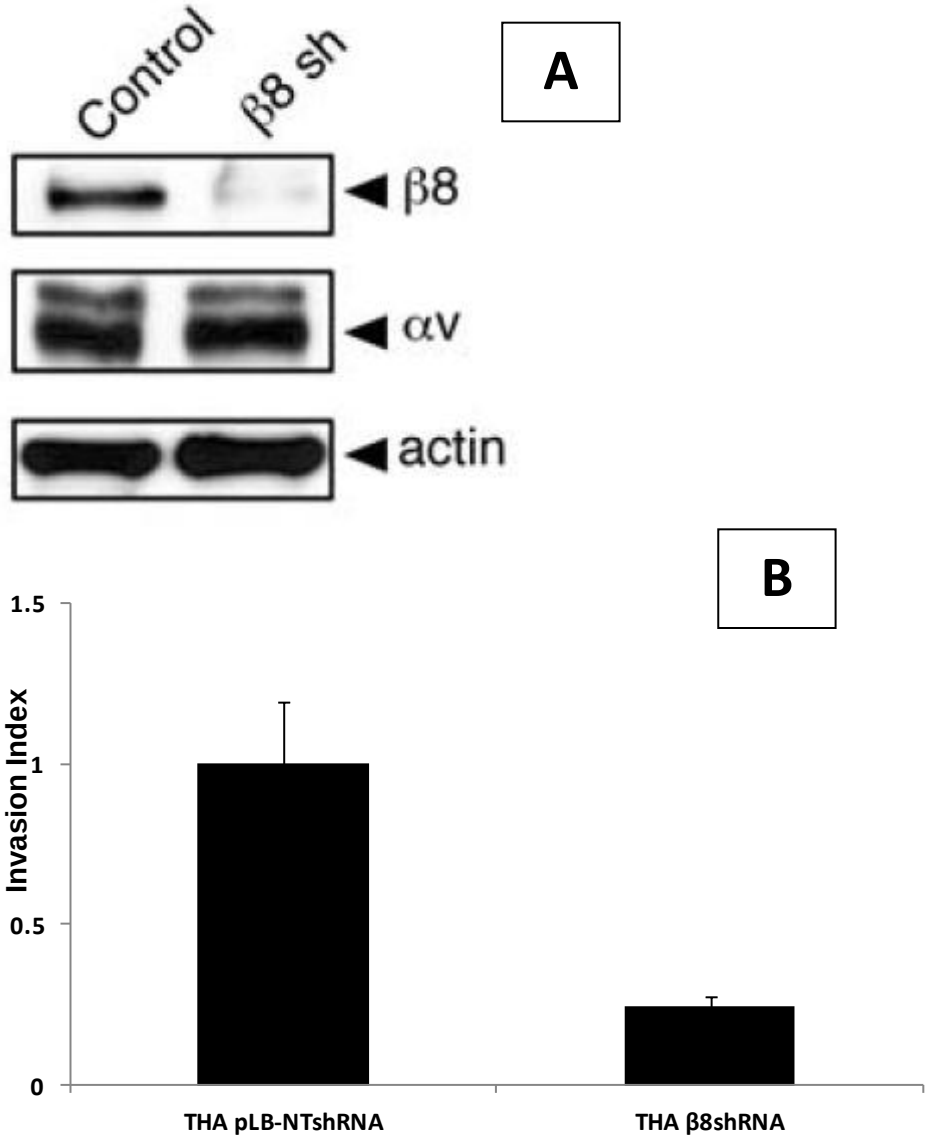


**Figure 17. Knockdown of β8 in Transformed Human Astrocytes Reduces Invasion**

**(A) Transformed human astrocytes (THAs) have the integrin β8 knocked down with β8 targeting shRNA. This blot was generated and previously published by Jeremy Tchaicha, Ph.D.(62) (B) Knocking down integrin β8 in THA cells reduced invasiveness by about 80%.**

**Integrin Subunit β8 Plays a Major Role in Invasion through TGFβ mediated signaling**

Considering the results of Figure 11 and the previous invasion results I then decided to probe the canonical TGFβ pathway. β8 integrin was previously examined for an extracellular presence (Figure 4-2) however it is possible that siRNA and shRNA may not knockdown the extracellular β8. To address this biotinylations were performed. Transformed mouse astrocytes were biotinylated to label all extracellular proteins and then immunoprecipitated with β8. This reveals that β8 knockout cells do not have β8 (Figure 18A). Next, SNB-19 cells that had β8shRNA were checked. These showed that when the integrin was knocked down there was also less of it being displayed on the surface (Figure 18B). LN229 cells were also checked. After biotinylations they were immunoprecipitated with αv to pull down all αv bound proteins. This revealed a significant band that correlated with integrin subunits β3, β5, and β8 and a reduction of this band when β8shRNA was present. To be more specific the same procedure was performed on LN229 cells pulling down β8. There was a significant reduction in β8 being expressed on the cell surface. Since no β subunits pair with β8, the band seen indicates residual β8 being expressed on the surface (Figure 18C).

A monoclonal antibody (MAB) directed against TGFβ was added to LN229 cells that had been serum starved. In doing so, TGFβ signaling could be stopped, preventing the phosphorylation of downstream Smads and TGFβ induced target genes that can lead to invasion(13,141,142). We can see that serum starved cells

express very little pSMAD3 as would be expected (Figure 18D). When active TGFβ was added to the cells that were in serum free media there was noticeable phosphorylation of SMAD3. However, when active TGFβ was pre-incubated with the MAB pSMAD3 signaling was not as active as without the MAB. This suggests that TGFβ can stimulate signaling downstream of the TGFβ1/2 receptor and that this activity can be attenuated by blocking the binding site of TGFβ. Proper controls were checked by mixing active TGFβ with IgG. Additionally, the inactive latent-TGFβ was added, which did not activate downstream signaling. Next an inhibitor of the TGFβ-receptor was analyzed for efficiency. Serum starved LN229 cells showed little to no SMAD2 and SMAD3 phosphorylation (Figure 18E). However after adding serum containing media both proteins became heavily phosphorylated indicating the ability of TGFβ to stimulate signaling downstream of the TGFβ receptor. The inhibitor was pre-incubated on the cells allowing for time to bind. When serum containing media was added the SMAD signaling decreased in a dose-dependent manner. A proliferation assay was then performed on the cells to determine if changes in SMAD signaling could affect cell growth in-vitro. There was no statistical or biological difference between the various conditions (Figure 18F). LN229 cells were then run through an invasion assay with the TGFβ MAB and the TGFβR1/2 inhibitor (Figure 18G). By blocking TGFβ signaling the cells invade 50-60% slower than those not treated; similar to the phenotype seen when β8 was knockdown or knocked out. As β8 is known to activate TGFβ these results suggest their heavy involvement in TGFβ signaling. Additionally, when β8 is knocked down TGFβ signaling also drops, as is indicated by a luciferase assay (Figure 18G).

**Figure 18.**

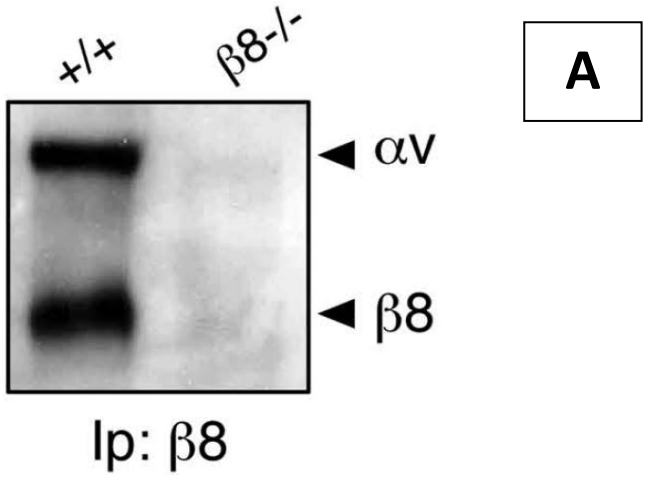


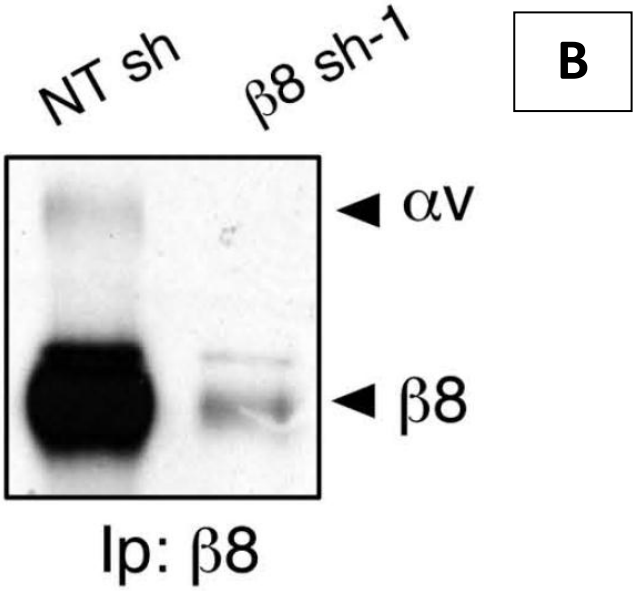

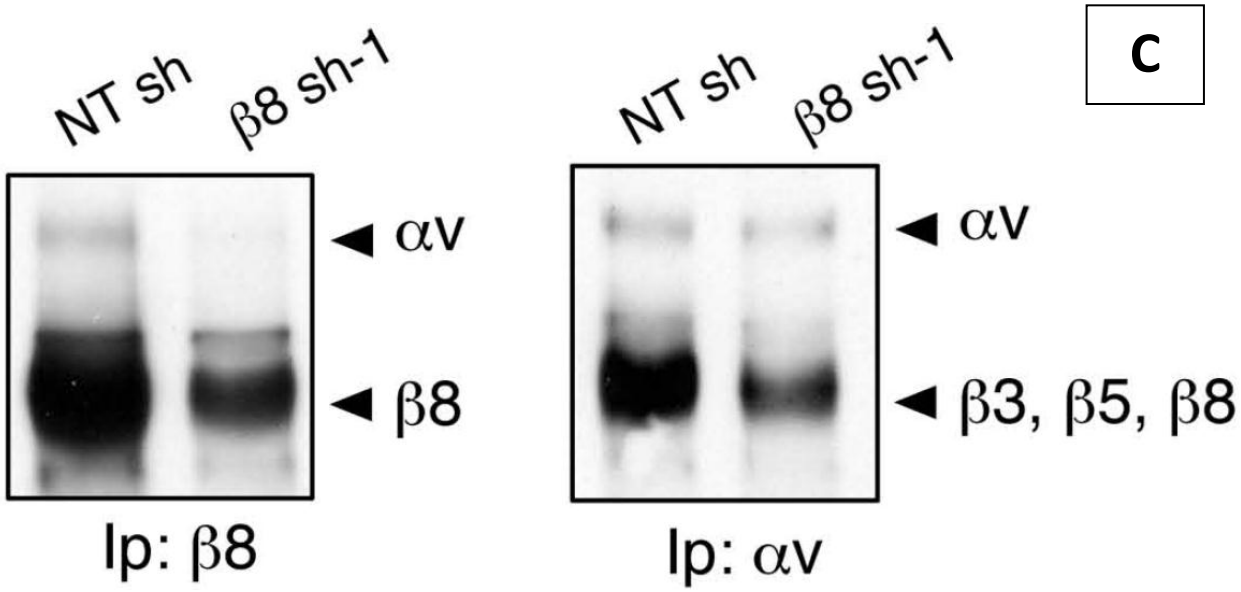
C
NT sh
β8 sh-1
αv
β8
Ip: β8
NT sh
β8 sh-1
αv
β3, β5, β8
Ip: αv

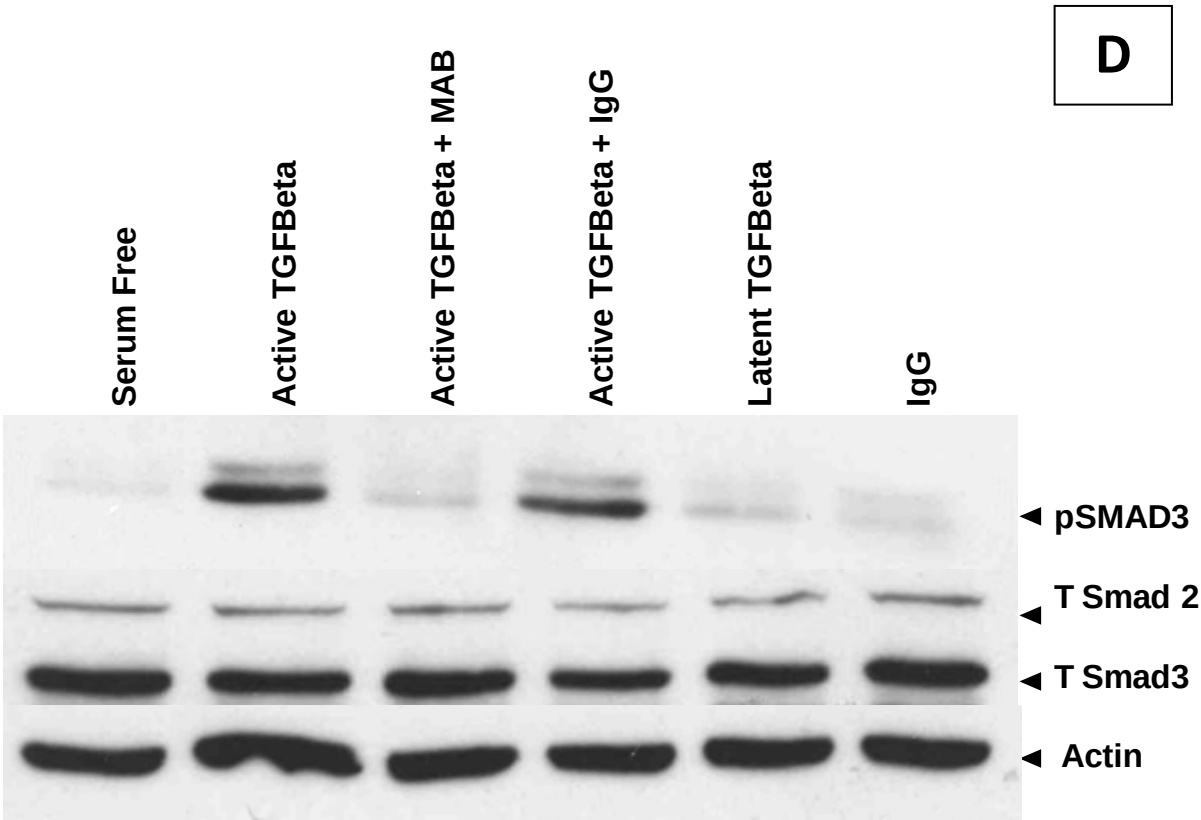
D
Serum Free
Active TGFBeta
Active TGFBeta + MAB
Active TGFBeta + IgG
Latent TGFBeta
IgG
pSMAD3
T Smad 2
T Smad3
Actin

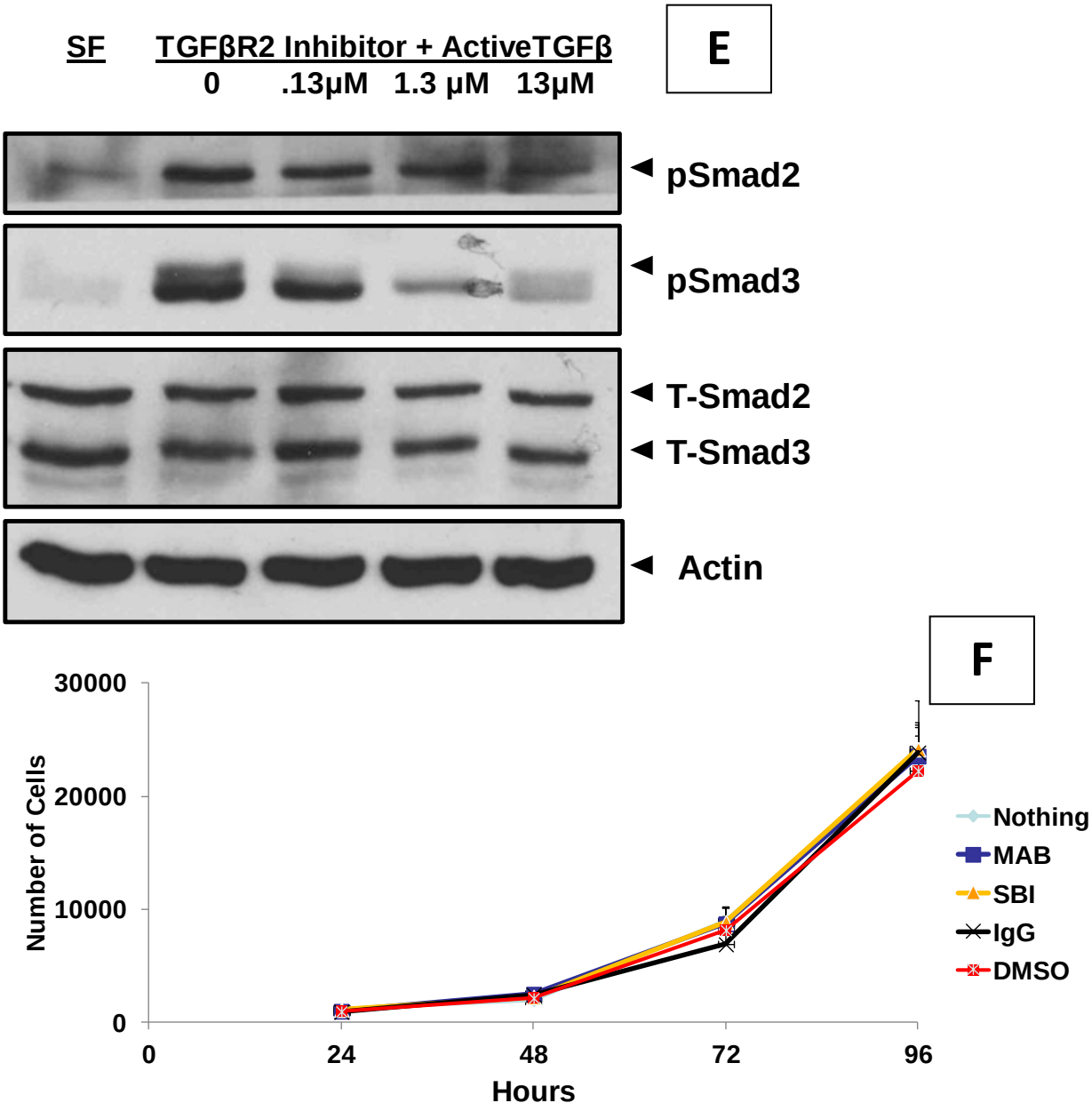
SF
TGFβR2 Inhibitor + ActiveTGFβ
0
.13μM
1.3 μM
13μM
E
pSmad2
pSmad3
T-Smad2
T-Smad3
Actin
F
30000
20000
10000
0
Number of Cells
0
24
48
72
96
Hours
Nothing
MAB
SBI
IgG
DMSO

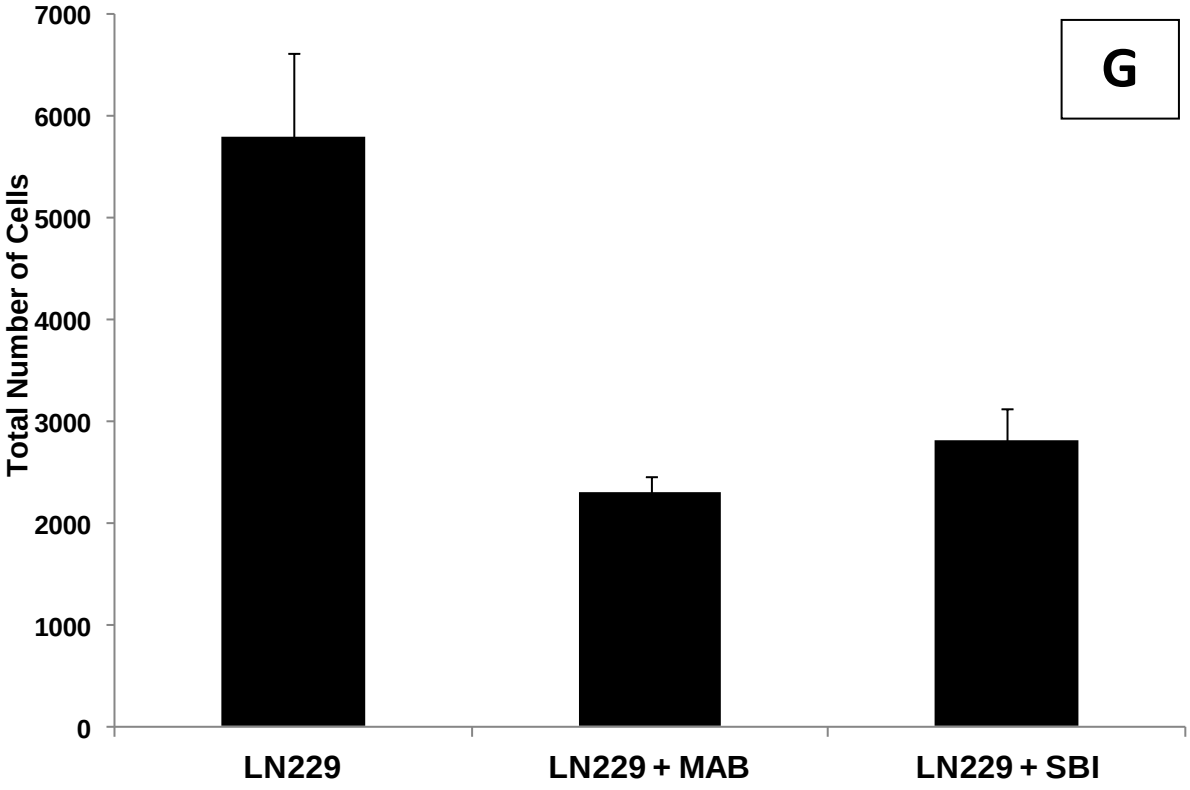
G
Total Number of Cells
7000
6000
5000
4000
3000
2000
1000
0
LN229
LN229 + MAB
LN229 + SBI

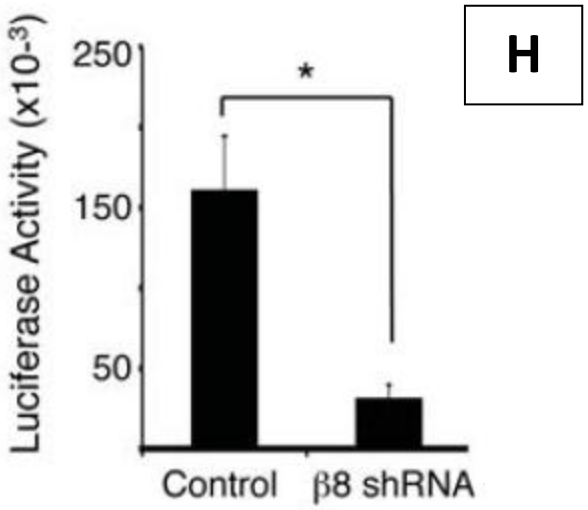
H
Luciferase Activity (x10-3)
250
150
50
*
Control
β8 shRNA

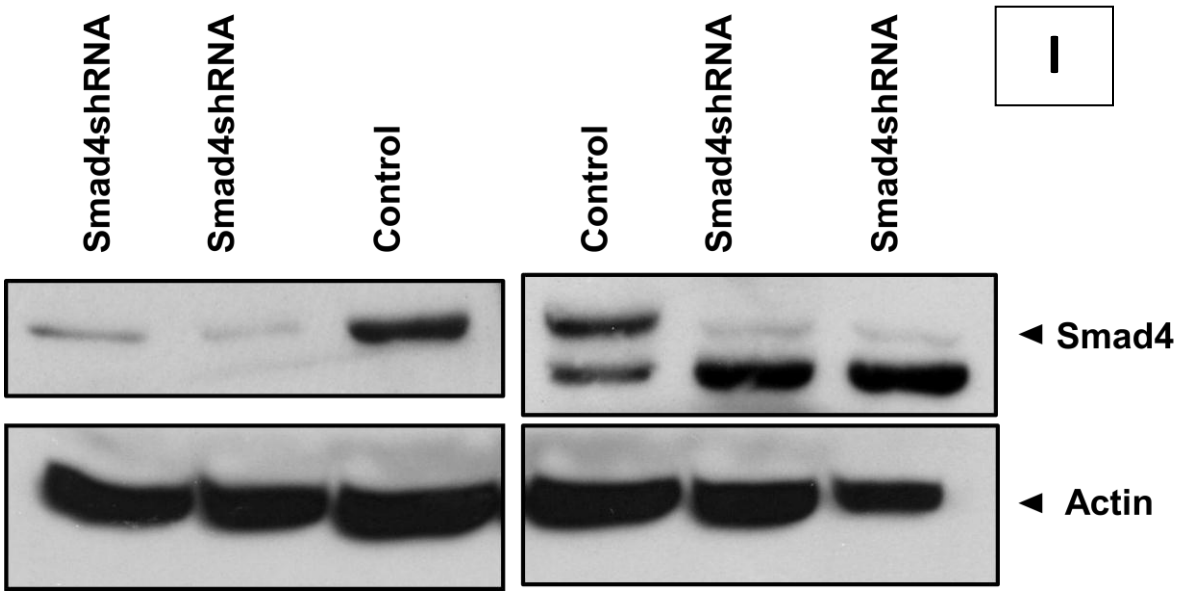
I
Smad4shRNA
Smad4shRNA
Control
Control
Smad4shRNA
Smad4shRNA
◄ Smad4
◄ Actin

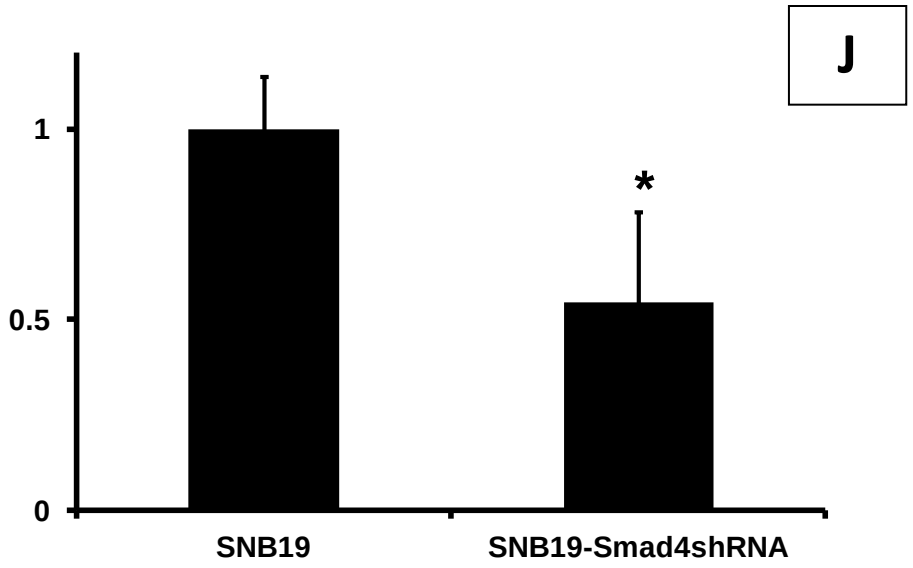
J
1
0.5
0
*
SNB19
SNB19-Smad4shRNA

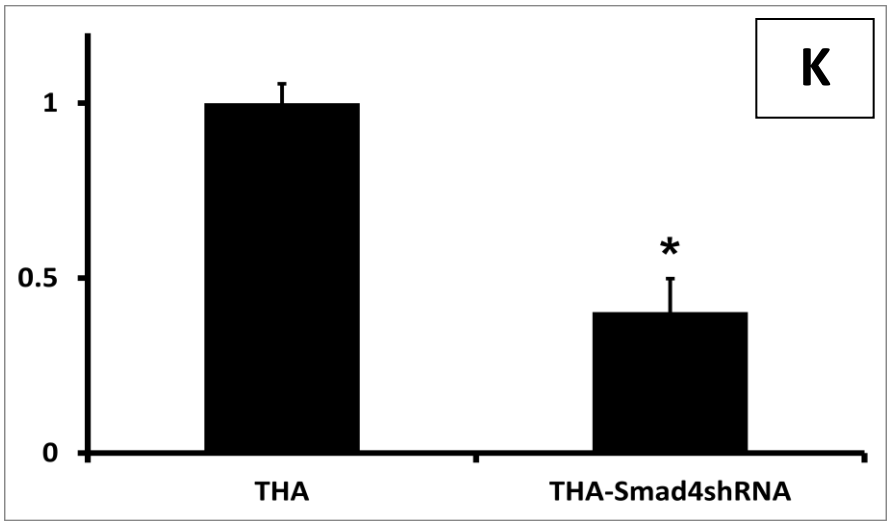
K
1
0.5
0
*
THA
THA-Smad4shRNA

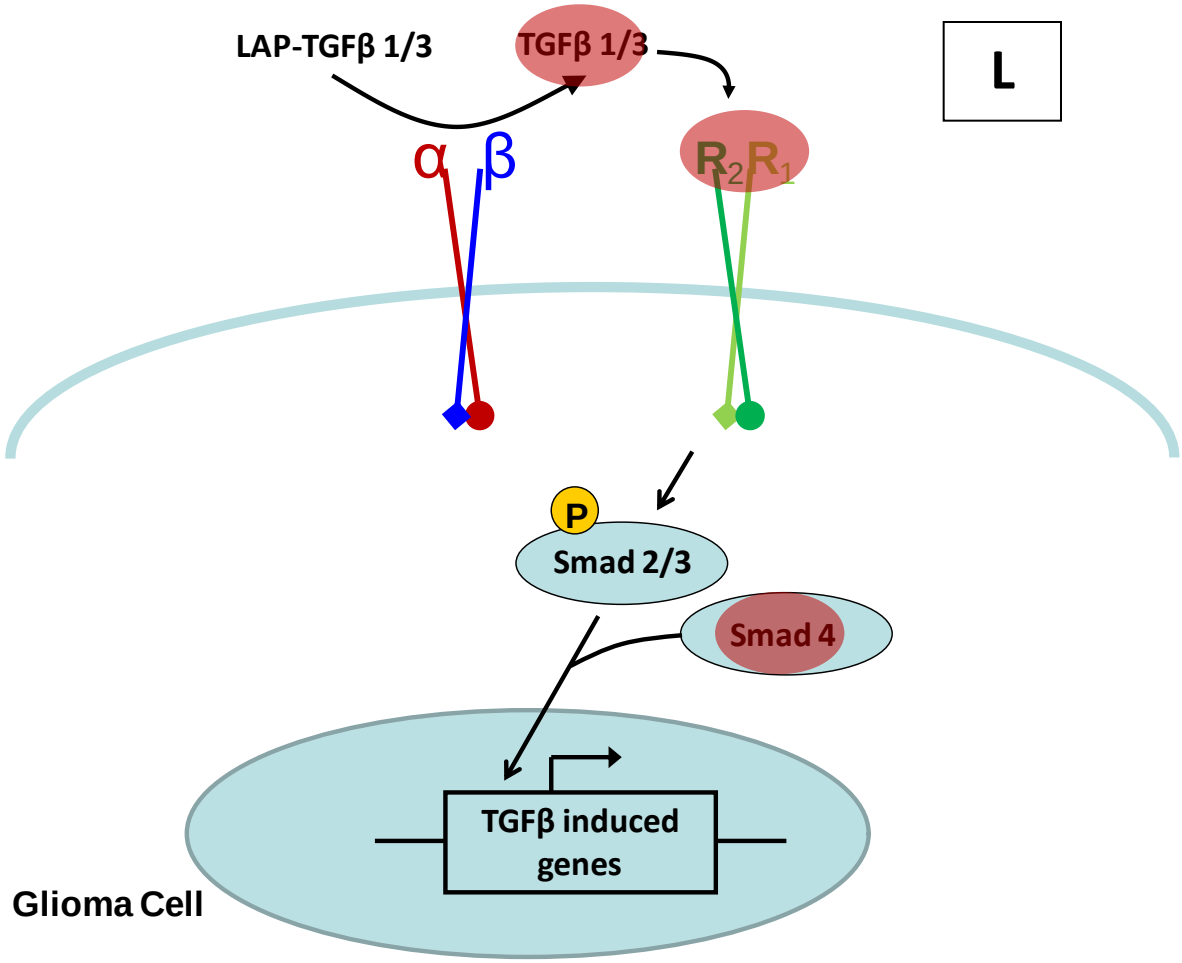
L
LAP-TGFβ 1/3
TGFβ 1/3
α
β
R2
R1
P
Smad 2/3
Smad 4
TGFβ induced genes
Glioma Cell

**Figure 18. Surface Expressed αvβ8 Mediates TGFβ Signaling and TGFβ Mediated Smad Signaling Mediates Invasion**

**(A) WT and β8$^{-/-}$ transformed mouse astrocytes were biotinylated and β8 was immunoprecipitated. Note the high expression of cell surface αv and β8 in WT cells but the lack thereof in β8 knockout cells. (B) SNB-19 GBM cells were biotinylated and β8 was immunoprecipitated. Note the large amount of surface β8 in the control cells and the reduced expression in cells with β8shRNA. (C) LN229 cells were biotinylated and immunoprecipitated with αv and β8 antibodies. Note the decreased surface expression of β8 when it is knocked down with shRNA. (D) Western blot of LN229 cells demonstrating the ability of exogenous active-TGFβ to stimulate SMAD2 phosphorylation and for an anti-TGFβ antibody to attenuate this response. (E) Western blot of LN229 cells demonstrating the ability of a TGFβ receptor inhibitor to block downstream SMAD2 and SMAD3 phosphorylation. (F) Proliferation assay of LN229 cells exposed to nothing, anti-TGFβ monoclonal blocking antibody, TGFβRI inhibitor (SBI), IgG, and DMSO (SBI is solubilized in DMSO). (G) LN229 cells were run through an invasion assay after being pre-incubated with MAB and TGFβR inhibitor. Note the decreased invasiveness in cells with blocked SMAD signaling. (H) The TGFβ responsive PAI-1 promoter drove luciferase in this luciferase assay of THA cells. Note roughly 80% decrease in luciferase activity in cells with β8 knocked down. Figure 18H was generated by former graduate student Dr. Tchaicha. (I) Smad4 is knocked down with shRNA in SNB19 GBM cells and transformed human astrocytes. (J) SNB19 cells with Smad4shRNA show reduced *in vitro* invasiveness. (K) THAs with Smad4shRNA show reduced *in vitro* invasiveness. (L) The previously discussed model of TGFβ activation shown with three points involved in TGFβ-mediated invasion, active-TGFβ, TGFβ Receptor, and Smad4 being targeted.**

## Discussion

Previously, our lab has seen that αvβ8 may play a role in primary mouse astrocyte migration. This however was not explored in depth or in the context of glioblastoma multiforme. The data generated and discussed in this chapter is the first to connect aberrant αvβ8 expression and function to invasive pathologies from normal astrocytes to transformed astrocytes to human GBMs.

Primary astrocytes were cultured from pups and the expression was verified. These were then immortalized with E6 and E7 to inhibit p53 and Rb as these proteins are known to experience loss of function in human GBMs. They were split and some cell lots further transformed with HRasV12. Since the mechanism being explored here involves the extracellular signaling, it is of importance to determine that αvβ8 is expressed on the surface. This was verified by biotinylation. It is interesting to note that as the primary mouse astrocytes become immortalized and then transformed they also begin to lose protein expression of both αv and β8 (Figure 2). As this loss is also seen on the cell surface it is likely to influence TGFβ signaling (Figure 1). The reasoning behind this is not clear as later experiments revealed that the majority of GBM cell lines and primary GBMs have higher expression levels of the integrin, though the levels do vary (Figure4)(62). One explanation may be that the primary and GBM cell lines analyzed are high grade GBMs while immediately after transformation the tumors cells are a lower grade.

Other integrin subunits were then analyzed whether they could potentially pair with β8. α5 and α6 are alpha subunits known to bind to β1 in astrocytes but it is unclear whether it has been checked if these interact with β8 on the cell surface.

We determined these subunits do not interact with β8 as a band would have been seen in the 100kDa range; they however are very likely to pair with β1 as is expected (Figure 3). This agrees with previous findings that β8 only pairs with αv. However, it conflicts with previous reports of α5 and α6 pairing with β1 (27,59,136).

Following characterization of transformed mouse astrocytes human GBM cell lines were analyzed. Here it was seen that while αv protein levels remains relatively unchanged in human GBM cell lines the levels of β8 vary (Figure 4). Additionally, it was again observed that a transformation of a primary cell line can cause loss of both αv and β8. This was the case for human astrocytes (Figure 4). Since THAs are more representative of human GBMs than transformed mouse astrocytes this cell type may be the best tool to use in analyzing why the integrin levels drop with immortalization and transformation events. The seven GBM cell lines were further characterized to determine the levels of these proteins on the cell surface. This is important because a difference in total αvβ8 from what is expressed on the surface could indicate defects in integrin transport and blur the conclusions that could be drawn from the hypothesis. However, it was determined that total protein levels and cell surface levels aligned; indicating that when the integrin is knocked down the surface expression is knocked down. Cell lines that were low in total β8 also had low expression on the cell surface. This allows us to hypothesize that cell lines with low endogenous levels of the integrin also have low levels of TGFβ activation, leading to different behaviors.

As angiogenic phenotypes were being discovered by Dr. Tchaicha it was hypothesized that VEGF levels may be influenced by integrin levels which

could further influence invasiveness. With this in mind a cell line with low endogenous β8 levels was chosen to check for basal VEGF expression and this cell line was over-expressed with β8 to record any influence (Figure 5A). This led to an increase in VEGF being secreted from the cells. This difference was so large that multiple clones were generated and the assay repeated many times. Additionally it was noticed that the cells were much longer when β8 was overexpressed (data not shown). This is in conflict with out hypothesis that low β8 leads to more angiogenic tumors. It would be predicted that low levels of the integrin *in vitro* would have high levels of VEGF to correlate with the large amount of vascularization seen in the *in vivo* tumors. However, it is interesting that this trend was not seen in LN229 and SNB-19 cells with β8shRNA, indicating there may be a factor exclusive to U87 cells that allows for this sensitivity. However, this statement is hard to claim because THA cells with β8shRNA showed ~60% less VEGF is secreted following knockdown of the integrin (Figure 5). This suggests that the results seen may not be the result of differences in cell type, but as a different in *in vitro* vs. *in vivo*. It is possible that communication with another cell type or the stroma of the tumor is influencing the signaling pathway in a way that VEGF is upregulated when the integrin is knocked down *in vivo*.

As previously mentioned, β8 was knocked down in LN229 and SNB-19 cell lines, which normally express high levels of the integrin. These utilized bicistronic expression of GFP and β8shRNA which allows for modulation of β8 levels by *Fluorescence Activated Cell Sorting (FACS*). From here the best β8 and αv targeting shRNAs were determined and chosen for further experiments. An in-

vitro growth assay was performed to determine potential growth differences with the integrin knocked down (Figure 6C and 7B). There were no growth differences between non-targeting and β8 targeting shRNA; however this was not true for αvshRNA. Cells with αv knocked down die after the first attempt at passaging or if left to grow unpassaged. This indicated the need for αv in cell survival. If trypsinized they would not adhere to a new culture dish, also indicating a disruption in adhesion. The need for αv for adhesion and survival was also seen with αvsiRNA (data not shown). For these reasons pLB-αvshRNA LN229 and SNB19 cells were not pursued for further in-vitro work. However, it remains to be seen whether αv integrin is required for in-vivo cell survival. Since knocking down β8 did not results in a difference it is likely that the cause is one of the other integrins that associates with αv. This may be αvβ3 or αvβ8. It also possible that no single integrin is responsible and knocking down multiple integrins is required for this effect in cell survival to occur. Additionally, β8 knockdown declined in LN229 and SNB-19 cells as they were passaged (data not show). Therefore consideration was taken to use cells only a few passages after sorting.

In contrast to human GBM cells, $\alpha v^{-/-}$ mouse transformed astrocytes (mTA) are able to adhere. Both of these cell types were analyzed by migration assay. While WT cells filled the wound $\alpha v^{-/-}$ mTA cells did not fill it at all. This appears as though the cells do not migrate whatsoever (Figure 8 and 9). The striking difference can be attributed to $\alpha v^{-/-}$ cells having no αv-associated integrin pairs forming, rendering their signaling and adhesion less functional. Further investigation though proved that the cells were not stopping all together, but were

just not moving across the wound region (data not shown). The cells were still motile as they move up and down the scratch region. These cells were also allowed to grow with a scratch region present until they became over confluent and died. They still would not cross the scratch. Though real time video capture cannot be displayed Figure 9 best represents the pattern of cells just after the scratch is made. Note the original scratch is not a smooth line (Figure 9). A rescue experiment was then attempted to see whether WT mTA cells could rescue the migration defect seen when αv is knocked out. It was anticipated that the inability of $\alpha v^{-/-}$ mTAs to activate TGFβ could be rescued by allowing WT cells to activate it. To distinguish between cells the WT and $\alpha v^{-/-}$ mTAs were given stably expressing RFP and GFP, respectively. After imaging separately to confirm the phenotypes while expressing the GFP and RFP proteins, the cells were mixed in a 50:50 ratio and then scratched and imaged. This revealed not only that WT cells could not rescue the knockouts, but they could prevent the WT cells from moving into the wound region. While WT cell migration into the scratch region was not 100% it was severely disrupted (Figure 10). Additionally it could be seen that an occasional $\alpha v^{-/-}$ cell could move into the scratch region but only so long as they were adhered to a WT cell. This suggests they had not lost all adhesive function as other cells could adhere to them. This is interesting because the knockout cells are able to adhere to other cell types and to the surface of the dish, yet do not fill the wound. Additionally exogenous active-TGFβ was added to these cells to see if the phenotype could be rescued, but this was not the case (data not shown). The scratch experiment was also duplicated with 293T cells stably expressing GFP. This non-astrocytic cell line

does not express β8 yet is able to migrate to fill in a scratch (data not shown). When mixed, it was seen that the $\alpha v^{-/-}$ mTAs also inhibited the 293T cells from crossing into the scratch region. This suggests that regardless of the whether a cell is of astrocytic origin $\alpha v^{-/-}$ mTAs would be able to inhibit their migration. This was the first evidence that I came across that suggests behavior of a second pathway that is independent of TGFβ activation. One possibility is that there are secreted factors the $\alpha v^{-/-}$ mTAs secrete that inhibit invasiveness. This hypothesis was initially tested by taking media conditioned by $\alpha v^{-/-}$ mTAs and placing it onto WT mTAs before conducting a scratch assay. This however did not result in a rescue of the phenotype (data not shown). If secreted factors did not alter the migration of the cells it was next thought that there may be a second mechanism that is independent of TGFβ activation. Since TGFβ activation was known to be taking place through the extracellular portion of β8 it was predicted that the cytoplasmic tail of the integrin was likely to be playing a role. Additionally, it may be possible that knocking out αv results in transcriptional differences that alter the expression of cell adhesion molecules such as cadherins. In the same line of thought it may also be possible that knocking out αv associated integrins results in a different expression of unknown αv-associating adhesion molecules. This might be tested by utilizing electric cell-substrate impedance sensing (ECIS) instrumentation. This consists of electrode arrays of gold with a surface area for the cells to attach. This allow for the resistance of cells on the tissue culture grade surface to be recorded. Changes can be measured between cell types with those that have high resistance having more cell-cell contacts. Additionally, these interactions can be distinguished from cell-

ECM contacts for more specific characterization. One potential mechanism might involve the integrins altering the recycling of cadherins(143). It may be possible that the αv associated integrins can signal through Src or integrin-linked kinase could upregulate the transcriptional repressors SLUG, SNAIL, and Src-family kinase to prevent the transcription of E-cadherin.

Following these mouse data a human cell line was sought. THAs with and without β8 knockdown were run through a scratch assay where it was determined that migration decreased with loss of the integrin. Exogenous active TGFβ was also added and it was seen that the phenotype could indeed be partially rescued (Figure 11). With a difference in migration being noticeable with down regulation of β8 polarity proteins were of interest. Therefore these THAs were allowed to partially migrate and then stained for actin and focal contacts. This revealed that normal THAs polarize into the wound region as expected with focal contacts at the leading edge and actin aligned in the direction the cells move. However, when β8 is knocked down with shRNA this is not the case. The cell contacts are on all sides of the cell and the actin shows up in a #-hashed form with the actin in many different directions. These indicated a disruption in polarity proteins that we wished to pursue (Figure 12).

Following a discovery of this role in migration effort was made to determine if these findings extended into *in vitro* invasion assays, something more closely mimicking the brain. First primary mouse astrocytes were examined by invasion assay. Here it was seen that when β8 is knocked out the cells invade about 40% less than WT cells. Additionally, when αv is knocked out, invasion is

almost entirely stopped (Figure 14A). Similar results were seen with transformed mouse astrocytes. When β8 was not present in the cells invasion dropped by over 50%, and it dropped over 95% when there were no αv-associated integrin pairs present (Figure 13B). This defect in invasion could be rescued by overexpressing β8 in $\beta8^{-/-}$ mTAs where it was seen that these cells invade about 60% faster than mock transfected $\beta8^{-/-}$ cells (Figure 13C). GBM cell lines were then analyzed. SNB-19 cells with β8siRNA was compared to scrambled siRNAs where it was seen that silencing integrin expression reduced invasion by about 50% (Figure 14A and 14B). A similar 50% reduction in invasiveness was seen in LN229 cells treated with β8siRNA (Figure 14 C and D). This was taken a step further with the use of a specific shRNA as opposed to the pool of siRNAs being used. LN229 and SNB-19 cells were stably transfected with β8shRNA and it was also seen that this reduced their invasiveness by about 65% and 55%, respectively (Figure 15A and 15B). Additionally two more alternative β8shRNAs were placed into LN229 cells where it was seen that these less efficient shRNAs were able to reduce invasiveness by about 40% each (Figure 16B). THAs were also checked for their response to a drop in β8 expression. They were given the same shRNA used with LN229 and SNB-19 cells , which significantly knocked the integrin down, resulting in about 80% reduction in invasiveness (Figure 17B). Here we see that in primary and transformed mouse astrocytes with the integrin knocked out as well as in transformed human astrocytes and GBM cell lines with the integrin knocked down (with both siRNA and multiple shRNAs) that β8 integrin reduces *in vitro*

invasiveness. Through these experiments we can reasonably state that β8 plays a major role in *in vitro* and warrants *in vivo* investigation.

Following these results the role of extracellular TGFβ signaling was probed. First it was determined that knocking out/down the integrin with shRNA reduces its total expression as well as its expression on the cell surface. WT and $\beta8^{-/-}$ mTAs were examined and shown to have no β8 expression on the cell surface. SNB-19 and LN229 cells with β8shRNA were shown to have reduced expression of the integrin on their cell surface when it is knocked down (Figure 18B and 18C). Additionally, when LN229 cells were biotinylated and αv was pulled down, a reduced size band was seen at the 100kDA mark. This is the same weight as β3, β5, and β5. However, since this band weakened significantly from the NTshRNA cells it is likely that β8 is the main integrin present.

With the knowledge that β8 surface expression was decreased in cells with β8 knocked down, the effect of extracellular TGFβ activation was analyzed. To accomplish this methods were explored to interrupt SMAD signaling downstream of the TGFβ receptor. This involved targeting TGFβ Receptor I and TGFβ itself. A monoclonal antibody specific for TGFβ was shown to be able to bind to active TGFβ and prevent its ability to induce downstream SMAD3 phosphorylation (Figure 18D). A small molecule inhibitor was used to target TGFβRI, which is required to pair with TGFβRII to induce downstream SMAD signaling (Figure 18E). When active TGFβ binds to the TGFβ receptor, SMAD2 and SMAD3 are normally autophosphorylated. With the inhibitor it was seen that there was a reduction in the phosphorylation of these SMADs in a dose dependent manner. These signaling disrupters were

subsequently shown to reduce the invasiveness of LN229 cells without affecting proliferation (Figure 18F and 18G). Since β8 activates TGFβ which signals through the SMAD receptors this was expected. Additionally a third target, SMAD4 was hit with shRNA (Figure 18I). After SMAD2 and SMAD3 are autophosphorylated, they are translocated to the nucleus by SMAD4. When the Smads were phosphorylated they were not able to be transported into the nucleus by Smad4 when the shRNA was added (Figure 18I). This led to a 50% reduction in invasiveness for SNB19 cells and about a 60% reduction in *in vitro* invasiveness for THAs (Figure 18J and 18K). Despite the drop in invasiveness correlating with the drops when β8 is knocked down in these cells, it is still possible that alternative integrins could be responsible for a percentage of the TGFβ activation. While I recognize that these unknown integrins may be responsible for residual TGFβ activation, β8 is the major integrin in TGFβ signaling (Figure 18H).

Taken together these data indicate that αvβ8 is an important player in human GBM invasiveness when analyzed from an in-vitro perspective. This integrin is responsible for translating ECM cues, that is inactive-TGFβ, into signals read by GBM cells and likely other cell types such as endothelial cells in the tumor niche.

**Chapter 4:**

**αvβ8 Intracellular Signaling: A Novel Mechanism of αvβ8 Cytoplasmic Tail Signaling and its Role in Glioma GTPase-Mediated Invasiveness.**

**Introduction:**

In this chapter we extended our studies of αvβ8 integrin from in-vitro extracellular adhesion studies to intracellular signaling roles that include in-vivo results. Previously we saw changes in polarity (Figure 12). Here were chose to pursued this phenotype and examined the activities of common polarity proteins Rac1, Cdc42, and RhoA. Additionally, a previous report has shown that the cytoplasmic tail of β8 may bind to Rho GDI-1. However, this system was artificial as it used a chimeric IL-2R/β8 to see if GDI bound. Despite this though, it is an attractive possibility that the integrin may be binding to this GDI which could signal to a GTPase and influence cell polarity. GDIs, or GDP dissociation inhibitors, inhibit the dissociation of GDP from GTPases. This allows them to regulate the GDP-GTP exchange reactions required for GTPase function and thus cell motility. Additionally, with only in-vitro previous wor, here we seek answers that can be given to us in an in-vivo context. Through this study we hope to better understand how changes in β8 levels can influence the invasiveness of GBM cells and hone in on what role it may be playing in patients.

**Integrin β8 suppresses Rac1 and Cdc42 GTPase activity**

LN229 cells were treated with the siRNA previously discussed (Figure 14C) and checked for PAK1 phosphorylation (Figure 19A). It was seen that knocking down the β8 integrin increased PAK1 phosphorylation, a readout for GTPase activity. This same lysate was used to also check RAC1, Cdc42, and RhoA basal levels and activation state. It was seen that Rac1 and Cdc42 are activated when the integrin is knocked down, however the RhoA activation state remains the same (Figure 19A). Additionally, LN229 cells had β8 knocked down using two separate shRNAs (Figure 19B). This also showed that PAK1 phosphorylation increases when the integrin is knocked down. B8 knockout transformed mouse astrocytes were also analyzed for Rac1, Cdc42, RhoA, and PAK1 activity. It was also seen here that the complete loss of β8 results in an increase in Rac1 activity (Figure 19C), and Cdc42 activity (Figure 19D). RhoA levels remained unchanged (data not shown) and PAK1 was phosphorylated (Figure 19E). Previously described β8-/- cells were transfected to over-express β8 (Figure 5A) and checked for their potential to activate Rac1 and phosphorylated PAK1. It was seen that expressing β8 in cells with it knocked out resulted in rescue with PAK1 phosphorylation and Rac1 activity both decreasing.

**Figure 19.**

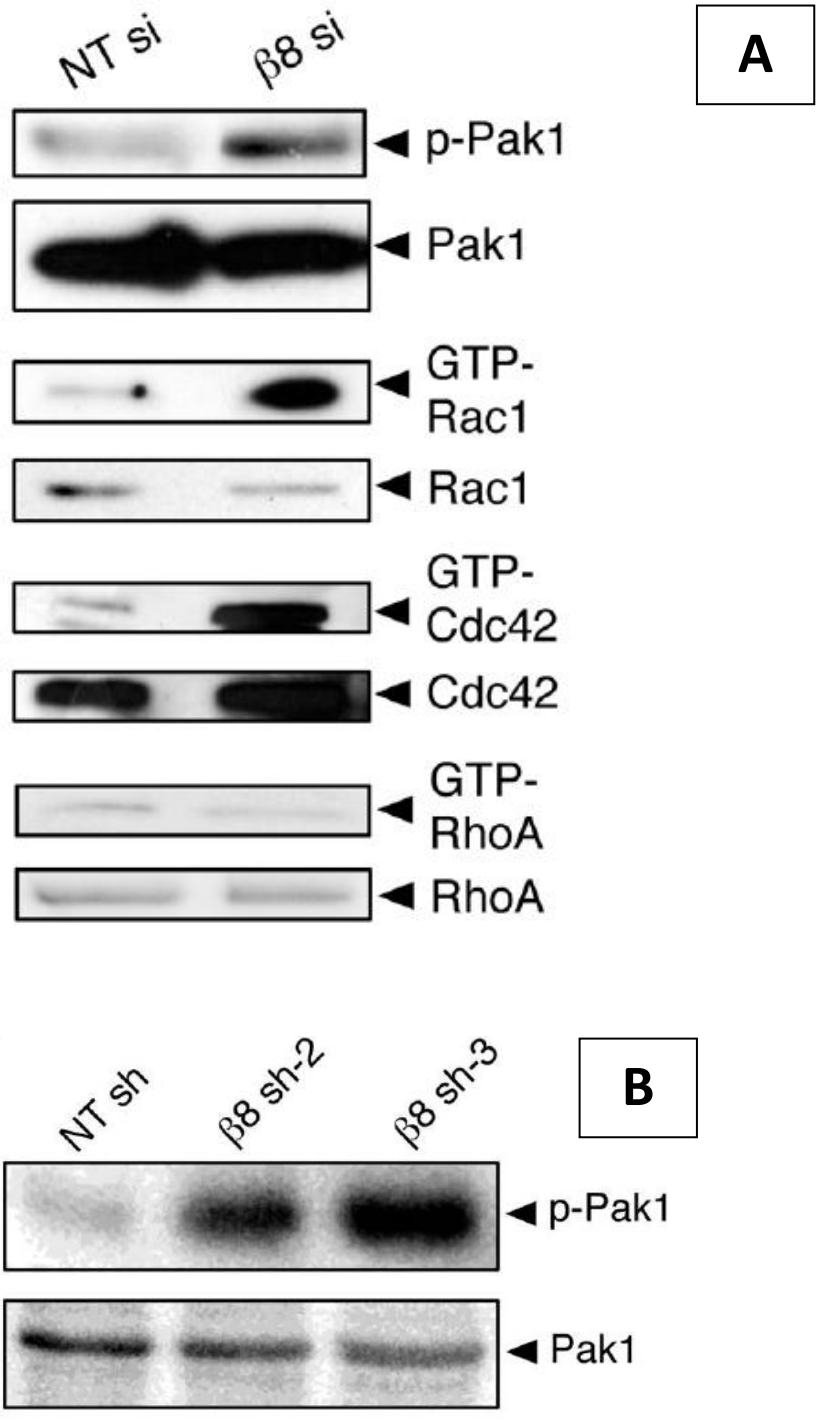
A
NT si
β8 si
p-Pak1
Pak1
GTP-
Rac1
Rac1
GTP-
Cdc42
Cdc42
GTP-
RhoA
RhoA
B
NT sh
β8 sh-2
β8 sh-3
p-Pak1
Pak1

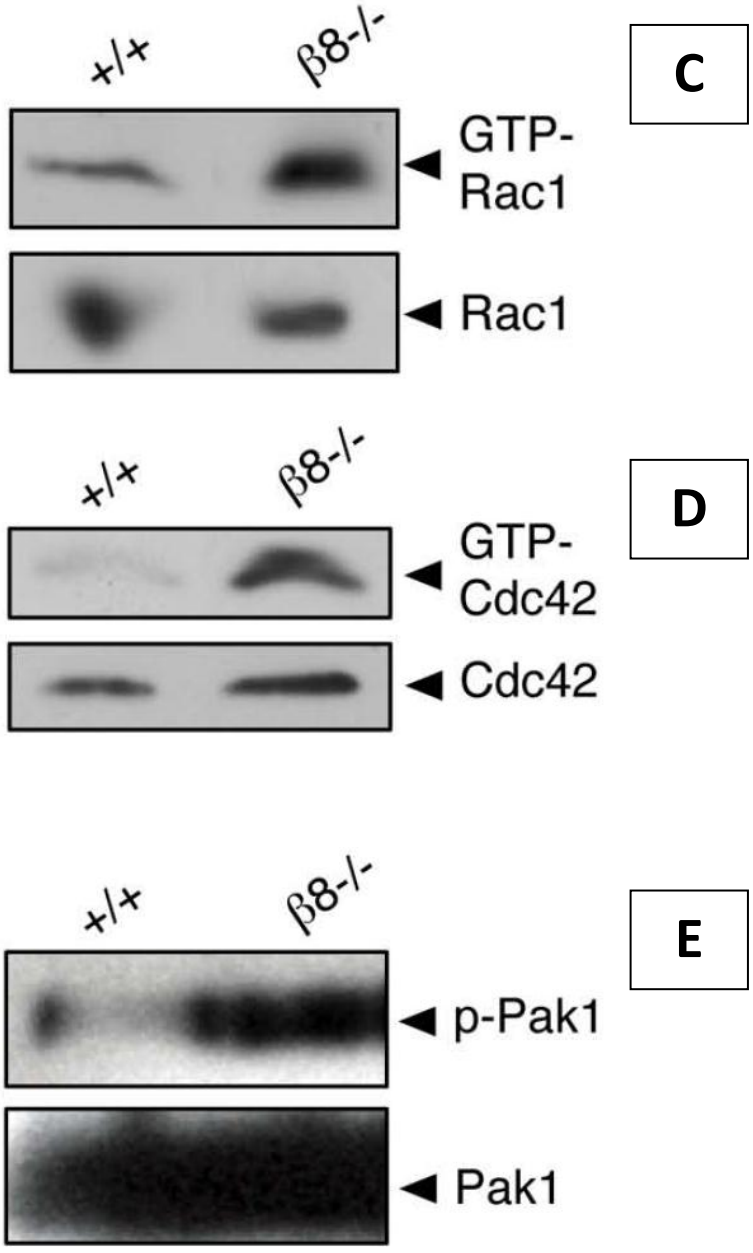
+/+
β8-/-
C
GTP-
Rac1
Rac1
+/+
β8-/-
D
GTP-
Cdc42
Cdc42
+/+
β8-/-
E
p-Pak1
Pak1

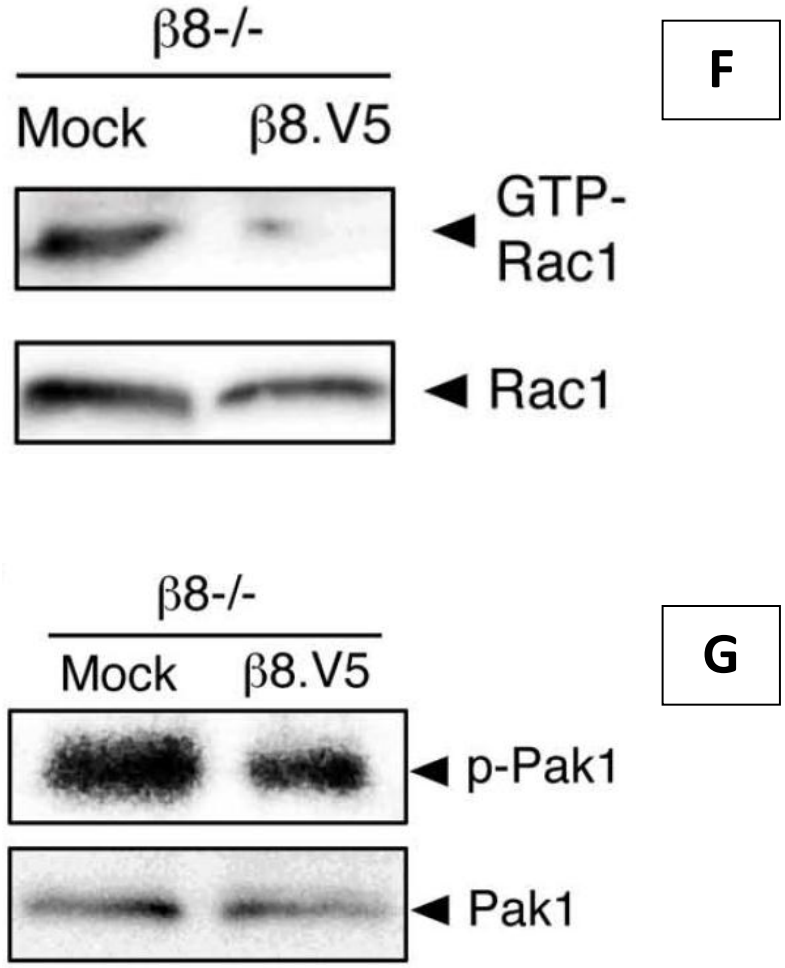


**Figure 19. Pak1 is Phosphorylated and Rac1 and Cdc42 are Activated in a β8 Dependent Manner**

**(A) LN229 cells treated with non-targeting and β8 targeting siRNA were examined by western blot for PAK1 phosphorylation and total PAK. They were also checked for RAC1, Cdc42, and RhoA activation. Note the increased levels of phosphorylated PAK1, active Rac1, and active Cdc42. The same siRNAs were used in figure 14C. (B) LN229 cells with β8 knocked down using two different shRNAs. Note the increased PAK1 phosphorylation when less integrin is present. WT and $\beta8^{-/-}$ transformed mouse astrocytes were analyzed for (C) Rac1 activation, (D) Cdc42 activation, and (E) PAK1 phosphorylation. $B8^{-/-}$ transformed mouse astrocytes were over-expressed with β8 and analyzed for (F) Rac1 activation and (G) PAK1 phosphorylation.**

**GDP Dissociation Inhibitor (GDI) Plays a Role in GTPase Activation and GBM Invasion**

Human GBM cell lines LN229 and SNB-19 were analyzed by western blot for Rho GDI-1 and Rho GDI-2 expression. It was determined that all of these cell lines expressed these GDIs and this expression was not affected by altering the level of integrin β8 (Figure 20A). LN229 cells were then transfected with GDI1 targeting siRNA. When GDI1 was knocked down no effect was seen on expression levels of β8. Additionally, when GDI1 was knocked down PAK-1 phosphorylation was up-regulated. Rac1 and Cdc42 were also hyper activated when compared with the control, non-targeting siRNA cells that had endogenous expression levels of GDI-1 (Figure 20B). This also corresponded with invasive characteristics. When GDI-1 was knocked down by siRNA in LN229 cells they became less invasive (Figure 20C). This was also seen in SNB-19 cells. The same Rho GDI-1 siRNA was used to knock down the GDI and the invasiveness of the cells significantly decreased (Figure 20D and 20E).

**Figure 20.**

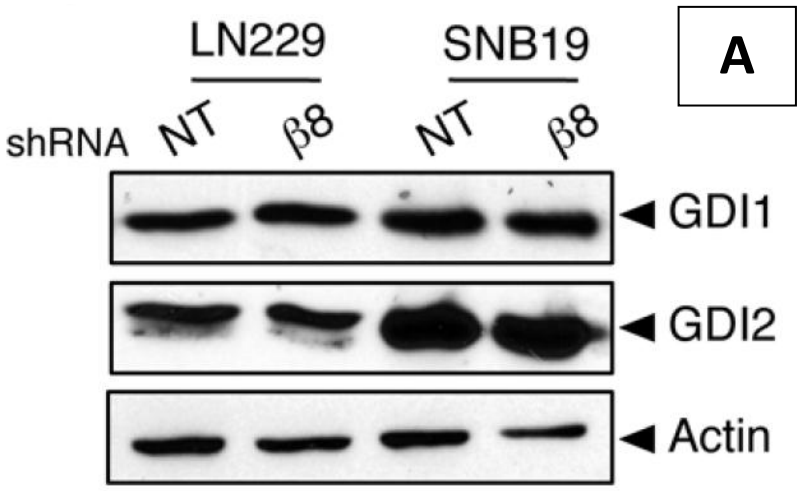

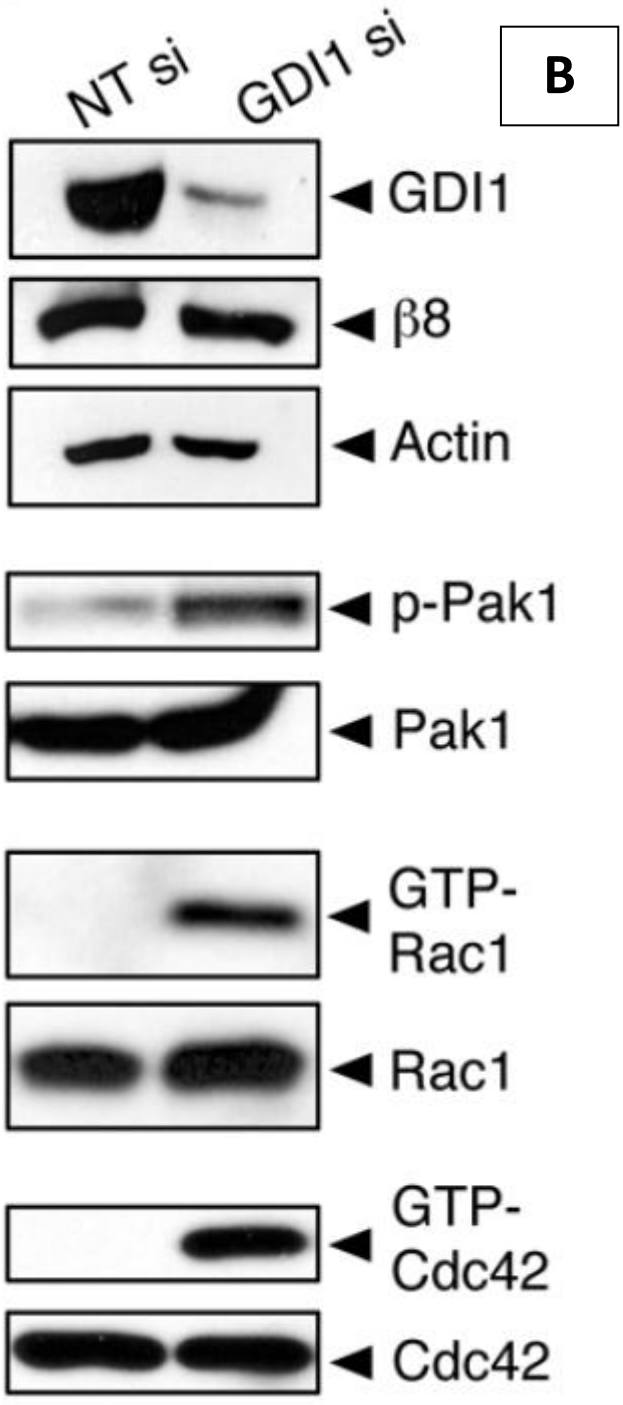
NT si
GDI1 si
B
GDI1
β8
Actin
p-Pak1
Pak1
GTP-
Rac1
Rac1
GTP-
Cdc42
Cdc42

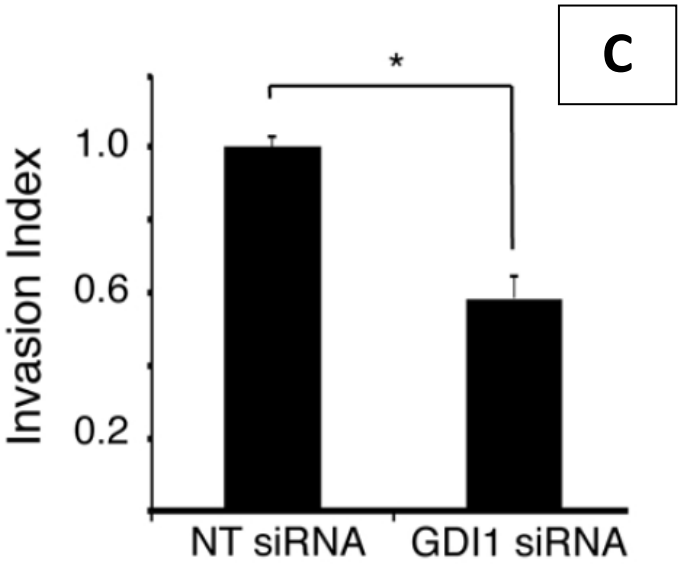
C
*
Invasion Index
1.0
0.6
0.2
NT siRNA
GDI1 siRNA

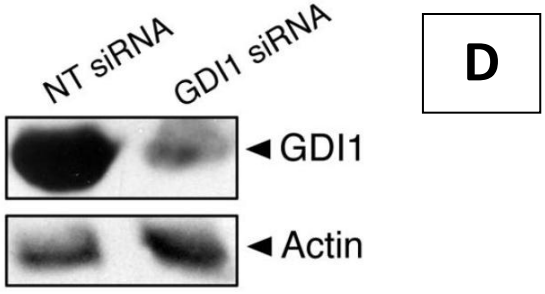
D
NT siRNA
GDI1 siRNA
GDI1
Actin

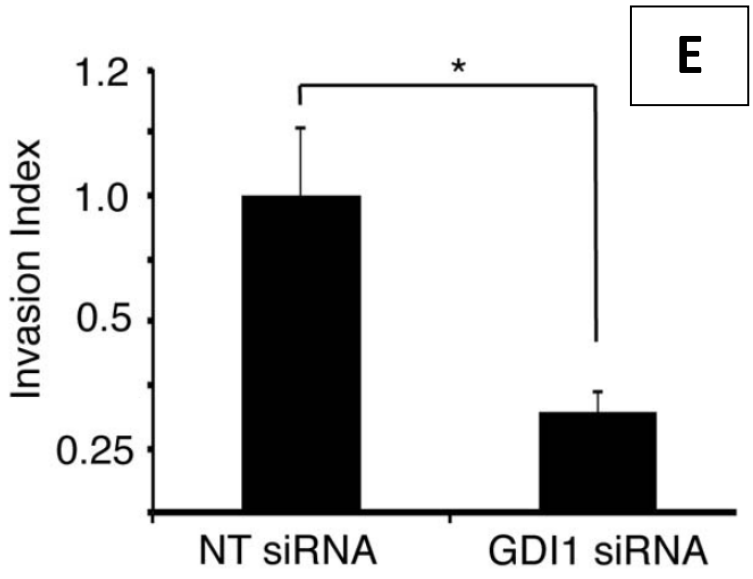
E
*
Invasion Index
1.2
1.0
0.5
0.25
NT siRNA
GDI1 siRNA

**Figure 20. Loss of Rho GDI-1 Activates Rac1 and Cdc42, Phosphorylates Pak1, and Reduces Invasiveness**

**(A) LN229 and SNB-19 cells were analyzed by western blot for protein expression levels of Rho GDI-1 and Rho GDI-2 in cells expressing β8 targeting shRNA. (B) LN229 cells were treated with Rho GDI-1 targeting siRNA and analyzed for GDI-1, β8, PAK1, Rac1, and Cdc42 expression as well as PAK1 phosphorylation. These same lysates were also checked for Rac1 and Cdc42 activation states. (C) LN229 cells treated with Rho GDI-1 siRNA were analyzed by invasion assay. Note the decreased invasiveness of cells with less available GDI-1. (D) SNB-19 cells were treated with RHO GDI-1 siRNA and analyzed by western blot. (E) SNB19 cells treated with Rho GDI-1 targeting siRNA were ran through an invasion assay. Note the substantial decrease in invasiveness that accompanies reduced Rho GDI-1 levels.**

**Constitutive Rac1 Activation Alters Cell Morphology and Reduces Invasiveness**

LN229 cells were transfected with either an empty YFP construct or constitutively active Rac1 tagged with YFP. This was verified by western blot. When blotted for Rac1, endogenous levels were seen, as well as an obvious band at the molecular weight corresponding to the additional 27kDa of the YFP (Figure 21A). These lysates were also probed for YFP. Distinctive bands were seen corresponding the YFP and to YFP-Rac1 (Figure 21B). Upon transfecting it was observed that efficiency was not 100%. The cells that were transfected with the empty YFP construct maintained their elongated morphology. The cells with the YFP tagged constitutively active Rac1 became flattened while the untransfected non-yellow cells in the same dish were still elongated (Figure 21C). This is more obvious at higher magnification (Figure 21D). These cells were sorted for YFP and then run through an invasion assay. It was seen that 50% fewer cells constitutively active Rac1 cells invaded compared to those expressing the empty-YFP construct (Figure 21E). Additionally, after the cells invaded through the membrane they were imaged before the membrane was stained and counted. The cells with empty-YFP invaded through as yellow cells. The YFP-Rac1 cells that invaded through were weakly expressing YFP (Figure 21F). As YFP expression is tied to the amount of active Rac1 in these cells, this suggests that the cells with higher expression of constitutively active Rac1 did not invade.

**Figure 21.**

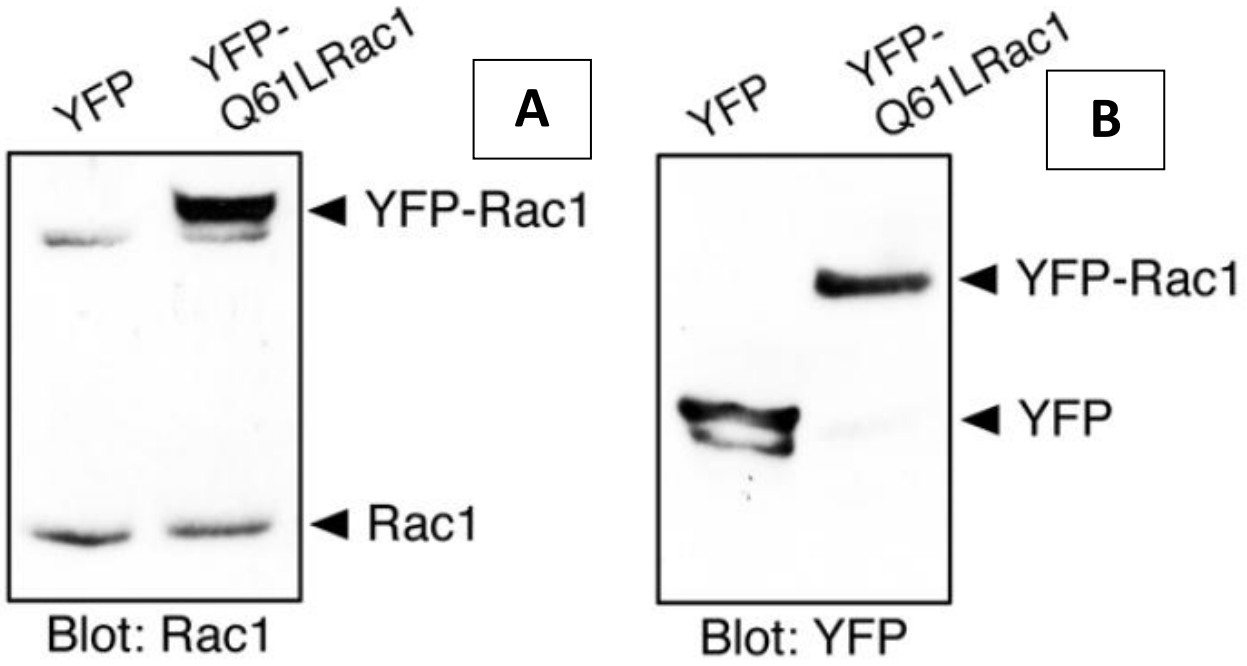
YFP
YFP-Q61LRac1
A
YFP-Rac1
Rac1
Blot: Rac1
YFP
YFP-Q61LRac1
B
YFP-Rac1
YFP
Blot: YFP

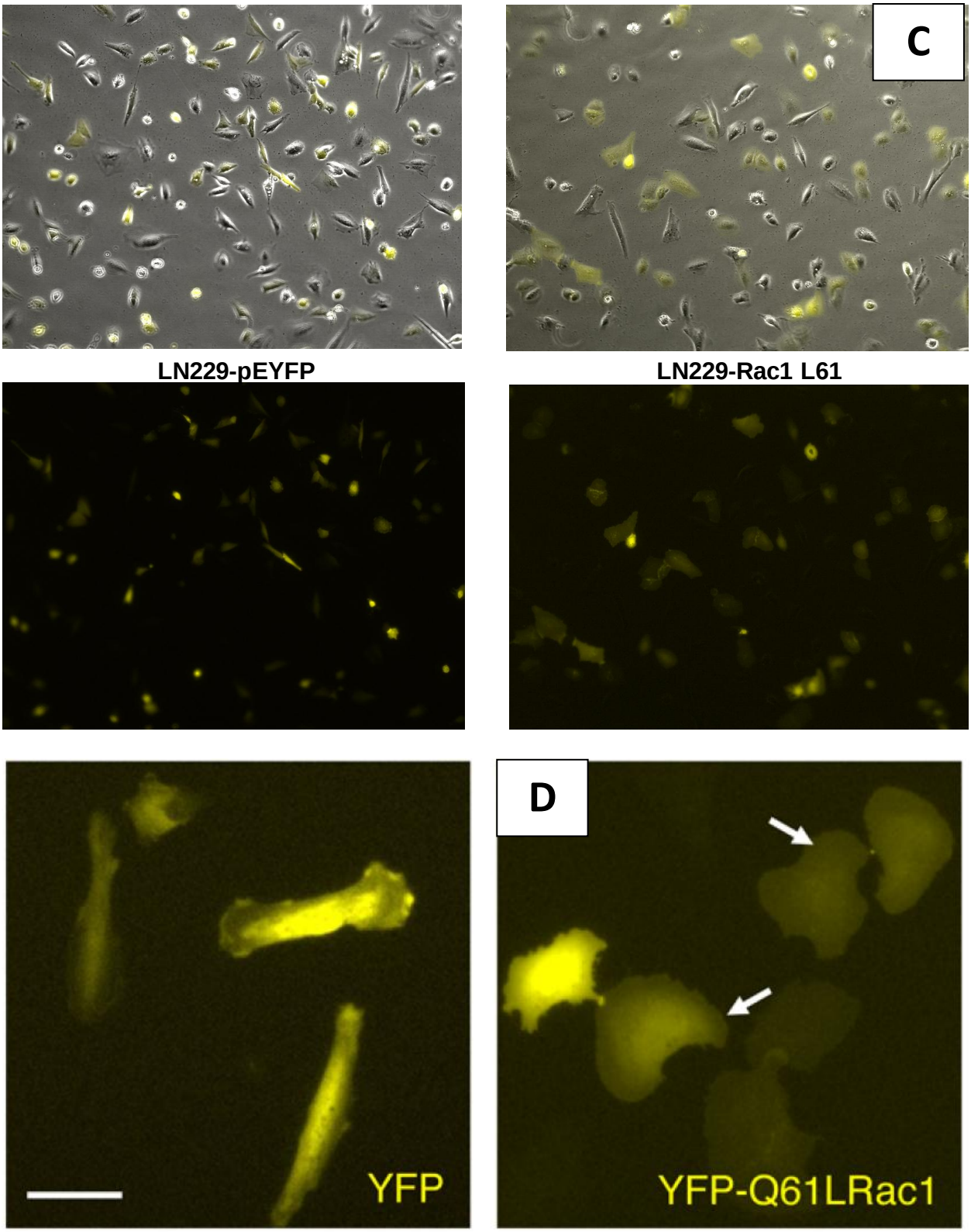
C
LN229-pEYFP
LN229-Rac1 L61
D
YFP
YFP-Q61LRac1

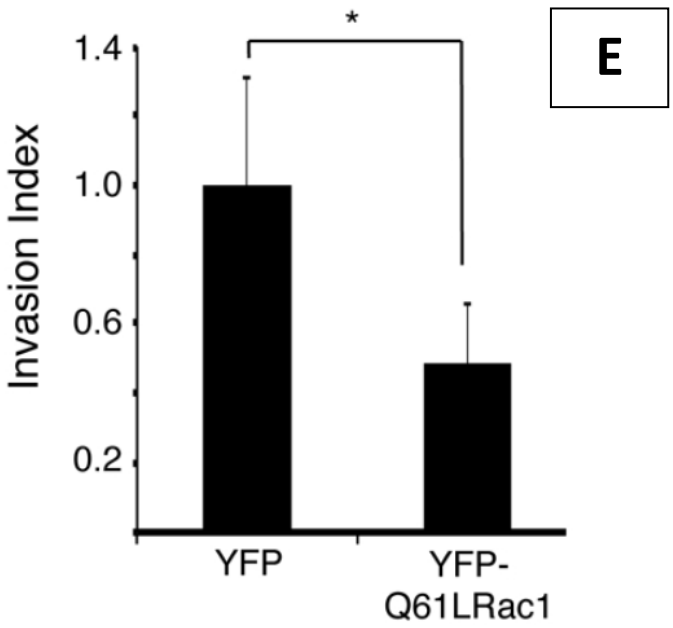
E
*
1.4
1.0
0.6
0.2
Invasion Index
YFP
YFP-
Q61LRac1

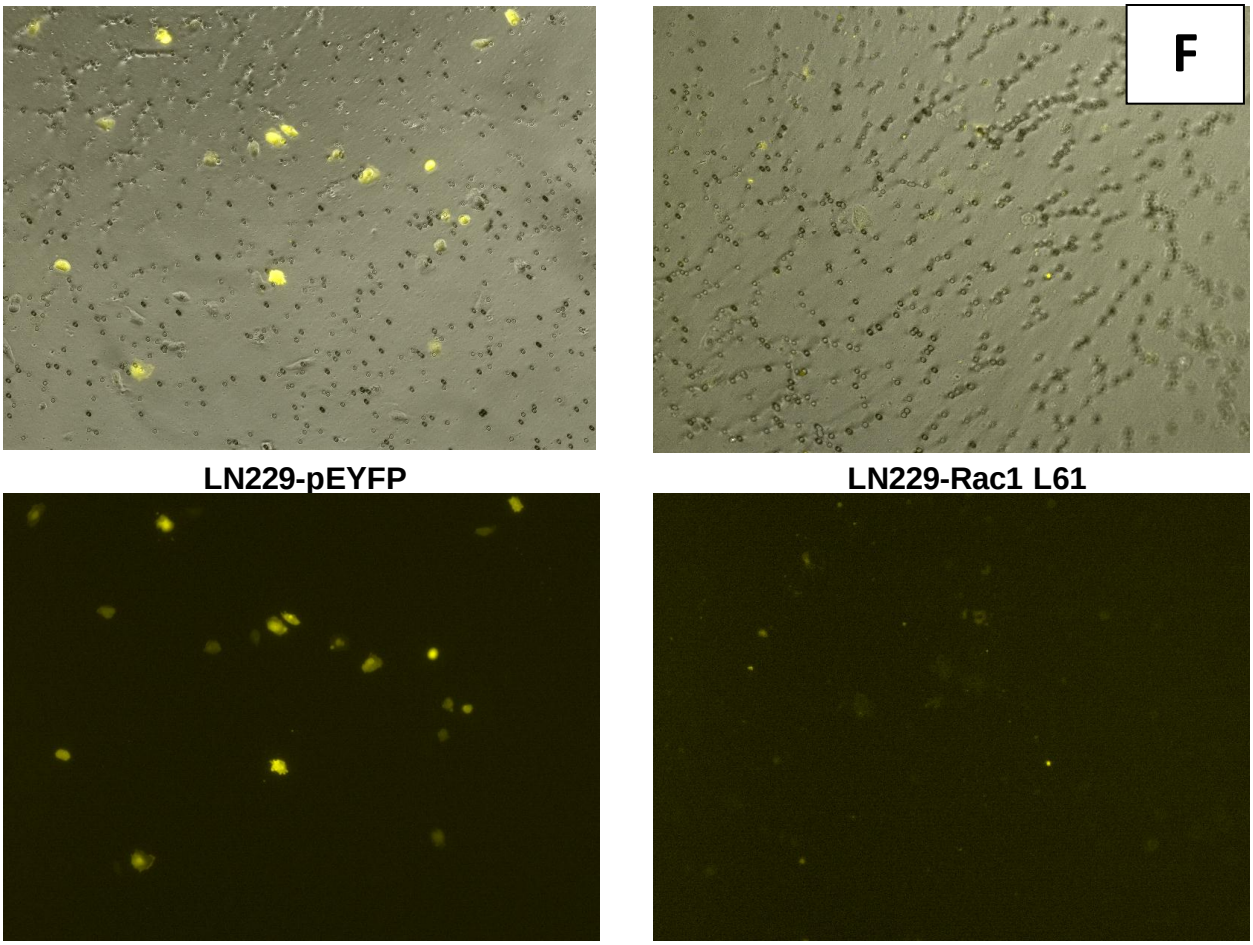


**Figure 21. Hyperactive Rac1 Induces Morphological changes and Reduces Invasion in LN229 GBM Cells**

**(A) LN229 cells were transfected with an empty YFP or a constitutively active Rac1 tagged with YFP. Western blot was used to verify Rac1 expression and also (B) YFP expression. (C) LN229 cells transfected with YFP and YFP-Rac1 were imaged 48 hours after transfection. The top panels show with bright-field and YFP images over layed. The bottom panels show just YFP. (D) LN229 cells transfected with YFP and YFP-Rac1 were imaged at a high magnification with the YFP filter. Note the elongated cells with the empty construct and the flattened morphology of those expressing constitutively active Rac1. Scale bar 60μm. (E) Sorted cells were run through an invasion assay. Note the decrease in invasiveness when Rac1 in constitutively active. (F) After 24 hours the invasion assay membranes were imaged. The top panels show bright field overlaying YFP and the bottom panels display YFP only. Note the weak expression of YFP among cells that invaded expressing active Rac1.**

**Rho GDI-1 Binds to Integrin β8**

LN229 cells were transfected with plasmids expressing GFP or GFP tagged Rho GDI-1. Additionally, one set of GRP-RhoGDI1 was treated with β8 targeting siRNA. These were then immunoprecipitated with mouse anti-GFP antibody and blotted with rabbit anti-β8 (top) or rabbit anti-GFP (bottom) antibodies (Figure 22A). Here it can be seen that Rho GDI-1 binds to integrin β8 and when the integrin is knocked down, less GDI can be pulled down by immunoprecipitation. The opposite immunoprecipitation was then carried out on these cells. They were immunoprecipitated with goat anti-β8 and blotted with mouse anti-GFP and rabbit anti-β8 (Figure 22B). When β8 was pulled down GFP can be seen just below the heavy chain. This indicates Rho GDI-1 binds to integrin β8.

**Figure 22.**

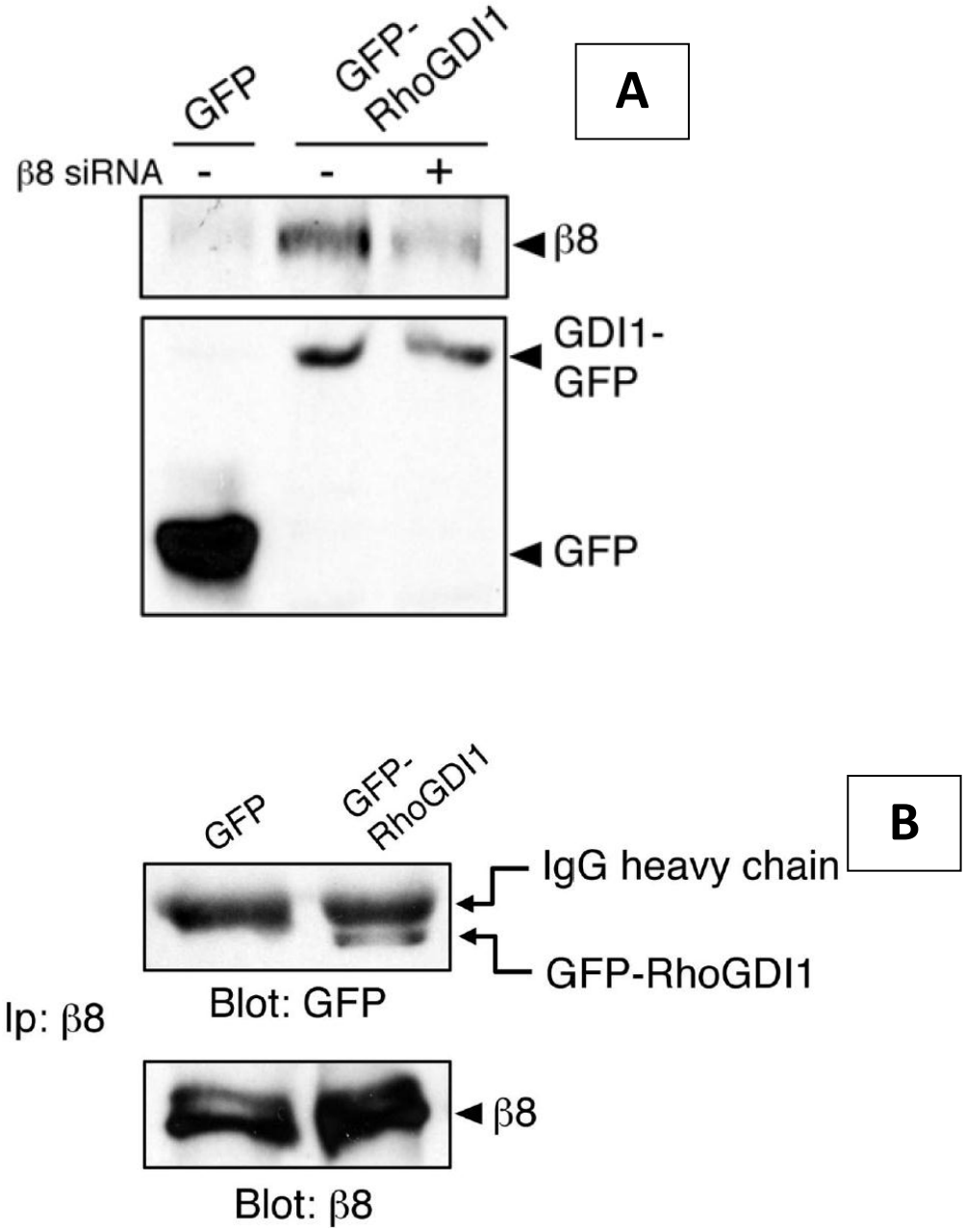


**Figure 22. Rho GDI-1 Co-Immunoprecipitates with β8 in LN229 GBM Cells**

**(A) LN229 cells were transfected with either GFP or GFP tagged Rho GDI-1. They were then immunoprecipitated with GFP and blotted for GFP or β8. Additionally, one set of cells was treated with β8 targeting siRNA. Note the**

**band indicated Rho GDI-1 is being pulled down and how this is reduced by reducing β8 expression. (B) Empty-GFP and GFP-RhoGDI1 cells were immunoprecipitated with β8 and blotted for either GFP. Note the band corresponding to GFP-RhoGDI1 being pulled down. The bottom blot shows immunoprecipitation with β8 and then blotting with β8. This reveals that β8 is indeed being pulled down in the first step.**

**Rho GDI1 Binds to the Cytoplasmic Tail of Integrin β8**

293T cells with no endogenous β8 were infected with lentivirus to express full length or truncated β8. These were verified by blotting with a cytoplasmic β8 specific antibody and an antibody targeting the extracellular portion (Figure 23A). When the extracellular β8 targeting antibody is used it can be seen that the truncated β8 expressed in the cells is a lower molecular weight than the full length. These cells were then biotinylated and immunoprecipitated with αv. The present band indicates that truncated β8 is still able to pair with its αv subunit (Figure 23B). Additionally, the full length and truncated β8 were placed into $\beta8^{-/-}$ transformed mouse astrocytes. This was verified by western blot where again the truncated β8 is seen to have a lower molecular weight as would be expected (Figure 23C). Additionally, Rac1 activation and Pak1 phosphorylation were checked to see if the signaling could be rescued. $\beta8^{-/-}$ cells with truncated β8 were seen to have similar levels of Rac1 activation to those without the integrin (Mock) (Figure 21C). However, cells with full length β8 had significantly less Rac1 activation. A similar trend was seen for Pak1 as cells with full length β8 are less phosphorylated than those with truncated β8 or no β8 (Figure 21C). These cells were then run through an invasion assay where it was seen that cells with no β8 and those with cytoplasmically truncated β8 invade at similar rates while cells with full length β8 invade about 40% faster (figure 23D).

**Figure 23.**

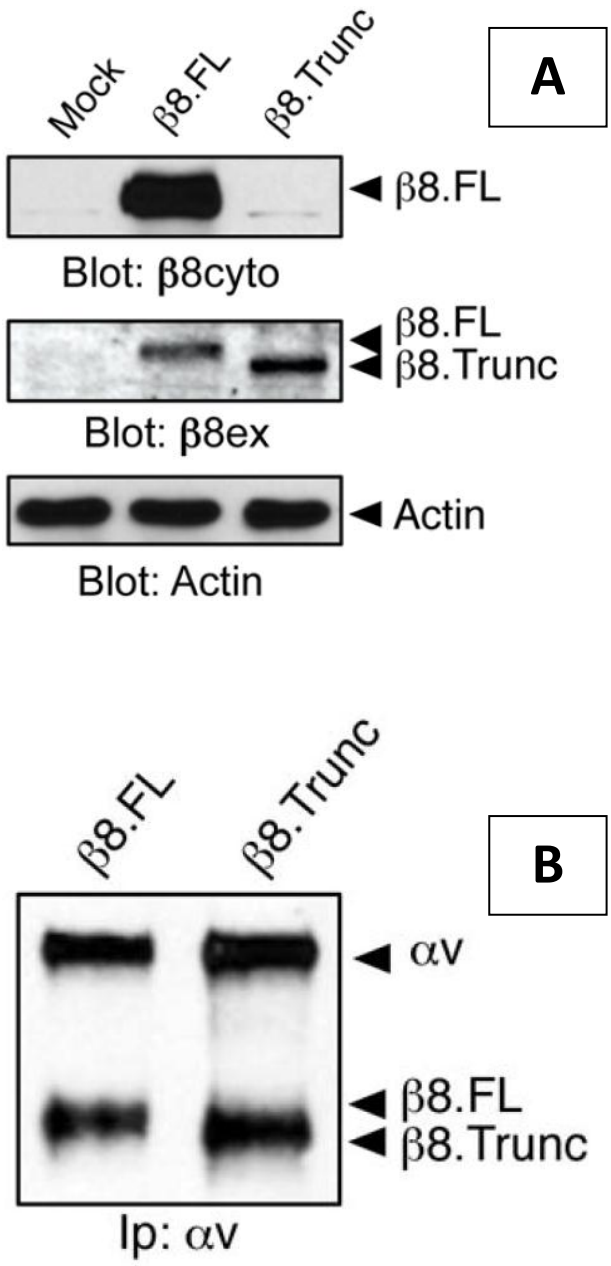
A
Mock
β8.FL
β8.Trunc
β8.FL
Blot: β8cyto
β8.FL
β8.Trunc
Blot: β8ex
Actin
Blot: Actin
B
β8.FL
β8.Trunc
αv
β8.FL
β8.Trunc
Ip: αv

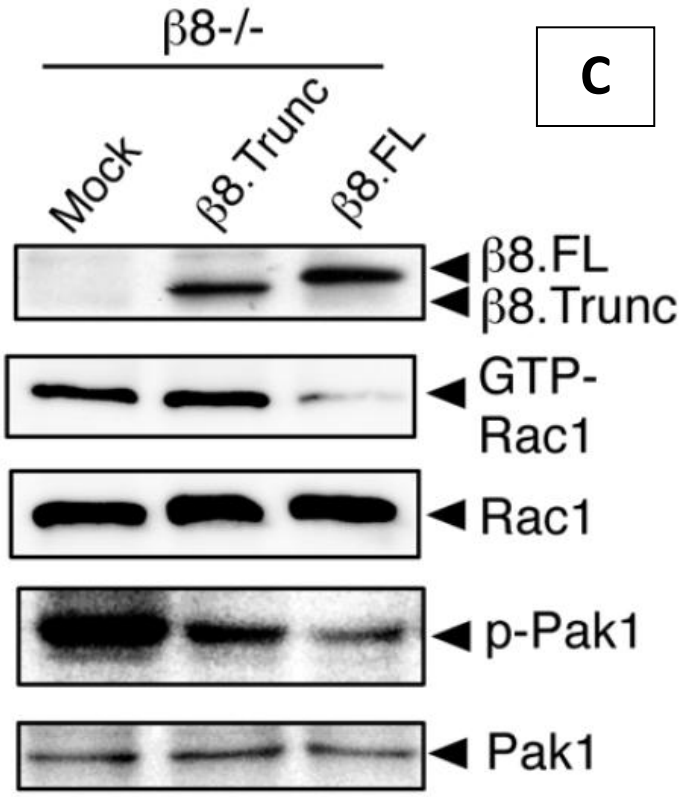
β8-/-
C
Mock
β8.Trunc
β8.FL
β8.FL
β8.Trunc
GTP-
Rac1
Rac1
p-Pak1
Pak1

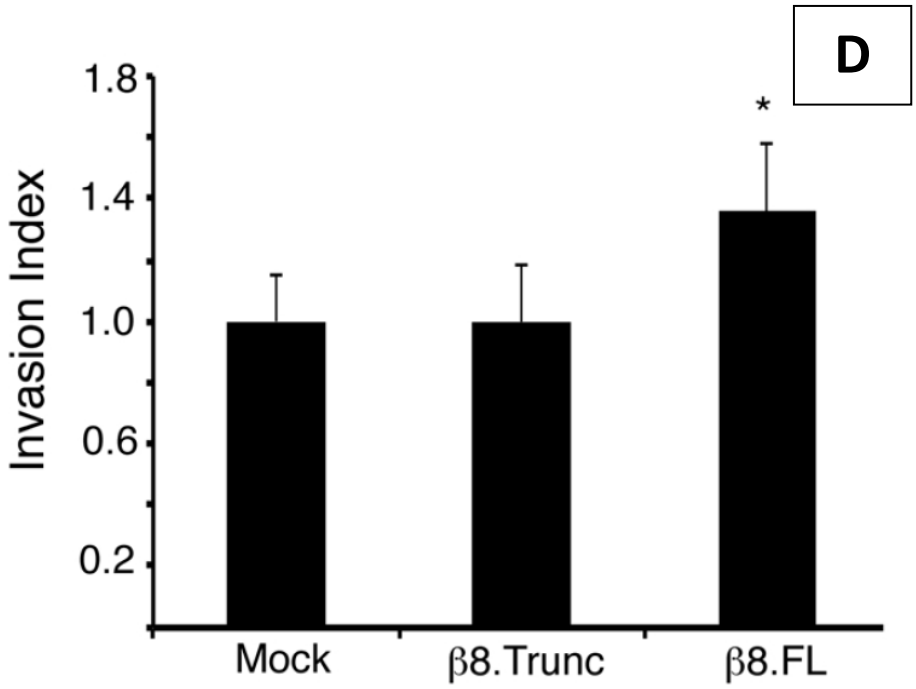
D
Invasion Index
1.8
1.4
1.0
0.6
0.2
*
Mock
β8.Trunc
β8.FL

**Figure 23. Rho GDI-1 Interacts with the Cytoplasmic Tail of β8 and Mediates Cell Invasion**

**(A) Full length and cytoplasmically truncated β8 were added to 293T cells which have no endogenous β8 but do have endogenous αv. A cytoplasmic specific β8 antibody was used to verify expression of the full length protein and no expression of truncated protein. (B) 293T cell expressing the full length and truncated β8 proteins were biotinylated and immunoprecipitated with and an-αv antibody. Note how β8 is able to bind with 293T's endogenous αv. (C) $\beta 8^{-/-}$ cells with and without full length and truncated β8 were checked by western blot for β8, Rac1, and Pak1 expression. Additionally, Pak1 phosphorylation and Rac1 activity were also checked. Note the low activity of Rac1 and the low phosphorylation of Pak1. (D) These cells were also ran through an invasion assay. Note the increased invasiveness of cells with full length β8 compared to those with truncated or no β8.**

**Human Patient GBMs Display High Levels of Integrin β8**

Immunohistochemistry was performed on human GBM sections. The following representative images show staining with goat IgG and goat anti-β8 (Figure 24A and 24B). The reactivity and specificity of the β8 antibody is evident in the copper toned staining (Figure 24B). This antibody was used on tumor sections that also had a section of normal non-tumorigenic brain (Figure 24C). The top panel shows a low level of β8 expression while the bottom panel shows a tumor margin with extremely high levels within the tumor. Four human GBM sections from the center of the tumor were also stained (Figure 24D). These reveal the large amount of integrin β8 within the tumor and the lack of β8 in intratumoral blood vessels.

**Figure 24.**

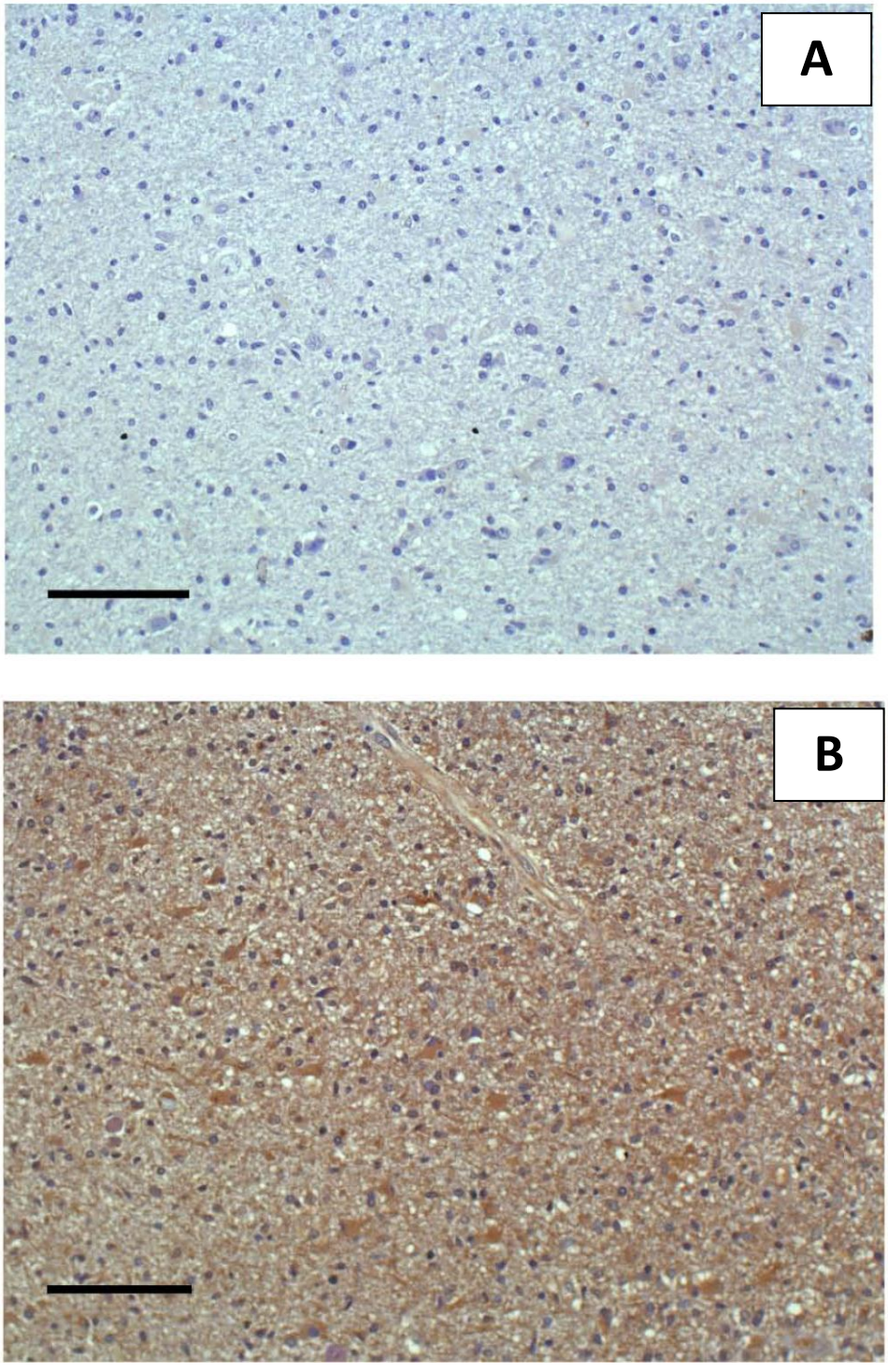

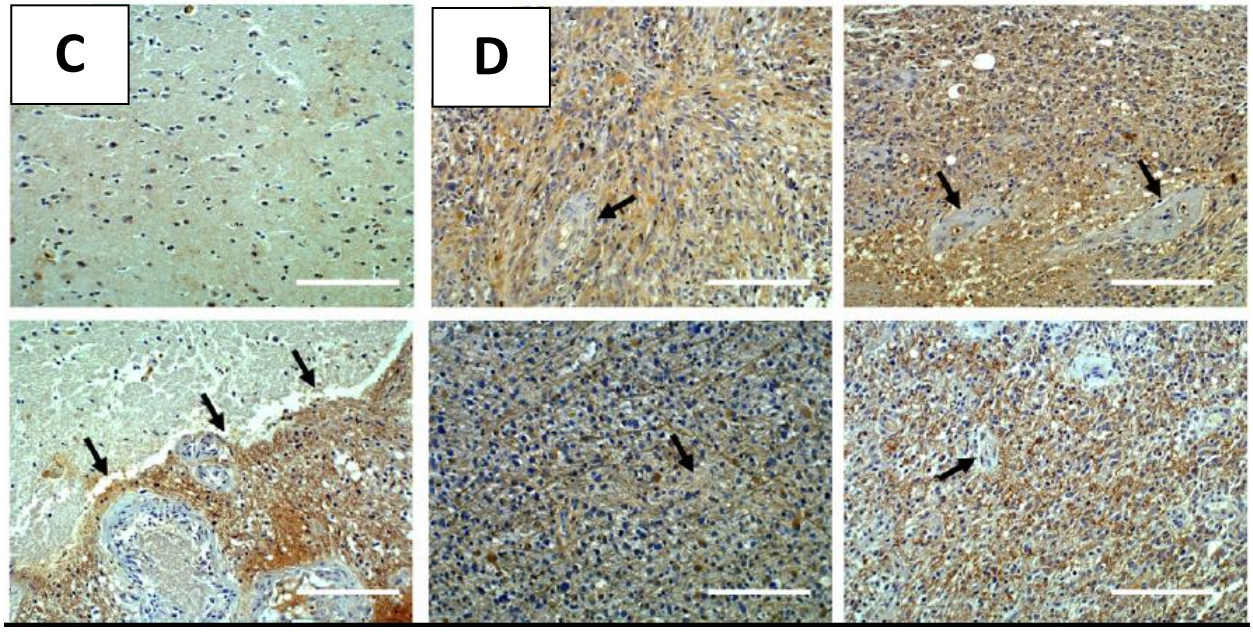


**Figure 24. Human Patient GBM Tumors Express High Levels of β8**

**Immunohistochemistry performed on human GBM samples with (A) goat IgG and (B) a goat anti-β8 antibody. (C) Two different human GBM sections were stained that contained normal non-tumorigenic tissue. The lower panel shows a tumor margin. (D) Immunohistochemistry was carried out with anti-β8 antibody on four human GBMs section taken from the center of the tumor. Note the high level of β8 within the tumor. Scale bar 200μm.**

## β8 Integrin Levels Direct Human GBM Cell Invasiveness and PAK1 Phosphorylation In-Vivo

LN229 GBM cells with either non-targeting shRNA or β8shRNA previously described (Figure 6) were stereotactically injected into the striatum of nude mice and sacrificed after 7 weeks. The brains were sectioned and H&E stained (Figure 25A). The tumors originating from control LN229 cells were very invasive, with many individual cells moving away from the primary tumor mass, while those with β8 knocked down lost invasiveness (these statements were verified by a pathologist specializing in brain tumors). Tumors with β8 knocked down were also much larger. This was quantified by measuring the two-dimensional surface area (Figure 25B). Immunofluorescence was also carried out on these tumors with an anti-GFP antibody to show tumor expression within the mouse brain (Figure 25C and 25D). In the bottom panel the tumor margin of the tumor with β8 knocked down is very distinct while in the upper panel the LN229 tumor with high levels of the integrin is very invasive. Additionally, the tumors were stained for KI-67 as it is known to be a marker for proliferation. The larger LN229-β8shRNA tumors did not show more KI-67 staining than the LN229-NTshRNA tumors (Figure 25E and 25F). These tumors were also doubled stained for GFP and pPAK1. It can be seen that invasive LN229 NT-shRNA tumor cells have little to no pPAK1 (Figure 25G). Alternatively, the non-invasive LN229 β8shRNA tumor cells have high levels of phosphorylated PAK1 (Figure 25H). These results correspond to those seen in-vivo (Figure 14D and 19B).

**Figure 25.**

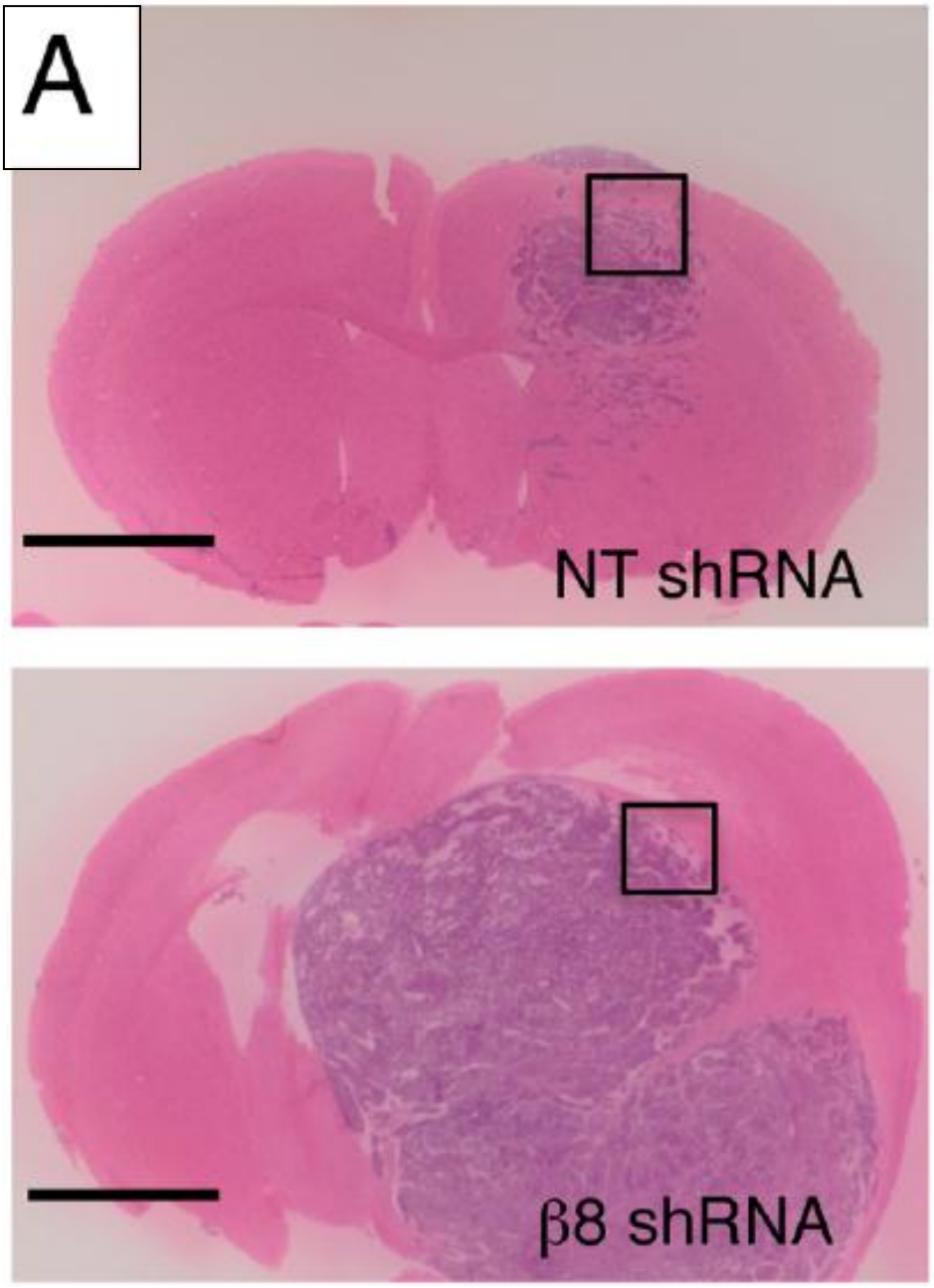

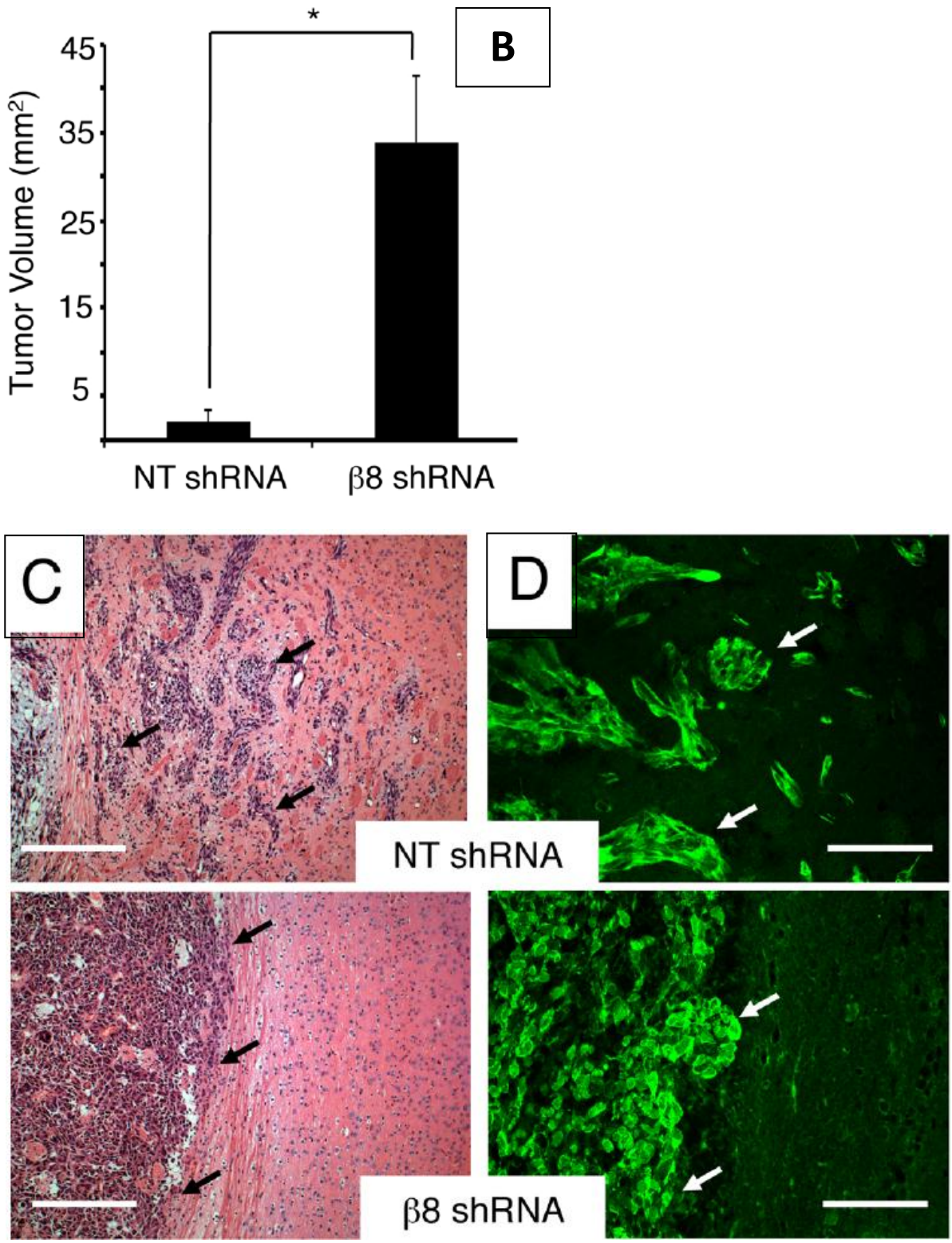
B
*
45
35
25
15
5
Tumor Volume (mm2)
NT shRNA
β8 shRNA
C
D
NT shRNA
β8 shRNA

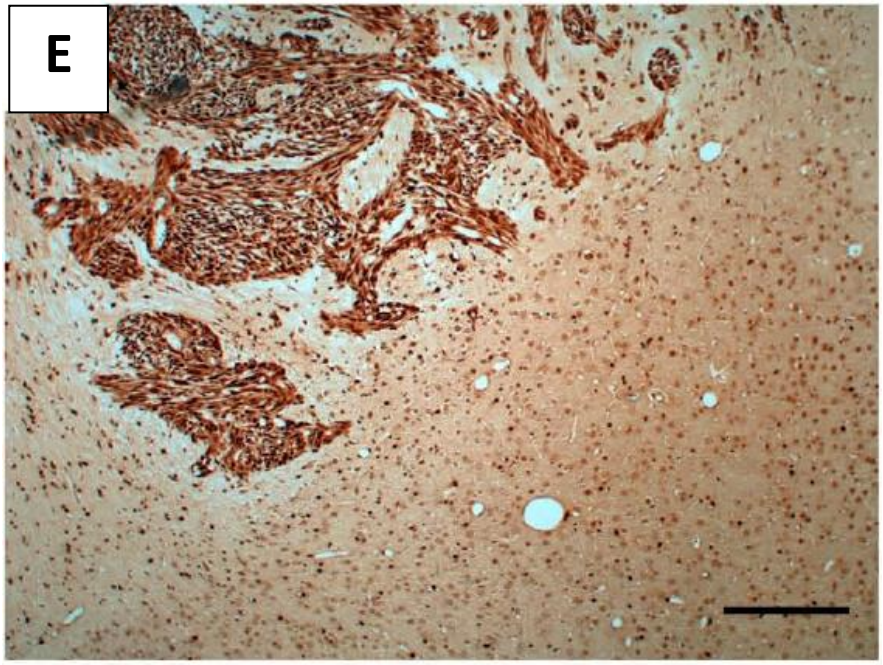
E

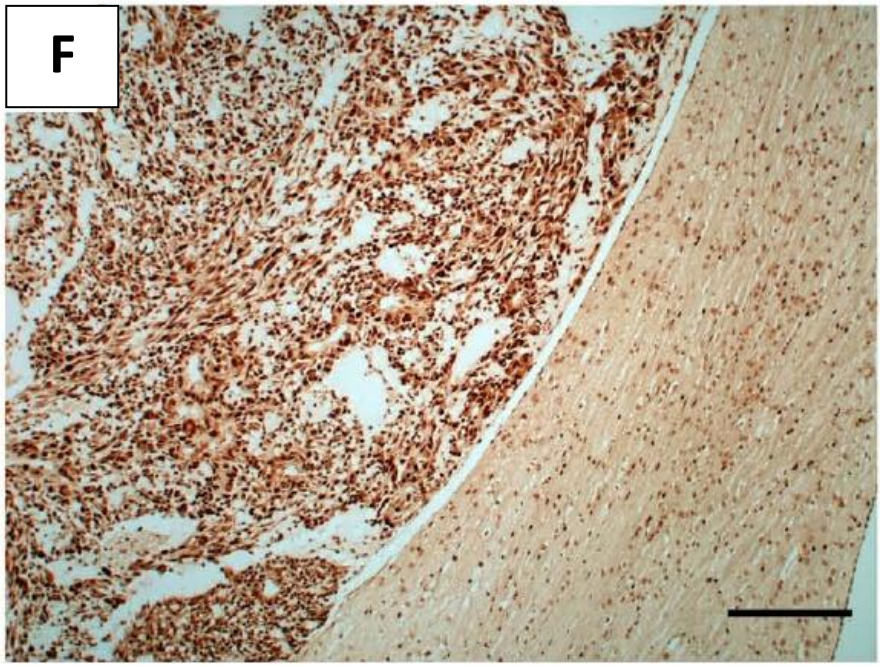
F

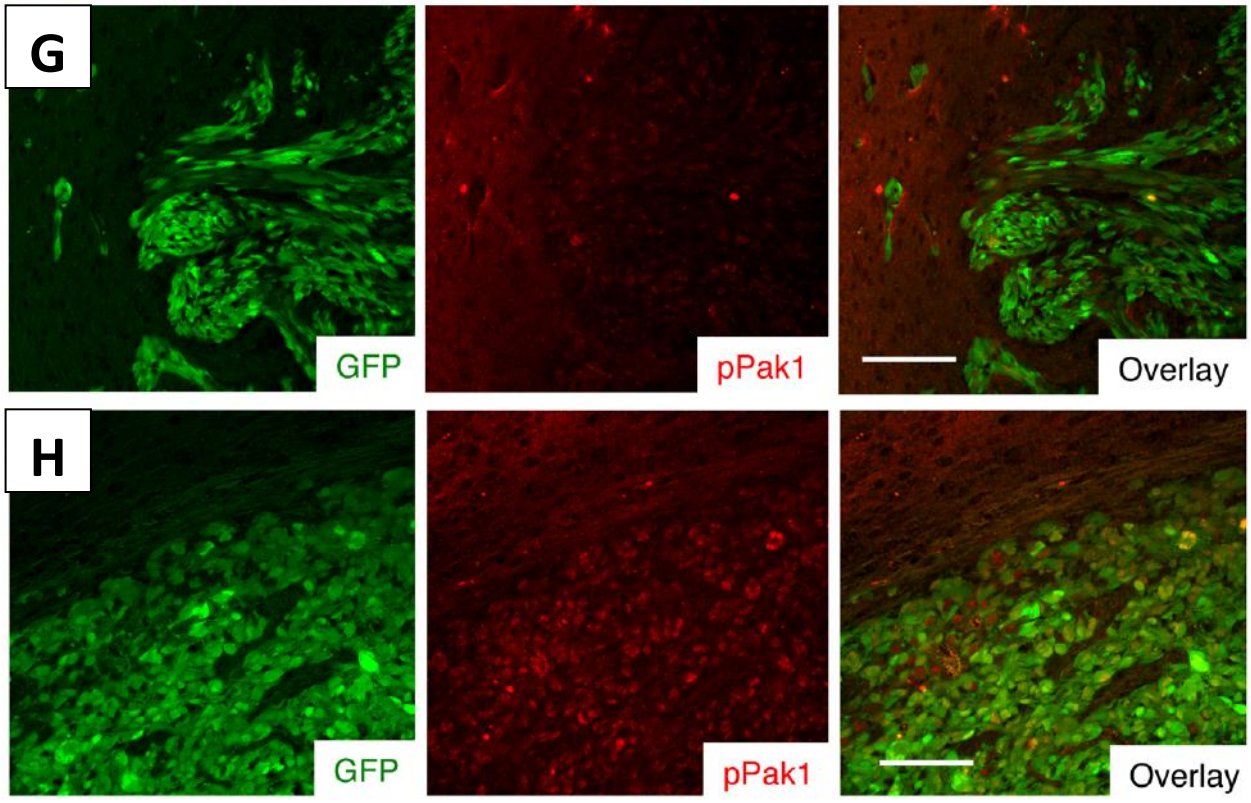
G
GFP
pPak1
Overlay
H
GFP
pPak1
Overlay

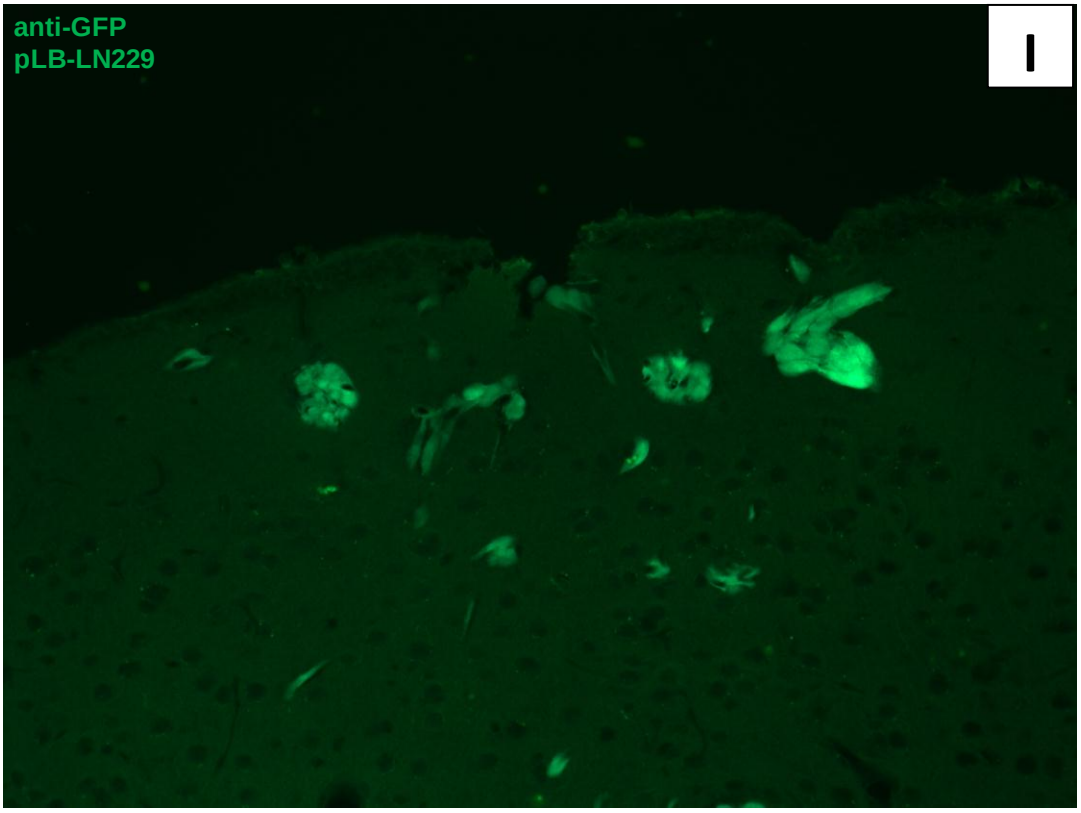
anti-GFP
pLB-LN229
I

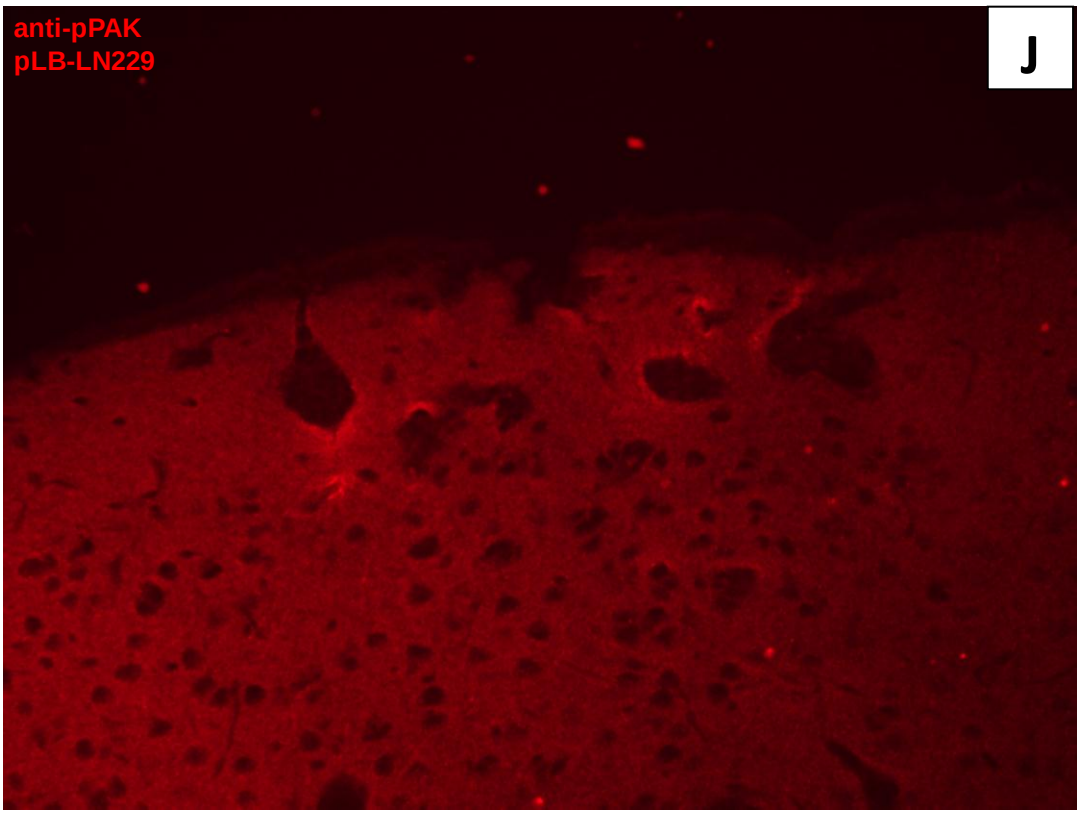
anti-pPAK
pLB-LN229
J

**Figure 25. αvβ8 Mediates Invasion and Pak1 Phosphorylation in an Orthotopic Mouse Model**

**(A) LN229 human GBM cells expressing either non-targeting shRNA or β8shRNA were injected into nude mice, sacrificed, perfused, sectioned, and H&E stained. (B) The surface area of the stained H&E sections was quantified. (C) H&E staining of LN229 non-targeting shRNA tumor (top) and LN229 β8shRNA tumor (bottom). (D) A different section of the same tumor shown in Figure C is shown that has been immunofluorescently GFP stained to reveal the tumor cells. Note the increased invasiveness of the β8shRNA containing tumors. (E) LN229-NTshRNA and (F) LN229-β8shRNA tumor were stained for KI-67. Note the larger tumor does not have more KI-67 staining. (G) LN229 NT-shRNA and (H) LN229 β8shRNA sections were stained with both anti-GFP and anti-pPAK1 antibodies. High resolution of (I) GFP and (J) pPAK staining in pLB-LN229 tumors. Note the lack of pPAK1 in invading LN229 NT-shRNA tumor cells.**

## Discussion

LN229 GBM cells were treated with scrambled, non-targeting or β8 targeting siRNA for analysis of PAK phosphorylation. p21 activated kinase-1 (PAK1) is autophosphorylated following binding to GTP-bound Rac1 or Cdc42. Thus PAK1 phosphorylation is used as a read out for Rac1 and Cdc42 activity. It was seen that when the integrin is knocked down more Pak1 is phosphorylated. Following this the activity states of three GTPases were checked for their activity. It was seen that both Rac1 and Cdc42 are activated when the integrin is knocked down, while the level of their protein expression does not change. Additionally, RhoA was checked which had no excess activity as measured by GTP bound levels (Figure 19A). As PAK1 is not known to be phosphorylated by active RhoA this fits with the previous results. siRNA experiments were preferred because they offered us better knockdown than shRNAs. However, I also checked two different β8shRNAs in LN229 cells where it was also shown that their levels of PAK phosphorylation go up significantly when the integrin in knocked down (Figure 19B). This trend was also seen in transformed mouse astrocytes where those with β8 knocked out had increased phosphorylation of PAK1 and increased levels of active Rac1 and Cdc42 (Figure 19C, 19D, and 19E). This signaling was also rescued when β8 was over expressed in $\beta8^{-/-}$ cells as PAK1 phosphorylation and Rac1 activation significantly decreased (Figure 19F and 19G).

It was previously reported that GDI1 could bind to the cytoplasmic tail of β8 in an artificial system(144). We therefore decided to pursue a GDI link. First we established that both Rho GDI-1 (GDIα or Rho GDI) and Rho GDI-2 (Rho GDIβ or

D4-GDI or Ly-GDI) are present in both LN229 and SNB-19 GBM cell lines. Additionally, the levels of GDI are not influenced by the levels of β8 (Figure 20A). Following this we knocked down Rho GDI-1 with siRNA. This revealed that GDI levels can influence Rac1 and Cdc42 activation states. PAK1 was phosphorylated and Rac1 and Cdc42 were activated in cells with less Rho GDI-1 (Figure 20B). This verified the known function of GDIs. GDP dissociation inhibitors (GDIs) work by binding to GDP bound Rho proteins. This GDP bound version is the inactive state while the protein become active when they are bound to GTP. By bind to GDP bound Rho proteins, the GDIs are able to hold them in their inactive state. However, when they are released these proteins are free to bind to GTP and become activated. The increase in PAK1 phosphorylation and the activation of Rac1 and Cdc42 Rho proteins when the GDI1 siRNA was present mimicked the signaling seen when the integrin is knocked down. When this GDI was knocked down in LN229 cells they also saw a reduction in invasiveness (Figure 20C). This increase in PAK1 phosphorylation and reduction in invasiveness was also seen when the GDI was knocked down in SNB-19 cells with ~75% reduction in invasiveness (Figure 20E).

As manipulation of GDI and β8 integrin levels were seen to alter Rac1 activation we then looked at Rac1 more closely. To do this we transfected YFP tagged constitutively active Rac1 into LN229 cells. When the expression was verified by anti-Rac1 the YFP levels were also checked (Figure 21A). This showed that the tagged active Rac1 was expressed at similar levels to that of the empty YFP construct (Figure 21B). Upon transfection an interesting phenotype was noted.

The YFP-positive active Rac1 cells appeared much flatter than the control cells. When checked under a fluorescent microscope this change was obvious as all of the $YFP^+$ cells had a flattened morphology while untransfected cells in the same culture appeared elongated like the control cells (Figure 21C). This is very apparent at high magnification where it can be seen that the cells are trying move in all directions at once; the result being a flattened morphology (Figure 21D). This would explain why the THA cells had focal contacts around all sides of the cell and had actin aligned in multiple directions (Figure 12). These cells were then sorted by FACS for YFP and run through an invasion assay where about a 50% drop in invasiveness was seen (Figure 21E). Additionally, before the cells were stained for quantification they were checked under a fluorescent microscope (Figure 21F). It was seen that the few LN229 cells that did migrate through were poorly expressing the YFP meaning they had lower levels of constitutively active Rac1. While the control cells that migrated through expressed much higher levels of YFP. Since both cell types started out with similar levels of YFP intensity this suggests that the constitutively active Rac1 cells were not invading through to the bottom of the chamber while those with less of the construct were. Therefore it is likely that cells that have more activated Rac1 are less invasive.

To connect the defects found for active Rac1 and β8 we looked at the ability of Rho GDI-1 to bind to the cytoplasmic tail of β8. As was previously mentioned, this interaction was detected using an artificial system. This included making a chimera protein of Interleukin-2 (IL-2) with a β8 cytoplasmic tail attached and transfecting it into human embryonic kidney 293T cells. The reason this was done

was due the lack of quality antibodies. With a chimeric protein they were able to target the IL-2 with and antibody and blot for the GDI. Instead of this artificial system I decided to look at this interaction in LN229 cells. The same cells I used for a majority of the *in vitro* and *in vivo* work. Due to antibody constraints this was first attempted with a GFP-RhoGDI1 construct. Rho GDI-1 was seen to bind to β8, and when the integrin was knocked down with siRNA the binding signal also decreased (Figure 22A and 22B). A GFP-GDI2 construct was also used, however no β8-GDI2 interaction was found (data not shown). These results were very interesting as the cytoplasmic tail of β8 shows little homology to the cytoplasmic tails of the β3 and β5 integrins. In the future a more definitive statement could be concluded regarding other integrins pairing with GDI1 by performing immunoprecipitations in cells that have higher levels of these integrins and with the corresponding antibodies. However since the predominant integrin expressed in all of the astrocytes analyzed is β8, its signaling in the context of a whole cell would like dominate any small contributions by the β3 and β5 integrins.

To strengthen the conclusion we utilized constructs with the cytoplasmic tail of the integrin truncated. Full length and truncated β8 was placed into 293T cells, which have no endogenous β8 expression, to verify its expression (Figure 23A). Additionally it was seen that the truncated β8 is still able to pair with αv by biotinylation (Figure 23B). This is important because the sequences that interact between αv and β8 are not known and removing the cytoplasmic tail could cause them to not form a pair. However, the biotinylation allows one to verify that αv and β8 are pairing on the cell surface. The constructs were then placed into $\beta8^{-/-}$ mTAs

to verify the role of the cytoplasmic tail. Indeed it was the case that the knockout cells and those with the cytoplasmic tail truncated lacked the invasive phenotype seen in GBMs. Addition of the cytoplasmic tail increased in-vitro invasiveness by about 40% meaning it is required for the downstream signaling events to take place (Figure 23D).

Despite a large amount of evidence of β8's role for invasiveness in-vitro, in-vivo work was sought for greater relevancy. Examining human GBMs by immunohistochemistry we were able to see how levels of the integrin vary between tumors but in general are high, just as seen in cell lines (Figure 24D and 4). The cell line used in most of the *in vitro* experiments, LN229, was used for animal studies. The previously described LN229-β8shRNA cells were seen to be incredibly non-invasive when injected into the mouse brain (Figure 15B and 25A). The control tumors were very invasive while those with the integrin knocked down were not invasive at all (verified by a pathologist). These knockdown tumors were also much larger (Figure 25). Staining for their GFP expression allowed for a better visualization of how invasive these cells really are (Figure 25D). As a size difference was apparent these were checked by KI-67 staining (Figure 25E and 25F). As a weak signal suggests slower proliferation, the β8shRNA tumors are not seen to be more proliferative than the control tumors, just as the case in-vitro (Figure 6C). Additionally, these tumors were stained for pPAK1 as a read out for Rac1 and Cdc42 activity. It is clear that pPAK levels are high in the control tumors while it is low in tumors with the integrin knocked down (Figure 25H and 25G). This is more apparent at higher magnification as the GFP+ tumor cells overlay exactly

with areas of the brain that have little to no PAK phosphorylation (Figure 25I and 25J). These in vivo finding suggest that the mechanism found *in vitro* is also taking place *in vivo*. That being GDI-1 bind to the cytoplasmic tail of β8, prevents Rac1 and Cdc42 from being activating and PAK1 from being phosphorylated. However, when the integrin is knocked down or knocked out there is no β8 for the GDI-1 to bind to. In this situation β8 is not able to increase the affinity for GDI-1 for GDP bound Cdc42 or Rac1. This leaves these be more easily converted to GTP and activated which leads to a loss of their invasiveness. In the future this model could be more closely explored with a FRET biosensor. CFP could be bound to GDI-1 and YFP to β8. These could then be imaged with a live imaging microscope that could excite the CYP. The emission wavelengths could then be read to watch the GDI1-β8 interaction in real time. When the CFP emission is read there is no interaction. However the emission wavelength from CFP can excite YFP if a change in protein conformation takes place. Therefore when GDI-1 binds to β8 the YFP fluorophore would be excited and emit a wavelength consistent with YFP only, revealing a β8 induced conformational change in GDI-1. This could also be repeated by placing the YFP onto the Rac1 (or Cdc42) instead of the β8 to record changes in the GDI1-Rac1GDP conformation induced by integrin β8.

## Chapter 5:

## Conclusion

This investigation is the first to link αvβ8 to the invasive pathologies associated with GBMs and identify a clear mechanism stemming from the cytoplasmic tail of the β8 subunit. Several key observations were made and are detailed below:

1. Overexpression of β8 in GBM U87 cells and knockdown of β8 in THAs correlates with VEGF expression.
2. $\alpha v^{-/-}$ primary and transformed mouse astrocytes have significantly inhibited migration and invasiveness that is not rescued by WT cell derived TGFβ activation.
3. Knocking down β8 in human GBM tumor cells and knocking it out in primary and transformed mouse astrocytes inhibits their invasive potential which can be rescued with over expression of β8.
4. Inhibiting TGFβ signaling reduces SMAD2/3 phosphorylation and invasiveness.
5. Silencing β8 and GDI causes Rac1 and Cdc2 activation and reduces invasiveness in-vitro. Re-expressing β8 in knockout cells knocks down Rac1 activation and PAK1 phosphorylation.
6. Silencing β8 causes PAK1 phosphorylation in-vitro and in-vivo.
7. Constitutively active Rac1 induces a flattened morphology and reduces invasiveness.
8. Rho GDI-1 binds to the cytoplasmic tail of β8.

9. Silencing β8 in GBM cells reduces invasiveness but increases tumor size in an orthotopic mouse model.

10. The $\beta 8^{-/-}$ Rac1/Cdc42 signaling and invasive defect is accounted for by the loss of signaling through the cytoplasmic tail.

## Chapter 6:

## Perspectives and Future Directions

I detail a previously unknown role for αvβ8 in GBM invasiveness. This knowledge could lead to better profiling of GBM tumors which has the potential to allow physicians to better predict tumor behavior and adjust the treatment plan appropriately. Additionally, the reported results raise several substantial curiosities and questions that are worthy of pursuit.

Among these are the possibility that β8 can function to modulate the invasiveness of the tumor. If this is the case different therapies could be given to patients with different β8 levels. This might mean an inhibitor of β8 could prevent invasiveness. However, our lab has extensive evidence suggesting a model of inverse pathophysiologies. When there is high αvβ8 the individual cells tend to be more invasive in-vitro and as a tumor function more invasively in-vivo. While when there are low levels of the integrin the tumors are more angiogenic. At face value this would present an interesting paradox for clinicians; too much β8 and the tumor cannot be caught with a scalpel, too little β8 and you feed the tumor. However, this may be attenuated if the pathways responsible for each phenotype can be independently addressed, without affecting the other. We have previously shown that manipulating levels of β8 correlate with changes in the amount of VEGF secreted by the cell and attributed the in-vivo angiogenic phenotype to this. If αvβ8 signaling levels could be knocked down in a patient with an inhibitor, VEGF transcription and secretion will increase. While it might be hard to directly target this transcription it would be feasible to reduce the function of the VEGF being secreted.

This could be accomplished with a VEGF blocking antibody. Bevacizumab (marketed as Avastin), is a drug being explored in the clinic that does just that(121). Further investigation into these pathways could lead to dual treatment with the inhibition of β8 and VEGF. However, a pitfall to this is that while Avastin has been seen to decrease angiogenesis, it has also been seen to increase the invasiveness of the tumor(145-150). One explanation to this is that a Bevacizumab treated tumor turns hypoxic as it becomes less angiogenic which is known to increase p38 activation. The Nishimura group has shown that p38 is directly involved in β8 transcription and inhibiting p38 reduces integrin transcription and protein expression(60). However, should this feedback mechanism be involved, excess β8 production would have a minimal effect as the drug could easily saturate it. A pitfall would be if a second mechanism, independent of β8, is activated by Bevacizumab. In this case the tumor would select for a population of cells that had a pro-invasive mechanism capable of overriding αvβ8's effects on Rac1 and Cdc42 signaling. This would result in the need for a different anti-angiogenic therapy(145,147-158).

Additionally, it remains to be seen whether one GTPase can override the activity of another, in terms of cell motility(159-162). We have seen mechanistically that β8 does not control RhoA. It may be the case that over-activating Cdc42 and Rac1 activity can halt invasiveness, but it not be an exclusive event. Aberrant RhoA behavior may result in changes in invasiveness independent of Cdc42 and Rac1(162-166). This could be addressed with dominant negative and dominant positive constructions. Additionally regulatory factors may be able to overcome excessive GTPase activity or inactivity(167-175). In the future it may be of interest

to look into GTPase-Activating Proteins (GAPs) and Guanine nucleotide Exchange Factors (GEFs)(176-184). GEFs regulate GTP to GDP exchange so that the GTPase is bound to GTP and activated(178,180,184-190). GAPs speed up the hydrolysis of GTP to GDP, allowing the removal of a phosphate and the GTPase to return to an inactive state(163,188,191-196). This gives GAPs and GEFs opposing functions, which harmonize to allow for the normal cycle to take place(160,170,189,197-202). When β8 is knocked down the activity of Cdc42 and Rac1 increase. It would be interesting to know which GAPs and GEFs are specifically used in these pathways in GBM cells. Once this is determined it could be seen if reducing the amount of GEF present would also reduce the amount of activation of the Cdc42 and Rac1 GTPases when β8 is knocked down. This could be accomplished with siRNAs. Conversely one would also want to analyze the GAP activity and see if adding a constitutively active GAP could cause the active GTPases to turn over much more quickly(203-207). This would be interesting as it could result in much faster moving cells than the wild-type normally display. The mechanisms upstream of these GAPs and GEFs could then be analyzed. If an αvβ8 targeting therapy initially works and relapse to an invasive phenotype, these upstream pathways would likely explain resistance. However, this would be no easy task as there are predicted to be between 59 and 70 proteins with RhoGAP domains that may be involved with Rho GTPases and an unknown number of GEFs, as there is no distinguishing motif(163,171,197,208-214).

Another intriguing possibility is that αvβ8 may be able to bind to TGFβRI or TGFβRII. Pilot studies have shown that TGFβRII may co-immunoprecipitate with

β8 however these could not be replicated (data not shown). It may be possible that the interaction is highly dynamic and responsive to other factors. This might be addressed by utilizing cross-linking reagents during the procedure. Additionally, one could utilize the truncated β8 construct to see if this tail is required for association with a TGFβ receptor. An alternative to this would be to engineer a FRET biosensor by expressing Cyan Fluorescent Protein (eCFP) on the cytoplasmic tail of β8 and express or commercially purchase TGFβRI and TGFβRII with a YFP tag on their cytoplasmic domains. This would allow for in-vitro characterization of this interaction as the CFP protein can excite the YFP to fluoresce. Additionally, one could inject GBM cell lines with these constructs, cut a window into the skull and then utilize a two-photon excitation microscope to image. This would allow for real time in-vivo imaging of the interaction taking place and would lend insight into how cells with more YFP excitation behave.

The cytoplasmically truncated β8 construct could also be used to determine if the cytoplasmic tail of the integrin is responsible for up-regulation of VEGF levels. U87 cells over expressing V5 tagged β8 were previously seen to up regulate VEGF secretion. It would be interesting to over express the non-tagged β8 or the truncated β8 in this cell line. This could verify that the v5 tag is not involved in the increase in VEGF. Another possibility would be to compare the β8-/- cells with the full length and truncated integrin. The truncated construct could define whether the signaling that led to VEGF up regulation is tied to the cytoplasmic tail (and possibly Rac1/Cdc42 signaling) or to the extracellular portion (and possibly TGFβ dependent signaling).

Interesting, I have also found that Cilengitide and a Cilengitide-like peptide may be able to bind to β8, preventing the binding of inactive-TGFβ (data not shown). This result has the most potential for a low effort, high impact project. As a direct protein-peptide interaction has been seen in mixing experiments, the next step would be to add the peptides to cells expressing robust levels of αvβ8 to determine the effect of this drug on Rac1 and Cdc42 activity. It may be the case that these peptides are able to block TGFβ activation by the integrin and/or manipulate the ability of the cytoplasmic tail to bind to Rho GDI-1. Additionally in-vivo experiments could be done to determine if Cilengitide treatment of a β8-high tumor results in a similar or reduced invasive phenotype. In parallel one could data-mine a tissue bank of human tumors. Should such resource be made available, one might select tissue samples of patients treated with Cilengitide and of patients treated with alternative drugs. It would be interesting to determine if Cilengitide treatment of patients with β8-high tumors results in a less invasive pathology. As a drug currently in Phase III clinical trials, further exploring this behavior of Cilengitide could lead to an immediate benefits for patients.

Taken together, this thesis has provided a significant advance in the research of integrin αvβ8. Further exploration is recommended to fully understand this protein's role in GBM invasiveness and its impact on patients.

## Bibliography


1. Ware, M. L., Berger, M. S., and Binder, D. K. (2003) Molecular biology of glioma tumorigenesis. *Histology and histopathology* **18**, 207-216
2. Shih, A. H., and Holland, E. C. (2004) Developmental neurobiology and the origin of brain tumors. *Journal of neuro-oncology* **70**, 125-136
3. Furnari, F. B., Fenton, T., Bachoo, R. M., Mukasa, A., Stommel, J. M., Stegh, A., Hahn, W. C., Ligon, K. L., Louis, D. N., Brennan, C., Chin, L., DePinho, R. A., and Cavenee, W. K. (2007) Malignant astrocytic glioma: genetics, biology, and paths to treatment. *Genes & development* **21**, 2683-2710
4. Broaddus, W. C., Liu, Y., Steele, L. L., Gillies, G. T., Lin, P. S., Loudon, W. G., Valerie, K., Schmidt-Ullrich, R. K., and Fillmore, H. L. (1999) Enhanced radiosensitivity of malignant glioma cells after adenoviral p53 transduction. *J Neurosurg* **91**, 997-1004
5. Abdollahi, A., Griggs, D. W., Zieher, H., Roth, A., Lipson, K. E., Saffrich, R., Grone, H. J., Hallahan, D. E., Reisfeld, R. A., Debus, J., Niethammer, A. G., and Huber, P. E. (2005) Inhibition of alpha(v)beta3 integrin survival signaling enhances antiangiogenic and antitumor effects of radiotherapy. *Clin Cancer Res.* **11**, 6270-6279
6. Ricci-Vitiani, L., Pallini, R., Biffoni, M., Todaro, M., Invernici, G., Cenci, T., Maira, G., Parati, E. A., Stassi, G., Larocca, L. M., and De Maria, R. (2010)

Tumour vascularization via endothelial differentiation of glioblastoma stem-like cells. *Nature* **468**, 824-828

7. Wang, R., Chadalavada, K., Wilshire, J., Kowalik, U., Hovinga, K. E., Geber, A., Fligelman, B., Leversha, M., Brennan, C., and Tabar, V. (2010) Glioblastoma stem-like cells give rise to tumour endothelium. *Nature* **468**, 829-833
8. Chen, Y., Saini, S., Zaman, M. S., Hirata, H., Shahryari, V., Deng, G., and Dahiya, R. (2011) Cytochrome P450 17 (CYP17) is involved in endometrial cancinogenesis through apoptosis and invasion pathways. *Mol Carcinog* **50**, 16-23
9. Wang, J. H., Wu, Q. D., Bouchier-Hayes, D., and Redmond, H. P. (2002) Hypoxia upregulates Bcl-2 expression and suppresses interferon-gamma induced antiangiogenic activity in human tumor derived endothelial cells. *Cancer* **94**, 2745-2755
10. Zeitlin, B. D., Joo, E., Dong, Z., Warner, K., Wang, G., Nikolovska-Coleska, Z., Wang, S., and Nor, J. E. (2006) Antiangiogenic effect of TW37, a small-molecule inhibitor of Bcl-2. *Cancer Res* **66**, 8698-8706
11. Zeitlin, B. D., Spalding, A. C., Campos, M. S., Ashimori, N., Dong, Z., Wang, S., Lawrence, T. S., and Nor, J. E. (2010) Metronomic small molecule inhibitor of Bcl-2 (TW-37) is antiangiogenic and potentiates the antitumor effect of ionizing radiation. *Int J Radiat Oncol Biol Phys* **78**, 879-887

12. Cancer Genome Atlas Research, N. (2008) Comprehensive genomic characterization defines human glioblastoma genes and core pathways. *Nature* **455**, 1061-1068

13. Kaminska, B., Kocyk, M., and Kijewska, M. (2013) TGF beta signaling and its role in glioma pathogenesis. *Advances in experimental medicine and biology* **986**, 171-187

14. Patyna, S., Laird, A. D., Mendel, D. B., O'Farrell A, M., Liang, C., Guan, H., Vojkovsky, T., Vasile, S., Wang, X., Chen, J., Grazzini, M., Yang, C. Y., Haznedar, J. O., Sukbuntherng, J., Zhong, W. Z., Cherrington, J. M., and Hu-Lowe, D. (2006) SU14813: a novel multiple receptor tyrosine kinase inhibitor with potent antiangiogenic and antitumor activity. *Mol Cancer Ther* **5**, 1774-1782

15. Roberts, W. G., Whalen, P. M., Soderstrom, E., Moraski, G., Lyssikatos, J. P., Wang, H. F., Cooper, B., Baker, D. A., Savage, D., Dalvie, D., Atherton, J. A., Ralston, S., Szewc, R., Kath, J. C., Lin, J., Soderstrom, C., Tkalcevic, G., Cohen, B. D., Pollack, V., Barth, W., Hungerford, W., and Ung, E. (2005) Antiangiogenic and antitumor activity of a selective PDGFR tyrosine kinase inhibitor, CP-673,451. *Cancer Res* **65**, 957-966

16. Lange, K., Kammerer, M., Hegi, M. E., Grotegut, S., Dittmann, A., Huang, W., Fluri, E., Yip, G. W., Gotte, M., Ruiz, C., and Orend, G. (2007) Endothelin receptor type B counteracts tenascin-C-induced endothelin receptor type A-dependent focal adhesion and actin stress fiber disorganization. *Cancer Res* **67**, 6163-6173

17. Skuli, N., Monferran, S., Delmas, C., Favre, G., Bonnet, J., Toulas, C., and Cohen-Jonathan Moyal, E. (2009) Alphavbeta3/alphavbeta5 integrins-FAK-RhoB: a novel pathway for hypoxia regulation in glioblastoma. *Cancer Res* **69**, 3308-3316

18. McCarty, J. H., Monahan-Earley, R. A., Brown, L. F., Keller, M., Gerhardt, H., Rubin, K., Shani, M., Dvorak, H. F., Wolburg, H., Bader, B. L., Dvorak, A. M., and Hynes, R. O. (2002) Defective associations between blood vessels and brain parenchyma lead to cerebral hemorrhage in mice lacking alphav integrins. *Mol Cell Biol* **22**, 7667-7677

19. McCarty, J. H., Lacy-Hulbert, A., Charest, A., Bronson, R. T., Crowley, D., Housman, D., Savill, J., Roes, J., and Hynes, R. O. (2005) Selective ablation of alphav integrins in the central nervous system leads to cerebral hemorrhage, seizures, axonal degeneration and premature death. *Development* **132**, 165-176

20. Hynes, R. O., Lively, J. C., McCarty, J. H., Taverna, D., Francis, S. E., Hodivala-Dilke, K., and Xiao, Q. (2002) The diverse roles of integrins and their ligands in angiogenesis. *Cold Spring Harb Symp Quant Biol* **67**, 143-153

21. VanMeter, T. E., Rooprai, H. K., Kibble, M. M., Fillmore, H. L., Broaddus, W. C., and Pilkington, G. J. (2001) The role of matrix metalloproteinase genes in glioma invasion: co-dependent and interactive proteolysis. *Journal of neuro-oncology* **53**, 213-235

22. Yabushita, H., Narumiya, H., Hiratake, K., Yamada, H., Shimazu, M., Sawaguchi, K., Noguchi, M., and Nakanishi, M. (2000) The association of transforming growth factor-beta 1 with myometrial invasion of endometrial carcinomas through effects on matrix metalloproteinase. *J Obstet Gynaecol Res* **26**, 163-170

23. Brooks, P. C., Stromblad, S., Sanders, L. C., von Schalscha, T. L., Aimes, R. T., Stetler-Stevenson, W. G., Quigley, J. P., and Cheresh, D. A. (1996) Localization of matrix metalloproteinase MMP-2 to the surface of invasive cells by interaction with integrin alpha v beta 3. *Cell* **85**, 683-693

24. Fillmore, H. L., VanMeter, T. E., and Broaddus, W. C. (2001) Membrane-type matrix metalloproteinases (MT-MMPs): expression and function during glioma invasion. *Journal of neuro-oncology* **53**, 187-202

25. Huang, S., Stupack, D., Liu, A., Cheresh, D., and Nemerow, G. R. (2000) Cell growth and matrix invasion of EBV-immortalized human B lymphocytes is regulated by expression of alpha(v) integrins. *Oncogene* **19**, 1915-1923

26. Gingras, M. C., Roussel, E., Bruner, J. M., Branch, C. D., and Moser, R. P. (1995) Comparison of cell adhesion molecule expression between glioblastoma multiforme and autologous normal brain tissue. *J Neuroimmunol* **57**, 143-153

27. Paulus, W., Baur, I., Schuppan, D., and Roggendorf, W. (1993) Characterization of integrin receptors in normal and neoplastic human brain. *Am J Pathol* **143**, 154-163

28. Friedlander, D. R., Zagzag, D., Shiff, B., Cohen, H., Allen, J. C., Kelly, P. J., and Grumet, M. (1996) Migration of brain tumor cells on extracellular matrix proteins in vitro correlates with tumor type and grade and involves alphaV and beta1 integrins. *Cancer Res* **56**, 1939-1947

29. Tysnes, B. B., Larsen, L. F., Ness, G. O., Mahesparan, R., Edvardsen, K., Garcia-Cabrera, I., and Bjerkvig, R. (1996) Stimulation of glioma-cell migration by laminin and inhibition by anti-alpha3 and anti-beta1 integrin antibodies. *Int J Cancer* **67**, 777-784

30. Kawataki, T., Yamane, T., Naganuma, H., Rousselle, P., Anduren, I., Tryggvason, K., and Patarroyo, M. (2007) Laminin isoforms and their integrin receptors in glioma cell migration and invasiveness: Evidence for a role of alpha5-laminin(s) and alpha3beta1 integrin. *Experimental cell research* **313**, 3819-3831

31. Fujiwara, H., Kikkawa, Y., Sanzen, N., and Sekiguchi, K. (2001) Purification and characterization of human laminin-8. Laminin-8 stimulates cell adhesion and migration through alpha3beta1 and alpha6beta1 integrins. *The Journal of biological chemistry* **276**, 17550-17558

32. Fukushima, Y., Ohnishi, T., Arita, N., Hayakawa, T., and Sekiguchi, K. (1998) Integrin alpha3beta1-mediated interaction with laminin-5 stimulates adhesion, migration and invasion of malignant glioma cells. *Int J Cancer* **76**, 63-72

33. Montet, X., Montet-Abou, K., Reynolds, F., Weissleder, R., and Josephson, L. (2006) Nanoparticle imaging of integrins on tumor cells. *Neoplasia* **8**, 214-222

34. Silva, R., D'Amico, G., Hodivala-Dilke, K. M., and Reynolds, L. E. (2008) Integrins: the keys to unlocking angiogenesis. *Arterioscler Thromb Vasc Biol* **28**, 1703-1713

35. Wilson, C. B., Leopard, J., Cheresh, D. A., and Nakamura, R. M. (1996) Extracellular matrix and integrin composition of the normal bladder wall. *World J Urol* **14 Suppl 1**, S30-37

36. Hu, B., Jarzynka, M. J., Guo, P., Imanishi, Y., Schlaepfer, D. D., and Cheng, S. Y. (2006) Angiopoietin 2 induces glioma cell invasion by stimulating matrix metalloprotease 2 expression through the alphavbeta1 integrin and focal adhesion kinase signaling pathway. *Cancer Res* **66**, 775-783

37. Ding, Q., Stewart, J., Jr., Prince, C. W., Chang, P. L., Trikha, M., Han, X., Grammer, J. R., and Gladson, C. L. (2002) Promotion of malignant astrocytoma cell migration by osteopontin expressed in the normal brain: differences in integrin signaling during cell adhesion to osteopontin versus vitronectin. *Cancer Res* **62**, 5336-5343

38. Schnell, O., Krebs, B., Wagner, E., Romagna, A., Beer, A. J., Grau, S. J., Thon, N., Goetz, C., Kretzschmar, H. A., Tonn, J. C., and Goldbrunner, R. H. (2008) Expression of integrin alphavbeta3 in gliomas correlates with tumor grade and is not restricted to tumor vasculature. *Brain Pathol* **18**, 378-386

39. Bello, L., Lucini, V., Giussani, C., Carrabba, G., Pluderi, M., Scaglione, F., Tomei, G., Villani, R., Black, P. M., Bikfalvi, A., and Carroll, R. S. (2003) IS20I, a specific alphavbeta3 integrin inhibitor, reduces glioma growth in vivo. *Neurosurgery* **52**, 177-185; discussion 185-176

40. Bello, L., Francolini, M., Marthyn, P., Zhang, J., Carroll, R. S., Nikas, D. C., Strasser, J. F., Villani, R., Cheresh, D. A., and Black, P. M. (2001) Alpha(v)beta3 and alpha(v)beta5 integrin expression in glioma periphery. *Neurosurgery* **49**, 380-389; discussion 390

41. Kenny, H. A., Kaur, S., Coussens, L. M., and Lengyel, E. (2008) The initial steps of ovarian cancer cell metastasis are mediated by MMP-2 cleavage of vitronectin and fibronectin. *J Clin Invest* **118**, 1367-1379

42. Baumann, F., Leukel, P., Doerfelt, A., Beier, C. P., Dettmer, K., Oefner, P. J., Kastenberger, M., Kreutz, M., Nickl-Jockschat, T., Bogdahn, U., Bosserhoff, A. K., and Hau, P. (2009) Lactate promotes glioma migration by TGF-beta2-dependent regulation of matrix metalloproteinase-2. *Neuro-oncology* **11**, 368-380

43. Lu, K. V., Jong, K. A., Rajasekaran, A. K., Cloughesy, T. F., and Mischel, P. S. (2004) Upregulation of tissue inhibitor of metalloproteinases (TIMP)-2 promotes matrix metalloproteinase (MMP)-2 activation and cell invasion in a human glioblastoma cell line. *Lab Invest* **84**, 8-20

44. Rupp, P. A., Visconti, R. P., Czirok, A., Cheresh, D. A., and Little, C. D. (2008) Matrix metalloproteinase 2-integrin alpha(v)beta3 binding is required

for mesenchymal cell invasive activity but not epithelial locomotion: a computational time-lapse study. *Mol Biol Cell* **19**, 5529-5540

45. Asano, Y., Ihn, H., Yamane, K., Jinnin, M., Mimura, Y., and Tamaki, K. (2005) Increased expression of integrin alpha(v)beta3 contributes to the establishment of autocrine TGF-beta signaling in scleroderma fibroblasts. *J Immunol* **175**, 7708-7718

46. Dickerson, E. B., Akhtar, N., Steinberg, H., Wang, Z. Y., Lindstrom, M. J., Padilla, M. L., Auerbach, R., and Helfand, S. C. (2004) Enhancement of the antiangiogenic activity of interleukin-12 by peptide targeted delivery of the cytokine to alphavbeta3 integrin. *Mol Cancer Res* **2**, 663-673

47. Reynolds, L. E., Wyder, L., Lively, J. C., Taverna, D., Robinson, S. D., Huang, X., Sheppard, D., Hynes, R. O., and Hodivala-Dilke, K. M. (2002) Enhanced pathological angiogenesis in mice lacking beta3 integrin or beta3 and beta5 integrins. *Nat Med* **8**, 27-34

48. Kanamori, M., Vanden Berg, S. R., Bergers, G., Berger, M. S., and Pieper, R. O. (2004) Integrin beta3 overexpression suppresses tumor growth in a human model of gliomagenesis: implications for the role of beta3 overexpression in glioblastoma multiforme. *Cancer Res* **64**, 2751-2758

49. Taga, T., Suzuki, A., Gonzalez-Gomez, I., Gilles, F. H., Stins, M., Shimada, H., Barsky, L., Weinberg, K. I., and Laug, W. E. (2002) alpha v-Integrin antagonist EMD 121974 induces apoptosis in brain tumor cells growing on vitronectin and tenascin. *Int J Cancer* **98**, 690-697

50. Yang, M., Adla, S., Temburni, M. K., Patel, V. P., Lagow, E. L., Brady, O. A., Tian, J., Boulos, M. I., and Galileo, D. S. (2009) Stimulation of glioma cell motility by expression, proteolysis, and release of the L1 neural cell recognition molecule. *Cancer Cell Int* **9**, 27

51. Asano, Y., Ihn, H., Jinnin, M., Mimura, Y., and Tamaki, K. (2006) Involvement of alphavbeta5 integrin in the establishment of autocrine TGF-beta signaling in dermal fibroblasts derived from localized scleroderma. *J Invest Dermatol* **126**, 1761-1769

52. Wipff, P. J., and Hinz, B. (2008) Integrins and the activation of latent transforming growth factor beta1 - an intimate relationship. *Eur J Cell Biol* **87**, 601-615

53. Asano, Y., Ihn, H., Yamane, K., Jinnin, M., Mimura, Y., and Tamaki, K. (2005) Involvement of alphavbeta5 integrin-mediated activation of latent transforming growth factor beta1 in autocrine transforming growth factor beta signaling in systemic sclerosis fibroblasts. *Arthritis Rheum* **52**, 2897-2905

54. Pijuan-Thompson, V., and Gladson, C. L. (1997) Ligation of integrin alpha5beta1 is required for internalization of vitronectin by integrin alphavbeta3. *The Journal of biological chemistry* **272**, 2736-2743

55. Ding, Q., Stewart, J., Jr., Olman, M. A., Klobe, M. R., and Gladson, C. L. (2003) The pattern of enhancement of Src kinase activity on platelet-derived growth factor stimulation of glioblastoma cells is affected by the integrin engaged. *The Journal of biological chemistry* **278**, 39882-39891

56. Fukushima, Y., Tamura, M., Nakagawa, H., and Itoh, K. (2007) Induction of glioma cell migration by vitronectin in human serum and cerebrospinal fluid. *J Neurosurg* **107**, 578-585

57. Mu, Z., Yang, Z., Yu, D., Zhao, Z., and Munger, J. S. (2008) TGFbeta1 and TGFbeta3 are partially redundant effectors in brain vascular morphogenesis. *Mech Dev* **125**, 508-516

58. Zhu, J., Motejlek, K., Wang, D., Zang, K., Schmidt, A., and Reichardt, L. F. (2002) beta8 integrins are required for vascular morphogenesis in mouse embryos. *Development* **129**, 2891-2903

59. Milner, R., Huang, X., Wu, J., Nishimura, S., Pytela, R., Sheppard, D., and ffrench-Constant, C. (1999) Distinct roles for astrocyte alphavbeta5 and alphavbeta8 integrins in adhesion and migration. *J Cell Sci* **112 ( Pt 23)**, 4271-4279

60. Cambier, S., Gline, S., Mu, D., Collins, R., Araya, J., Dolganov, G., Einheber, S., Boudreau, N., and Nishimura, S. L. (2005) Integrin alpha(v)beta8-mediated activation of transforming growth factor-beta by perivascular astrocytes: an angiogenic control switch. *Am J Pathol* **166**, 1883-1894

61. Fang, L., Deng, Z., Shatseva, T., Yang, J., Peng, C., Du, W. W., Yee, A. J., Ang, L. C., He, C., Shan, S. W., and Yang, B. B. MicroRNA miR-93 promotes tumor growth and angiogenesis by targeting integrin-beta8. *Oncogene* **30**, 806-821

62. Tchaicha, J. H., Reyes, S. B., Shin, J., Hossain, M. G., Lang, F. F., and McCarty, J. H. (2011) Glioblastoma angiogenesis and tumor cell

invasiveness are differentially regulated by beta8 integrin. *Cancer Res* **71**, 6371-6381

63. Chen, X., Park, R., Shahinian, A. H., Tohme, M., Khankaldyyan, V., Bozorgzadeh, M. H., Bading, J. R., Moats, R., Laug, W. E., and Conti, P. S. (2004) 18F-labeled RGD peptide: initial evaluation for imaging brain tumor angiogenesis. *Nucl Med Biol* **31**, 179-189

64. Cianfrocca, M. E., Kimmel, K. A., Gallo, J., Cardoso, T., Brown, M. M., Hudes, G., Lewis, N., Weiner, L., Lam, G. N., Brown, S. C., Shaw, D. E., Mazar, A. P., and Cohen, R. B. (2006) Phase 1 trial of the antiangiogenic peptide ATN-161 (Ac-PHSCN-NH(2)), a beta integrin antagonist, in patients with solid tumours. *Br J Cancer* **94**, 1621-1626

65. da Silva, R. G., Tavora, B., Robinson, S. D., Reynolds, L. E., Szekeres, C., Lamar, J., Batista, S., Kostourou, V., Germain, M. A., Reynolds, A. R., Jones, D. T., Watson, A. R., Jones, J. L., Harris, A., Hart, I. R., Iruela-Arispe, M. L., Dipersio, C. M., Kreidberg, J. A., and Hodivala-Dilke, K. M. Endothelial alpha3beta1-integrin represses pathological angiogenesis and sustains endothelial-VEGF. *Am J Pathol* **177**, 1534-1548

66. Donate, F., Parry, G. C., Shaked, Y., Hensley, H., Guan, X., Beck, I., Tel-Tsur, Z., Plunkett, M. L., Manuia, M., Shaw, D. E., Kerbel, R. S., and Mazar, A. P. (2008) Pharmacology of the novel antiangiogenic peptide ATN-161 (Ac-PHSCN-NH2): observation of a U-shaped dose-response curve in several preclinical models of angiogenesis and tumor growth. *Clin Cancer Res.* **14**, 2137-2144

67. Erdreich-Epstein, A., Tran, L. B., Cox, O. T., Huang, E. Y., Laug, W. E., Shimada, H., and Millard, M. (2005) Endothelial apoptosis induced by inhibition of integrins alphavbeta3 and alphavbeta5 involves ceramide metabolic pathways. *Blood* **105**, 4353-4361

68. Schor-Bardach, R., Alsop, D. C., Pedrosa, I., Solazzo, S. A., Wang, X., Marquis, R. P., Atkins, M. B., Regan, M., Signoretti, S., Lenkinski, R. E., and Goldberg, S. N. (2009) Does arterial spin-labeling MR imaging-measured tumor perfusion correlate with renal cell cancer response to antiangiogenic therapy in a mouse model? *Radiology* **251**, 731-742

69. Senger, D. R., Claffey, K. P., Benes, J. E., Perruzzi, C. A., Sergiou, A. P., and Detmar, M. (1997) Angiogenesis promoted by vascular endothelial growth factor: regulation through alpha1beta1 and alpha2beta1 integrins. *Proc Natl Acad Sci U S A* **94**, 13612-13617

70. Stupack, D. G., and Cheresh, D. A. (2003) Apoptotic cues from the extracellular matrix: regulators of angiogenesis. *Oncogene* **22**, 9022-9029

71. Sun, X., Qiao, H., Jiang, H., Zhi, X., Liu, F., Wang, J., Liu, M., Dong, D., Kanwar, J. R., Xu, R., and Krissansen, G. W. (2005) Intramuscular delivery of antiangiogenic genes suppresses secondary metastases after removal of primary tumors. *Cancer Gene Ther* **12**, 35-45

72. Wang, W., Wang, F., Lu, F., Xu, S., Hu, W., Huang, J., Gu, Q., and Sun, X. (2011) The antiangiogenic effects of integrin alpha5beta1 inhibitor (ATN-161) in vitro and in vivo. *Invest Ophthalmol Vis Sci* **52**, 7213-7220

73. Albo, D., Wang, T. N., and Tuszynski, G. P. (2004) Antiangiogenic therapy. *Curr Pharm Des* **10**, 27-37

74. Beaudry, P., Force, J., Naumov, G. N., Wang, A., Baker, C. H., Ryan, A., Soker, S., Johnson, B. E., Folkman, J., and Heymach, J. V. (2005) Differential effects of vascular endothelial growth factor receptor-2 inhibitor ZD6474 on circulating endothelial progenitors and mature circulating endothelial cells: implications for use as a surrogate marker of antiangiogenic activity. *Clin Cancer Res* **11**, 3514-3522

75. MacDonald, T. J., Taga, T., Shimada, H., Tabrizi, P., Zlokovic, B. V., Cheresh, D. A., and Laug, W. E. (2001) Preferential susceptibility of brain tumors to the antiangiogenic effects of an alpha(v) integrin antagonist. *Neurosurgery* **48**, 151-157

76. Pfeifer, A., Kessler, T., Silletti, S., Cheresh, D. A., and Verma, I. M. (2000) Suppression of angiogenesis by lentiviral delivery of PEX, a noncatalytic fragment of matrix metalloproteinase 2. *Proc Natl Acad Sci U S A* **97**, 12227-12232

77. Ren, B., Hoti, N., Rabasseda, X., Wang, Y. Z., and Wu, M. (2003) The antiangiogenic and therapeutic implications of endostatin. *Methods and findings in experimental and clinical pharmacology* **25**, 215-224

78. Teng, L. S., Jin, K. T., He, K. F., Wang, H. H., Cao, J., and Yu, D. C. (2010) Advances in combination of antiangiogenic agents targeting VEGF-binding and conventional chemotherapy and radiation for cancer treatment. *J Chin Med Assoc* **73**, 281-288

79. Wang, J., Chen, L. T., Tsang, Y. M., Liu, T. W., and Shih, T. T. (2004) Dynamic contrast-enhanced MRI analysis of perfusion changes in advanced hepatocellular carcinoma treated with an antiangiogenic agent: a preliminary study. *AJR Am J Roentgenol* **183**, 713-719

80. Woltering, E. A., Lewis, J. M., Maxwell, P. J. t., Frey, D. J., Wang, Y. Z., Rothermel, J., Anthony, C. T., Balster, D. A., O'Leary, J. P., and Harrison, L. H. (2003) Development of a novel in vitro human tissue-based angiogenesis assay to evaluate the effect of antiangiogenic drugs. *Ann Surg* **237**, 790-798; discussion 798-800

81. Yuan, P., Wang, L., Wei, D., Zhang, J., Jia, Z., Li, Q., Le, X., Wang, H., Yao, J., and Xie, K. (2007) Therapeutic inhibition of Sp1 expression in growing tumors by mithramycin a correlates directly with potent antiangiogenic effects on human pancreatic cancer. *Cancer* **110**, 2682-2690

82. Zhang, J., Zhang, Y., Zhang, S., Wang, S., and He, L. (2010) Discovery of novel taspine derivatives as antiangiogenic agents. *Bioorg Med Chem Lett* **20**, 718-721

83. Zhang, N., Wang, L., Liang, Y., Zhao, Y. M., Xue, Q., Wu, W. Z., Sun, H. C., Fan, J., and Tang, Z. Y. (2009) The antiangiogenic effects of tyroservatide on animal models of hepatocellular carcinoma. *J Cancer Res Clin Oncol* **135**, 1447-1453

84. Zhang, Q., Kang, X., Yang, B., Wang, J., and Yang, F. (2008) Antiangiogenic effect of capecitabine combined with ginsenoside Rg3 on breast cancer in mice. *Cancer Biother Radiopharm* **23**, 647-653

85. Zhang, W., Zhu, X. D., Sun, H. C., Xiong, Y. Q., Zhuang, P. Y., Xu, H. X., Kong, L. Q., Wang, L., Wu, W. Z., and Tang, Z. Y. (2010) Depletion of tumor-associated macrophages enhances the effect of sorafenib in metastatic liver cancer models by antimetastatic and antiangiogenic effects. *Clin Cancer Res.* **16**, 3420-3430

86. Zhang, Z., Zou, W., Wang, J., Gu, J., Dang, Y., Li, B., Zhao, L., Qian, C., Qian, Q., and Liu, X. (2005) Suppression of tumor growth by oncolytic adenovirus-mediated delivery of an antiangiogenic gene, soluble Flt-1. *Mol Ther* **11**, 553-562

87. Zhang, Z. L., Wang, J. H., and Liu, X. Y. (2003) Current strategies and future directions of antiangiogenic tumor therapy. *Sheng Wu Hua Xue Yu Sheng Wu Wu Li Xue Bao (Shanghai)* **35**, 873-880

88. Zhao, Y. L., Wang, S. F., Li, Y., He, Q. X., Liu, K. C., Yang, Y. P., and Li, X. L. (2011) Isolation of chemical constituents from the aerial parts of Verbascum thapsus and their antiangiogenic and antiproliferative activities. *Arch Pharm Res* **34**, 703-707

89. Zhu, X. D., Zhang, J. B., Fan, P. L., Xiong, Y. Q., Zhuang, P. Y., Zhang, W., Xu, H. X., Gao, D. M., Kong, L. Q., Wang, L., Wu, W. Z., Tang, Z. Y., Ding, H., and Sun, H. C. (2011) Antiangiogenic effects of pazopanib in xenograft hepatocellular carcinoma models: evaluation by quantitative contrast-enhanced ultrasonography. *BMC Cancer* **11**, 28

90. Milner, R., and Campbell, I. L. (2002) Developmental regulation of beta1 integrins during angiogenesis in the central nervous system. *Mol Cell Neurosci* **20**, 616-626

91. Senger, D. R., Perruzzi, C. A., Streit, M., Koteliansky, V. E., de Fougerolles, A. R., and Detmar, M. (2002) The alpha(1)beta(1) and alpha(2)beta(1) integrins provide critical support for vascular endothelial growth factor signaling, endothelial cell migration, and tumor angiogenesis. *Am J Pathol* **160**, 195-204

92. Ling, Y., Yang, Y., Lu, N., You, Q. D., Wang, S., Gao, Y., Chen, Y., and Guo, Q. L. (2007) Endostar, a novel recombinant human endostatin, exerts antiangiogenic effect via blocking VEGF-induced tyrosine phosphorylation of KDR/Flk-1 of endothelial cells. *Biochemical and biophysical research communications* **361**, 79-84

93. Anand, M., Van Meter, T. E., and Fillmore, H. L. (2011) Epidermal growth factor induces matrix metalloproteinase-1 (MMP-1) expression and invasion in glioma cell lines via the MAPK pathway. *Journal of neuro-oncology* **104**, 679-687

94. Pozzi, A., Moberg, P. E., Miles, L. A., Wagner, S., Soloway, P., and Gardner, H. A. (2000) Elevated matrix metalloprotease and angiostatin levels in integrin alpha 1 knockout mice cause reduced tumor vascularization. *Proc Natl Acad Sci U S A* **97**, 2202-2207

95. Kamisasanuki, T., Tokushige, S., Terasaki, H., Khai, N. C., Wang, Y., Sakamoto, T., and Kosai, K. (2011) Targeting CD9 produces stimulus-

independent antiangiogenic effects predominantly in activated endothelial cells during angiogenesis: a novel antiangiogenic therapy. *Biochemical and biophysical research communications* **413**, 128-135

96. Kessler, T. A., Pfeifer, A., Silletti, S., Mesters, R. M., Berdel, W. E., Verma, I., and Cheresh, D. (2002) Matrix metalloproteinase/integrin interactions as target for anti-angiogenic treatment strategies. *Ann Hematol* **81 Suppl 2**, S69-70

97. Kumar, M., Liu, Z. R., Thapa, L., Chang, Q., Wang, D. Y., and Qin, R. Y. (2004) Antiangiogenic effect of somatostatin receptor subtype 2 on pancreatic cancer cell line: Inhibition of vascular endothelial growth factor and matrix metalloproteinase-2 expression in vitro. *World J Gastroenterol* **10**, 393-399

98. Pullen, N. A., and Fillmore, H. L. (2010) Induction of matrix metalloproteinase-1 and glioma cell motility by nitric oxide. *Journal of neuro-oncology* **96**, 201-209

99. San Antonio, J. D., Zoeller, J. J., Habursky, K., Turner, K., Pimtong, W., Burrows, M., Choi, S., Basra, S., Bennett, J. S., DeGrado, W. F., and Iozzo, R. V. (2009) A key role for the integrin alpha2beta1 in experimental and developmental angiogenesis. *Am J Pathol* **175**, 1338-1347

100. Cailleteau, L., Estrach, S., Thyss, R., Boyer, L., Doye, A., Domange, B., Johnsson, N., Rubinstein, E., Boucheix, C., Ebrahimian, T., Silvestre, J. S., Lemichez, E., Meneguzzi, G., and Mettouchi, A. alpha2beta1 integrin

controls association of Rac with the membrane and triggers quiescence of endothelial cells. *J Cell Sci* **123**, 2491-2501

101. Francis, S. E., Goh, K. L., Hodivala-Dilke, K., Bader, B. L., Stark, M., Davidson, D., and Hynes, R. O. (2002) Central roles of alpha5beta1 integrin and fibronectin in vascular development in mouse embryos and embryoid bodies. *Arterioscler Thromb Vasc Biol* **22**, 927-933
102. Taverna, D., and Hynes, R. O. (2001) Reduced blood vessel formation and tumor growth in alpha5-integrin-negative teratocarcinomas and embryoid bodies. *Cancer Res* **61**, 5255-5261
103. Sun, Z., Martinez-Lemus, L. A., Trache, A., Trzeciakowski, J. P., Davis, G. E., Pohl, U., and Meininger, G. A. (2005) Mechanical properties of the interaction between fibronectin and alpha5beta1-integrin on vascular smooth muscle cells studied using atomic force microscopy. *Am J Physiol Heart Circ Physiol* **289**, H2526-2535
104. Hynes, R. O. (2002) A reevaluation of integrins as regulators of angiogenesis. *Nat Med* **8**, 918-921
105. Bouvard, D., Brakebusch, C., Gustafsson, E., Aszodi, A., Bengtsson, T., Berna, A., and Fassler, R. (2001) Functional consequences of integrin gene mutations in mice. *Circ Res* **89**, 211-223
106. Almokadem, S., and Belani, C. P. (2012) Volociximab in cancer. *Expert opinion on biological therapy* **12**, 251-257

107. Barkan, D., and Chambers, A. F. (2011) beta1-integrin: a potential therapeutic target in the battle against cancer recurrence. *Clin Cancer Res.* **17**, 7219-7223

108. Besse, B., Tsao, L. C., Chao, D. T., Fang, Y., Soria, J. C., Almokadem, S., and Belani, C. P. (2013) Phase Ib safety and pharmacokinetic study of volociximab, an anti-alpha5beta1 integrin antibody, in combination with carboplatin and paclitaxel in advanced non-small-cell lung cancer. *Annals of oncology : official journal of the European Society for Medical Oncology / ESMO* **24**, 90-96

109. Bhaskar, V., Fox, M., Breinberg, D., Wong, M. H., Wales, P. E., Rhodes, S., DuBridge, R. B., and Ramakrishnan, V. (2008) Volociximab, a chimeric integrin alpha5beta1 antibody, inhibits the growth of VX2 tumors in rabbits. *Investigational new drugs* **26**, 7-12

110. Bhaskar, V., Zhang, D., Fox, M., Seto, P., Wong, M. H., Wales, P. E., Powers, D., Chao, D. T., Dubridge, R. B., and Ramakrishnan, V. (2007) A function blocking anti-mouse integrin alpha5beta1 antibody inhibits angiogenesis and impedes tumor growth in vivo. *Journal of translational medicine* **5**, 61

111. Kuwada, S. K. (2007) Drug evaluation: Volociximab, an angiogenesis-inhibiting chimeric monoclonal antibody. *Current opinion in molecular therapeutics* **9**, 92-98

112. Ricart, A. D., Tolcher, A. W., Liu, G., Holen, K., Schwartz, G., Albertini, M., Weiss, G., Yazji, S., Ng, C., and Wilding, G. (2008) Volociximab, a chimeric

monoclonal antibody that specifically binds alpha5beta1 integrin: a phase I, pharmacokinetic, and biological correlative study. *Clin Cancer Res* **14**, 7924-7929

113. Tomillero, A., and Moral, M. A. (2009) Gateways to clinical trials. *Methods and findings in experimental and clinical pharmacology* **31**, 397-417

114. Oleszewski, M., Beer, S., Katich, S., Geiger, C., Zeller, Y., Rauch, U., and Altevogt, P. (1999) Integrin and neurocan binding to L1 involves distinct Ig domains. *The Journal of biological chemistry* **274**, 24602-24610

115. Mahesparan, R., Read, T. A., Lund-Johansen, M., Skaftnesmo, K. O., Bjerkvig, R., and Engebraaten, O. (2003) Expression of extracellular matrix components in a highly infiltrative in vivo glioma model. *Acta Neuropathol* **105**, 49-57

116. Lee, T. H., Seng, S., Li, H., Kennel, S. J., Avraham, H. K., and Avraham, S. (2006) Integrin regulation by vascular endothelial growth factor in human brain microvascular endothelial cells: role of alpha6beta1 integrin in angiogenesis. *The Journal of biological chemistry* **281**, 40450-40460

117. Bhatt, R. S., Wang, X., Zhang, L., Collins, M. P., Signoretti, S., Alsop, D. C., Goldberg, S. N., Atkins, M. B., and Mier, J. W. (2010) Renal cancer resistance to antiangiogenic therapy is delayed by restoration of angiostatic signaling. *Mol Cancer Ther* **9**, 2793-2802

118. Chen, C. P., Hu, C. B., Yeh, K. C., Song, J. S., Yeh, T. K., Tung, F. F., Hwang, L. L., Tseng, H. Y., Huang, Y. C., Shy, H. S., Hsieh, S. H., Shen, C. C., Wang, H. S., Hsieh, H. P., Liou, J. P., Chao, Y. S., and Chen, C. T.

(2010) Antiangiogenic activities and cisplatin-combined antitumor activities of BPR0L075. *Anticancer Res* **30**, 2813-2822

119. Chen, S. C., Lu, M. K., Cheng, J. J., and Wang, D. L. (2005) Antiangiogenic activities of polysaccharides isolated from medicinal fungi. *FEMS Microbiol Lett* **249**, 247-254

120. Hu, C. C., Ji, H. M., Chen, S. L., Zhang, H. W., Wang, B. Q., Zhou, L. Y., Zhang, Z. P., Sun, X. L., Chen, Z. Z., Cai, Y. Q., Qin, L. S., Lu, L., Jiang, X. D., Xu, R. X., and Ke, Y. Q. (2010) Investigation of a plasmid containing a novel immunotoxin VEGF165-PE38 gene for antiangiogenic therapy in a malignant glioma model. *Int J Cancer* **127**, 2222-2229

121. Jia, Z., Zhang, J., Wei, D., Wang, L., Yuan, P., Le, X., Li, Q., Yao, J., and Xie, K. (2007) Molecular basis of the synergistic antiangiogenic activity of bevacizumab and mithramycin A. *Cancer Res* **67**, 4878-4885

122. Li, L. H., Guo, Z. J., Yan, L. L., Yang, J. C., Xie, Y. F., Sheng, W. H., Huang, Z. H., and Wang, X. H. (2007) Antitumor and antiangiogenic activities of anti-vascular endothelial growth factor hairpin ribozyme in human hepatocellular carcinoma cell cultures and xenografts. *World J Gastroenterol* **13**, 6425-6432

123. Wang, B., Atherton, P., Patel, R., Manning, G., and Donnelly, R. (2010) Antiangiogenic effects and transcriptional regulation of pigment epithelium-derived factor in diabetic retinopathy. *Microvasc Res* **80**, 31-36

124. Wang, L., Guan, X., Zhang, J., Jia, Z., Wei, D., Li, Q., Yao, J., and Xie, K. (2008) Targeted inhibition of Sp1-mediated transcription for antiangiogenic

therapy of metastatic human gastric cancer in orthotopic nude mouse models. *Int J Oncol* **33**, 161-167

125. Yano, S., Li, Q., Wang, W., Yamada, T., Takeuchi, S., Nakataki, E., Ogino, H., Goto, H., Nishioka, Y., and Sone, S. (2011) Antiangiogenic therapies for malignant pleural mesothelioma. *Frontiers in bioscience : a journal and virtual library* **16**, 740-748
126. Wang, J., and Milner, R. (2006) Fibronectin promotes brain capillary endothelial cell survival and proliferation through alpha5beta1 and alphavbeta3 integrins via MAP kinase signalling. *J Neurochem* **96**, 148-159
127. Flintoff-Dye, N. L., Welser, J., Rooney, J., Scowen, P., Tamowski, S., Hatton, W., and Burkin, D. J. (2005) Role for the alpha7beta1 integrin in vascular development and integrity. *Dev Dyn* **234**, 11-21
128. Weinlander, K., Naschberger, E., Lehmann, M. H., Tripal, P., Paster, W., Stockinger, H., Hohenadl, C., and Sturzl, M. (2008) Guanylate binding protein-1 inhibits spreading and migration of endothelial cells through induction of integrin alpha4 expression. *FASEB J* **22**, 4168-4178
129. Hodivala-Dilke, K. M., Reynolds, A. R., and Reynolds, L. E. (2003) Integrins in angiogenesis: multitalented molecules in a balancing act. *Cell Tissue Res* **314**, 131-144
130. Xu, J., Millard, M., Ren, X., Cox, O. T., and Erdreich-Epstein, A. c-Abl mediates endothelial apoptosis induced by inhibition of integrins alphavbeta3 and alphavbeta5 and by disruption of actin. *Blood* **115**, 2709-2718

131. Ren, X., Xu, J., Cooper, J. P., Kang, M. H., and Erdreich-Epstein, A. (2012) c-Abl is an upstream regulator of acid sphingomyelinase in apoptosis induced by inhibition of integrins alphavbeta3 and alphavbeta5. *PloS one* **7**, e42291

132. Xu, J., Millard, M., Ren, X., Cox, O. T., and Erdreich-Epstein, A. (2010) c-Abl mediates endothelial apoptosis induced by inhibition of integrins alphavbeta3 and alphavbeta5 and by disruption of actin. *Blood* **115**, 2709-2718

133. Hynes, R. O. (2002) Integrins: bidirectional, allosteric signaling machines. *Cell* **110**, 673-687

134. Milner, R., Relvas, J. B., Fawcett, J., and ffrench-Constant, C. (2001) Developmental regulation of alphav integrins produces functional changes in astrocyte behavior. *Mol Cell Neurosci* **18**, 108-118

135. Haring, H. P., Akamine, B. S., Habermann, R., Koziol, J. A., and Del Zoppo, G. J. (1996) Distribution of integrin-like immunoreactivity on primate brain microvasculature. *J Neuropathol Exp Neurol* **55**, 236-245

136. Milner, R., and Ffrench-Constant, C. (1994) A developmental analysis of oligodendroglial integrins in primary cells: changes in alpha v-associated beta subunits during differentiation. *Development* **120**, 3497-3506

137. Staniszewska, I., Zaveri, S., Del Valle, L., Oliva, I., Rothman, V. L., Croul, S. E., Roberts, D. D., Mosher, D. F., Tuszynski, G. P., and Marcinkiewicz, C. (2007) Interaction of alpha9beta1 integrin with thrombospondin-1 promotes angiogenesis. *Circ Res* **100**, 1308-1316

138. Weil, R. J. (2006) Glioblastoma multiforme--treating a deadly tumor with both strands of RNA. *PLoS medicine* **3**, e31

139. Hall, P. E., Lathia, J. D., Caldwell, M. A., and Ffrench-Constant, C. (2008) Laminin enhances the growth of human neural stem cells in defined culture media. *BMC neuroscience* **9**, 71

140. Silletti, S., Kessler, T., Goldberg, J., Boger, D. L., and Cheresh, D. A. (2001) Disruption of matrix metalloproteinase 2 binding to integrin alpha vbeta 3 by an organic molecule inhibits angiogenesis and tumor growth in vivo. *Proc Natl Acad Sci U S A* **98**, 119-124

141. Meulmeester, E., and Ten Dijke, P. (2011) The dynamic roles of TGF-beta in cancer. *The Journal of pathology* **223**, 205-218

142. Samanta, D., and Datta, P. K. (2012) Alterations in the Smad pathway in human cancers. *Frontiers in bioscience : a journal and virtual library* **17**, 1281-1293

143. Guo, W., and Giancotti, F. G. (2004) Integrin signalling during tumour progression. *Nature reviews. Molecular cell biology* **5**, 816-826

144. Lakhe-Reddy, S., Khan, S., Konieczkowski, M., Jarad, G., Wu, K. L., Reichardt, L. F., Takai, Y., Bruggeman, L. A., Wang, B., Sedor, J. R., and Schelling, J. R. (2006) Beta8 integrin binds Rho GDP dissociation inhibitor-1 and activates Rac1 to inhibit mesangial cell myofibroblast differentiation. *The Journal of biological chemistry* **281**, 19688-19699

145. Lucio-Eterovic, A. K., Piao, Y., and de Groot, J. F. (2009) Mediators of glioblastoma resistance and invasion during antivascular endothelial growth factor therapy. *Clin Cancer Res.* **15**, 4589-4599

146. Ahluwalia, M. S., de Groot, J., Liu, W. M., and Gladson, C. L. (2010) Targeting SRC in glioblastoma tumors and brain metastases: rationale and preclinical studies. *Cancer letters* **298**, 139-149

147. de Groot, J. F., Fuller, G., Kumar, A. J., Piao, Y., Eterovic, K., Ji, Y., and Conrad, C. A. (2010) Tumor invasion after treatment of glioblastoma with bevacizumab: radiographic and pathologic correlation in humans and mice. *Neuro-oncology* **12**, 233-242

148. de Groot, J. F. (2011) High-dose antiangiogenic therapy for glioblastoma: less may be more? *Clin Cancer Res.* **17**, 6109-6111

149. de Groot, J., Liang, J., Kong, L. Y., Wei, J., Piao, Y., Fuller, G., Qiao, W., and Heimberger, A. B. (2012) Modulating antiangiogenic resistance by inhibiting the signal transducer and activator of transcription 3 pathway in glioblastoma. *Oncotarget* **3**, 1036-1048

150. Piao, Y., Liang, J., Holmes, L., Zurita, A. J., Henry, V., Heymach, J. V., and de Groot, J. F. (2012) Glioblastoma resistance to anti-VEGF therapy is associated with myeloid cell infiltration, stem cell accumulation, and a mesenchymal phenotype. *Neuro-oncology* **14**, 1379-1392

151. Amemiya, M., Mori, H., Imamura, S., Toyoda, A., Funayama, I., Asano, Y., Kusano, E., and Tabei, K. (2004) Stimulation of NHE3 in OKP cells by an autocrine mechanism. *Nephron Exp Nephrol* **96**, e23-30

152. Drake, C. J., Cheresh, D. A., and Little, C. D. (1995) An antagonist of integrin alpha v beta 3 prevents maturation of blood vessels during embryonic neovascularization. *J Cell Sci* **108 ( Pt 7)**, 2655-2661

153. Dupont, E., Falardeau, P., Mousa, S. A., Dimitriadou, V., Pepin, M. C., Wang, T., and Alaoui-Jamali, M. A. (2002) Antiangiogenic and antimetastatic properties of Neovastat (AE-941), an orally active extract derived from cartilage tissue. *Clin Exp Metastasis* **19**, 145-153

154. Dupont, E., Wang, B., Mamelak, A. J., Howell, B. G., Shivji, G., Zhuang, L., Dimitriadou, V., Falardeau, P., and Sauder, D. N. (2003) Modulation of the contact hypersensitivity response by AE-941 (Neovastat), a novel antiangiogenic agent. *J Cutan Med Surg* **7**, 208-216

155. Guo, Y. L., Wang, S., and Colman, R. W. (2002) Kininostatin as an antiangiogenic inhibitor: what we know and what we do not know. *Int Immunopharmacol* **2**, 1931-1940

156. Ko, E., Luo, W., Peng, L., Wang, X., and Ferrone, S. (2007) Mouse dendritic-endothelial cell hybrids and 4-1BB costimulation elicit antitumor effects mediated by broad antiangiogenic immunity. *Cancer Res* **67**, 7875-7884

157. Lebedeva, I. V., Emdad, L., Su, Z. Z., Gupta, P., Sauane, M., Sarkar, D., Staudt, M. R., Liu, S. J., Taher, M. M., Xiao, R., Barral, P., Lee, S. G., Wang, D., Vozhilla, N., Park, E. S., Chatman, L., Boukerche, H., Ramesh, R., Inoue, S., Chada, S., Li, R., De Pass, A. L., Mahasreshti, P. J., Dmitriev, I. P., Curiel, D. T., Yacoub, A., Grant, S., Dent, P., Senzer, N., Nemunaitis, J. J., and Fisher, P. B. (2007) mda-7/IL-24, novel anticancer cytokine: focus on

bystander antitumor, radiosensitization and antiangiogenic properties and overview of the phase I clinical experience (Review). *Int J Oncol* **31**, 985-1007

158. Liu, C., Wang, S., Deb, A., Nath, K. A., Katusic, Z. S., McConnell, J. P., and Caplice, N. M. (2005) Proapoptotic, antimigratory, antiproliferative, and antiangiogenic effects of commercial C-reactive protein on various human endothelial cell types in vitro: implications of contaminating presence of sodium azide in commercial preparation. *Circ Res* **97**, 135-143
159. Doherty, K. J., McKay, C., Chan, K. K., and El-Tanani, M. K. (2011) RAN GTPase as a target for cancer therapy: Ran binding proteins. *Current molecular medicine* **11**, 686-695
160. Mardilovich, K., Olson, M. F., and Baugh, M. (2012) Targeting Rho GTPase signaling for cancer therapy. *Future oncology* **8**, 165-177
161. Mizukawa, B., Wei, J., Shrestha, M., Wunderlich, M., Chou, F. S., Griesinger, A., Harris, C. E., Kumar, A. R., Zheng, Y., Williams, D. A., and Mulloy, J. C. (2011) Inhibition of Rac GTPase signaling and downstream prosurvival Bcl-2 proteins as combination targeted therapy in MLL-AF9 leukemia. *Blood* **118**, 5235-5245
162. van der Meel, R., Symons, M. H., Kudernatsch, R., Kok, R. J., Schiffelers, R. M., Storm, G., Gallagher, W. M., and Byrne, A. T. (2011) The VEGF/Rho GTPase signalling pathway: a promising target for anti-angiogenic/anti-invasion therapy. *Drug discovery today* **16**, 219-228

163. Karlsson, R., Pedersen, E. D., Wang, Z., and Brakebusch, C. (2009) Rho GTPase function in tumorigenesis. *Biochimica et biophysica acta* **1796**, 91-98

164. Van den Broeke, C., and Favoreel, H. W. (2011) Actin' up: herpesvirus interactions with Rho GTPase signaling. *Viruses* **3**, 278-292

165. Vernoud, V., Horton, A. C., Yang, Z., and Nielsen, E. (2003) Analysis of the small GTPase gene superfamily of Arabidopsis. *Plant physiology* **131**, 1191-1208

166. Wittinghofer, A., Scheffzek, K., and Ahmadian, M. R. (1997) The interaction of Ras with GTPase-activating proteins. *FEBS letters* **410**, 63-67

167. Baranwal, S., and Alahari, S. K. (2011) Rho GTPase effector functions in tumor cell invasion and metastasis. *Current drug targets* **12**, 1194-1201

168. Beckers, C. M., van Hinsbergh, V. W., and van Nieuw Amerongen, G. P. (2010) Driving Rho GTPase activity in endothelial cells regulates barrier integrity. *Thrombosis and haemostasis* **103**, 40-55

169. Beier, F., and Loeser, R. F. (2010) Biology and pathology of Rho GTPase, PI-3 kinase-Akt, and MAP kinase signaling pathways in chondrocytes. *Journal of cellular biochemistry* **110**, 573-580

170. Bement, W. M., Miller, A. L., and von Dassow, G. (2006) Rho GTPase activity zones and transient contractile arrays. *BioEssays : news and reviews in molecular, cellular and developmental biology* **28**, 983-993

171. Bollag, G., and McCormick, F. (1992) GTPase activating proteins. *Seminars in cancer biology* **3**, 199-208

172. Bosco, E. E., Mulloy, J. C., and Zheng, Y. (2009) Rac1 GTPase: a "Rac" of all trades. *Cellular and molecular life sciences : CMLS* **66**, 370-374

173. Bosgraaf, L., and Van Haastert, P. J. (2003) Roc, a Ras/GTPase domain in complex proteins. *Biochimica et biophysica acta* **1643**, 5-10

174. Braga, V. M., and Yap, A. S. (2005) The challenges of abundance: epithelial junctions and small GTPase signalling. *Current opinion in cell biology* **17**, 466-474

175. Bryan, B. A., and D'Amore, P. A. (2007) What tangled webs they weave: Rho-GTPase control of angiogenesis. *Cellular and molecular life sciences : CMLS* **64**, 2053-2065

176. Burbelo, P., Wellstein, A., and Pestell, R. G. (2004) Altered Rho GTPase signaling pathways in breast cancer cells. *Breast cancer research and treatment* **84**, 43-48

177. Chardin, P. (2003) GTPase regulation: getting aRnd Rock and Rho inhibition. *Current biology : CB* **13**, R702-704

178. Coleman, M. L., and Olson, M. F. (2002) Rho GTPase signalling pathways in the morphological changes associated with apoptosis. *Cell death and differentiation* **9**, 493-504

179. Davis, G. E., and Bayless, K. J. (2003) An integrin and Rho GTPase-dependent pinocytic vacuole mechanism controls capillary lumen formation in collagen and fibrin matrices. *Microcirculation* **10**, 27-44

180. Deacon, S. W., and Peterson, J. R. (2008) Chemical inhibition through conformational stabilization of Rho GTPase effectors. *Handbook of experimental pharmacology*, 431-460

181. DerMardirossian, C., and Bokoch, G. M. (2005) GDIs: central regulatory molecules in Rho GTPase activation. *Trends in cell biology* **15**, 356-363

182. Donovan, S., Shannon, K. M., and Bollag, G. (2002) GTPase activating proteins: critical regulators of intracellular signaling. *Biochimica et biophysica acta* **1602**, 23-45

183. Dovas, A., and Couchman, J. R. (2005) RhoGDI: multiple functions in the regulation of Rho family GTPase activities. *The Biochemical journal* **390**, 1-9

184. Ferguson, S. M., and De Camilli, P. (2012) Dynamin, a membrane-remodelling GTPase. *Nature reviews. Molecular cell biology* **13**, 75-88

185. Friedman, E. (1995) The role of ras GTPase activating protein in human tumorigenesis. *Pathobiology : journal of immunopathology, molecular and cellular biology* **63**, 348-350

186. Fukuhra, S., Sakurai, A., Yamagishi, A., Sako, K., and Mochizuki, N. (2006) Vascular endothelial cadherin-mediated cell-cell adhesion regulated by a small GTPase, Rap1. *Journal of biochemistry and molecular biology* **39**, 132-139

187. Gamblin, S. J., and Smerdon, S. J. (1998) GTPase-activating proteins and their complexes. *Current opinion in structural biology* **8**, 195-201

188. Goldfinger, L. E. (2008) Choose your own path: specificity in Ras GTPase signaling. *Molecular bioSystems* **4**, 293-299

189. Gomez del Pulgar, T., Benitah, S. A., Valeron, P. F., Espina, C., and Lacal, J. C. (2005) Rho GTPase expression in tumourigenesis: evidence for a significant link. *BioEssays : news and reviews in molecular, cellular and developmental biology* **27**, 602-613

190. Grunicke, H. H., and Maly, K. (1993) Role of GTPases and GTPase regulatory proteins in oncogenesis. *Critical reviews in oncogenesis* **4**, 389-402

191. Hakoshima, T. (2002) [Structural biology of the Rho GTPase signaling]. *Seikagaku. The Journal of Japanese Biochemical Society* **74**, 1237-1243

192. Hakoshima, T., Shimizu, T., and Maesaki, R. (2003) Structural basis of the Rho GTPase signaling. *Journal of biochemistry* **134**, 327-331

193. Johnson, D. I. (1999) Cdc42: An essential Rho-type GTPase controlling eukaryotic cell polarity. *Microbiology and molecular biology reviews : MMBR* **63**, 54-105

194. Kandpal, R. P. (2006) Rho GTPase activating proteins in cancer phenotypes. *Current protein & peptide science* **7**, 355-365

195. Karnoub, A. E., Symons, M., Campbell, S. L., and Der, C. J. (2004) Molecular basis for Rho GTPase signaling specificity. *Breast cancer research and treatment* **84**, 61-71

196. Leve, F., and Morgado-Diaz, J. A. (2012) Rho GTPase signaling in the development of colorectal cancer. *Journal of cellular biochemistry* **113**, 2549-2559

197. McCormick, F. (1993) The GTPase superfamily. Introduction. *Ciba Foundation symposium* **176**, 1-5

198. Moon, S. Y., and Zheng, Y. (2003) Rho GTPase-activating proteins in cell regulation. *Trends in cell biology* **13**, 13-22

199. Narumiya, S. (1996) The small GTPase Rho: cellular functions and signal transduction. *Journal of biochemistry* **120**, 215-228

200. Nishimoto, T. (1999) A new role of ran GTPase. *Biochemical and biophysical research communications* **262**, 571-574

201. Olson, M. F. (2004) Contraction reaction: mechanical regulation of Rho GTPase. *Trends in cell biology* **14**, 111-114

202. Pedersen, E., and Brakebusch, C. (2012) Rho GTPase function in development: how in vivo models change our view. *Experimental cell research* **318**, 1779-1787

203. Pfeffer, S. (2005) A model for Rab GTPase localization. *Biochemical Society transactions* **33**, 627-630

204. Quimby, B. B., and Dasso, M. (2003) The small GTPase Ran: interpreting the signs. *Current opinion in cell biology* **15**, 338-344

205. Rao, V. P., and Epstein, D. L. (2007) Rho GTPase/Rho kinase inhibition as a novel target for the treatment of glaucoma. *BioDrugs : clinical immunotherapeutics, biopharmaceuticals and gene therapy* **21**, 167-177

206. Rensen, W. M., Mangiacasale, R., Ciciarello, M., and Lavia, P. (2008) The GTPase Ran: regulation of cell life and potential roles in cell transformation. *Frontiers in bioscience : a journal and virtual library* **13**, 4097-4121

207. Rutherford, S., and Moore, I. (2002) The Arabidopsis Rab GTPase family: another enigma variation. *Current opinion in plant biology* **5**, 518-528

208. Scheffzek, K., and Ahmadian, M. R. (2005) GTPase activating proteins: structural and functional insights 18 years after discovery. *Cellular and molecular life sciences : CMLS* **62**, 3014-3038

209. Scheffzek, K., Ahmadian, M. R., and Wittinghofer, A. (1998) GTPase-activating proteins: helping hands to complement an active site. *Trends in biochemical sciences* **23**, 257-262

210. Schwefel, D., and Daumke, O. (2011) GTP-dependent scaffold formation in the GTPase of Immunity Associated Protein family. *Small GTPases* **2**, 27-30

211. Steggerda, S. M., and Paschal, B. M. (2002) Regulation of nuclear import and export by the GTPase Ran. *International review of cytology* **217**, 41-91

212. Stenmark, H., and Olkkonen, V. M. (2001) The Rab GTPase family. *Genome biology* **2**, REVIEWS3007

213. Toksoz, D., and Merdek, K. D. (2002) The Rho small GTPase: functions in health and disease. *Histology and histopathology* **17**, 915-927

214. Tolias, K. F., Duman, J. G., and Um, K. (2011) Control of synapse development and plasticity by Rho GTPase regulatory proteins. *Progress in neurobiology* **94**, 133-148

215. Reyes, S. B., Narayanan, A. S., Lee, H. S., Tchaicha, J. H., Aldape, K. D., Lang, F. F., Tolias, K. F., McCarty, J. H. (2013) αvβ 8 Integrin Interacts with RhoGDI1 to Regulate Rac1 and Cdc42 Activation and Drive Glioblastoma Cell Invasion. *Molecular Biology of the Cell* [Epub ahead of print]

## Vita

Steve Bradley Reyes was born in Houston, Texas on October 6, 1985, the son of Brenda Reyes and Sebastian Reyes. After completing his work at Nimitz High School, Houston, Texas in 2004 he entered Lone Star North Harris Community College. In 2006 he entered University of Houston in Houston, Texas. He received a Bachelor of Science with a major in Biochemical & Biophysical Sciences from UH in May, 2008. In August of 2008 he entered The University of Texas Health Science Center at Houston Graduate School of Biomedical Sciences. In May 2009 he joined the laboratory of Dr. Joseph H. McCarty at the University of Texas M. D. Anderson Cancer Center to study the invasive role of αvβ8 integrin in glioma. Three and a half years later he defended his research in January of 2013.